HYDROGEOLOGICAL CHARACTERIZATION OF A MINE SITE IN EASTERN
ANATOLIA

A THESIS SUBMITTED TO
THE GRADUATE SCHOOL OF NATURAL AND APPLIED SCIENCES
OF
MIDDLE EAST TECHNICAL UNIVERSITY

BY

DOĞUKAN TAYYAR

IN PARTIAL FULFILLMENT OF THE REQUIREMENTS
FOR
THE DEGREE OF MASTER SCIENCE
IN
GEOLOGICAL ENGINEERING

SEPTEMBER 2020

Approval of the thesis:

HYDROGEOLOGICAL CHARACTERIZATION OF A MINE SITE IN EASTERN ANATOLIA

submitted by **DOĞUKAN TAYYAR** in partial fulfillment of the requirements for the degree of **Master of Science in Geological Engineering Department, Middle East Technical University** by,

Prof. Dr. Halil Kalıpçılar
Dean, Graduate School of **Natural and Applied Sciences** _____

Prof. Dr. Erdin Bozkurt
Head of Department, **Geological Engineering** _____

Prof. Dr. Hasan Yazıcıgil
Supervisor, **Geological Engineering Dept., METU** _____

Examining Committee Members:

Prof. Dr. M. Zeki Çamur
Geological Engineering Dept., METU _____

Prof. Dr. Hasan Yazıcıgil
Geological Engineering Dept., METU _____

Assoc. Prof. Dr. Harun Aydın
Hydrogeological Engineering Dept., Hacettepe University _____

Assoc. Prof. Dr. Özlem Yağbasan
Department of Geography Education, Gazi University _____

Assist. Prof. Dr. Levent Tezcan
Hydrogeological Engineering Dept., Hacettepe University _____

Date: 07.09.2020

I hereby declare that all information in this document has been obtained and presented in accordance with academic rules and ethical conduct. I also declare that, as required by these rules and conduct, I have fully cited and referenced all material and results that are not original to this work.

Name, Surname: Doğukan Tayyar

Signature:

ABSTRACT

HYDROGEOLOGICAL CHARACTERIZATION OF A MINE SITE IN EASTERN ANATOLIA

Tayyar, Doğukan

Master of Science, Geological Engineering

Supervisor: Prof. Dr. Hasan Yazıcıgil

September 2020, 100 pages

Characterization of hydrogeological properties of water bearing rocks in a mine site is important for controlling groundwater flow to provide safe operating conditions. This study aims to characterize the groundwater flow in an active mine site in eastern Anatolia. Large diameter pumping wells were drilled in the surrounding carbonate rocks to determine the groundwater flow and boundary conditions along some critical cross-sections. Large diameter wells were also drilled in the mine site for hydraulic testing of the metasediments. Constant rate pumping tests and monitoring of groundwater levels were conducted at each well. Furthermore, twelve diamond core drilling were done in the mine site and a total 33 vibrating wire piezometers were installed at different depths for monitoring pore water pressures. Packer tests were applied on these wells to determine localized hydraulic conductivity of diorite and metasediments at different depths. The results obtained from these tests are used for developing hydrogeological conceptual model for groundwater flow. According to the results, the carbonate unit in the immediate vicinity on the mine site does not contain groundwater in significant amount because of diorite intrusion at the Uzundere-Zangardere area and the metasediments and diorite have low permeability and heterogeneous medium. Also, downward hydraulic gradient was observed in almost all piezometers drilled in the metasediments and diorite and it generally increases with depth. Stable isotope analysis has indicated that the metasediments-diorite are recharged by infiltration from local precipitation.

ÖZ

DOĞU ANADOLUDAKİ BİR MADEN SAHASININ HİDROJEOLOJİK KARAKTERİZASYONU

Tayyar, Doğukan

Yüksek Lisans, Jeoloji Mühendisliği

Tez Danışmanı: Prof. Dr. Hasan Yazıcıgil

Eylül 2020, 100 sayfa

Bir maden sahasındaki su taşıyan kayaçların hidrojeolojik özelliklerinin karakterizasyonu, güvenli çalışma koşulları sağlamak üzere yeraltı suyu akışını kontrol etmek için önemlidir. Bu çalışma, doğu Anadolu'daki aktif maden sahasındaki yeraltı suyu akışını karakterize etmeyi amaçlamaktadır. Bazı kritik kesitler boyunca yeraltı suyu akışını ve sınır koşullarını belirlemek için çevreleyen karbonat kayaçlarında büyük çaplı pompa kuyuları açılmıştır. Metasedimentlerin hidrolik testi için maden sahasında büyük çaplı kuyular da açılmıştır Her bir kuyuda sabit debili pompa testleri ve yeraltı suyu seviyelerinin izlenmesi gerçekleştirilmiştir. Ayrıca, maden sahasında on iki adet elmas karotlu sondaj yapılmış ve yeraltı suyu basınçlarının izlenmesi için farklı derinliklerde toplam 33 adet titreşimli tel piyezometre yerleştirilmiştir. Farklı derinliklerde, diyorit ve metasediment birimlerinin lokal hidrolik iletkenliğini belirlemek için bu kuyularda paker testleri uygulanmıştır. Bu testlerden elde edilen sonuçlar yeraltı suyu akışını karakterize eden hidrojeolojik kavramsal model geliştirmek için kullanılmıştır. Elde edilen sonuçlara göre, maden alanı yakın civarındaki karbonatlı birim, Uzundere-Zangardere bölgesindeki diyorit intirüzyonu nedeni ile önemli miktarda yeraltı suyu içermemekte olup, metasedimanlar ve diyorit düşük geçirimliliğe ve heterojen ortama sahiptir. Ayrıca, metasedimanlar ve diyoritte açılan hemen hemen tüm piyezometrelerde düşey yönlü derinlikle artan hidrolik gradyan gözlenmiştir. Kararlı izotop analizi, metasedimanlar-diyoritin yerel yağıştan beslendiğini göstermiştir.

Anahtar Kelimeler: Hidrojeolojik Özellikler, Pompa Testi, Titreşimli Tel Piyezometresi, Paker Testi, Hidrojeolojik Kavramsal Model

TO BELOVED FAMILY AND FRIENDS…

ACKNOWLEDGMENTS

TABLE OF CONTENTS

LIST OF FIGURES

FIGURES

LIST OF TABLES

CHAPTER 1

INTRODUCTION

1.1. Problem Statement and Scope of Study

Çöpler mine site is located in İliç town of Erzincan Province and operated by Anagold Madencilik Sanayi and Ticaret A.Ş. (Anagold A.Ş). The mine site is formed by a series of side-by-side open pits. Groundwater seepages are observed along the pit walls, mainly in sheared zones of the highly altered areas where faults intersect the pit walls. Consequently, Anagold A.Ş. requested Hacettepe Mineral Technologies (HMT) to study groundwater occurrence and its control for effective and safe mining. Eventually the hydrogeological characterization of the mine site and development of a site hydrogeological conceptual model became necessary to develop techniques and methods for a more effective and safe dewatering and/or depressurization, if needed. Thus, the purpose of this study is to characterize the groundwater occurrence and distribution at the mine site and to develop hydrogeological conceptual model for the site.The study program divided into two main phases to achieve the objectives and scope of the study. Phase-I: Data collection and Gap Analysis, Phase-II: Field Investigations and Preparation of a Conceptual Hydrogeological Model. Six cross-sections are determined by another study to obtain field data regarding hydraulic properties and pore water pressure distributions. Drilling and installation of piezometers and pumping wells in karstic rock masses, metasediments and diorite have been conducted to obtain in situ values. The data collected from the hydraulic testing and monitoring are used to characterize the hydrogeology of the mine site. Finally, the study is completed by developing a conceptual hydrogeological model of the site.

1.2. Location of the Study Area

The Çöpler mine site is in 120 km west of the Erzincan city and 7 km west of İliç town (Figure 1.1). Topographically the mine site surrounded by high carbonate masses of the Munzur mountain range. Altitude of carbonate rocks reaches about 1500 m in the north and about 2500 m in the south of the mine site, while elevation of valley ranges changes between 1100 m and 1300 m. In the north of the study area, there are Karasu River and Bağıştaş-I Dam, in the north-west Bağıştaş-II Dam, in the north-east Çöpler Creek and in the south-east Sabırlı Creek.
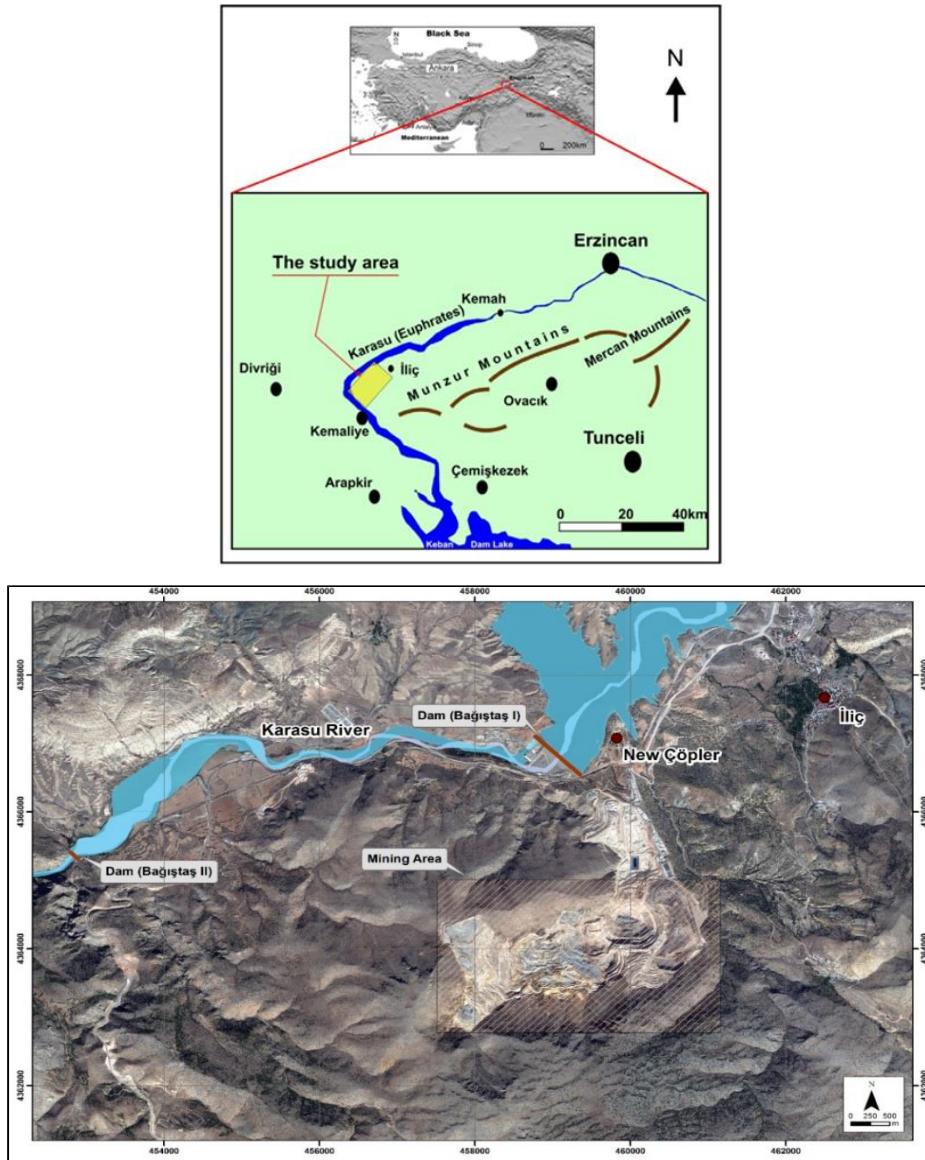
Figure 1.1. Location map of the study area

1.3. Previous Studies

The geology of the region at a scale of 1/100000 covering the mine site was conducted by Özgül et al. (1981). This study was regional in nature and does not give detailed information for the geology of the mine site. Ekmekçi and Tezcan (2007) documented extractions from this report to explain the geology of the area including Çöpler mine site.

The studies at the Çöpler mine site mainly focused on mineralization of economic interest. Technical feasibility and economic viability of recovering precious metals were main targets. These studies are prefeasibility and feasibility report (SE, 2010), mineral source report (Alacer Gold, 2013) and geotechnical reports (Alacer Gold, 2016; Golder, 2014 & 2015).

Four water management studies have been conducted at the mine site. The first one is completed by Schlumberger Water Services (UK) Ltd. (SWS, 2010). The main purpose of this study was to develop a sediment control and surface drainage management plan for the Çöpler mine site (SWS 2010). The report also included conceptual design recommendations for sediment ponds and diversion channels.

The second study conducted by Golder Associates in 2013 about Flood Control Management to support the feasibility study and Environmental Impact Assessment (EIA) for the Sulfide project (Golder, 2013). This study focused on the major surface water diversions that collected water from upgradient, undisturbed land around the mine area.

Third study was also prepared by Golder Associates in 2016 about surface water management plan (Golder, 2016). The study results were used to design surface water collection and sediment control structures.

The final study about surface water management plan was conducted by INR Engineering Consultancy in 2017 (INR, 2017). This study mainly focused on open pit

drainage design in addition to side-wide surface water management plan.

Ekmekçi et al. (2018) conducted a study about optimization of groundwater control for slope stability at mine site. The study included numerical modeling to simulate the pore water pressure distribution and general conceptual model of the Çöpler Mine site. This master thesis is conducted as a part of to above mentioned study.

1.4. Methodology

The work program to achieve the objectives and scope defined above consisted of the following specific tasks;

1.4.1. Data Collection and Gap Analysis

Compiling and evaluating previously collected data regarding geology, hydrology, hydrogeology, meteorology, topography and geo-technics with the aim of a gap analysis to fully develop a conceptual hydrogeological model of the site.

1.4.2. Field Studies

Field studies consisted of drilling large diameter wells in the carbonate rock mass surrounding the mine site. These wells were mainly drilled to gather information regarding the boundary conditions and to determine the groundwater potential of the carbonate rocks. Pumping tests are conducted in the large diameter wells and groundwater levels were monitored over a period of almost two years on a monthly basis. Nested large diameter wells were also drilled in the metasediments and diorites in the mine site for testing, sampling and monitoring purposes. Furthermore, PQ diameter (122.6 mm) core drilling were conducted along critical cross sections for geotechnical analyses and vibrating wire piezometers were installed at various depths in these boreholes to monitor pore pressure distributions. The packer tests conducted in these boreholes together with the data obtained from geotechnical logs helped to develop vertical distribution of the hydraulic conductivities and identify vertical heterogeneities. As mentioned in section 1.1, six critical cross-sections were selected, namely A through F (Figure 1.2). The number of cross-sections to study reduced to four (A, B, C and E), D was cancelled, and E and F considered as one cross-section. Totally 10 large diameter wells and 11 small diameter piezometer wells were drilled.

A total of 33 vibrating wire pressure transducers were installed at different depths.

1.4.3. Preparation of a Conceptual Hydrogeological Model

Using the information generated from first and second steps, a conceptual hydrogeological model of the mine site is developed to aid in the analyses of appropriate dewatering/or depressurization techniques to control groundwater.
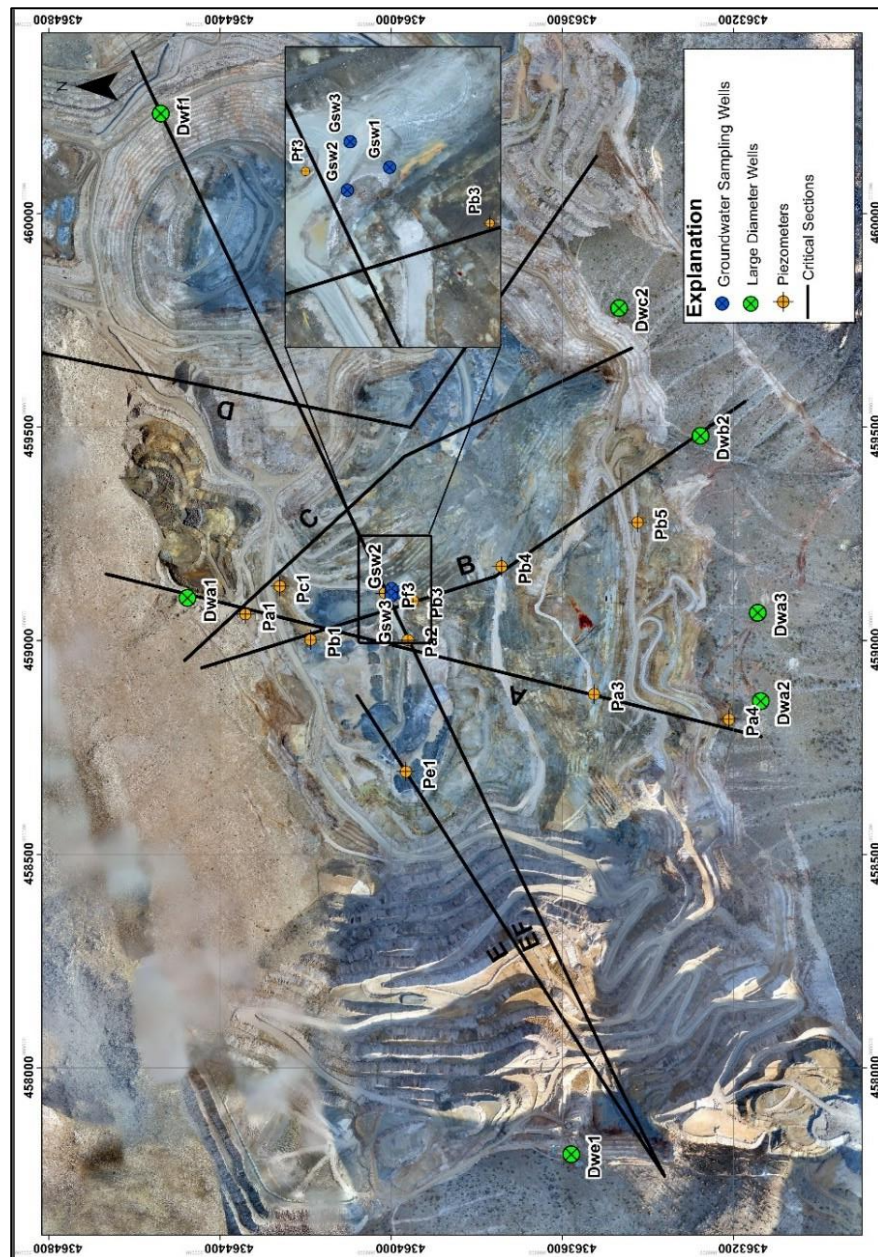
Figure 1.2 Location of wells with respect to critical cross-sections (From Ekmekçi et al., 2018)

CHAPTER 2

DESCRIPTION OF THE STUDY SITE

2.1. Topography and Drainage

The Çöpler mine site situated in a topographical depression which is created by the Çöpler stream, a small tributary of the Karasu River (Figure 2.1). The pre-mining elevation of the study site is around 1200 meters above sea level (m.a.s.l). The carbonate rock mass surrounding the site has an elevation higher than 1700 m.a.s.l.

The main surface water is the Karasu River which limits the study area from the north. The other surface water resources are dry or temporary. Two streams are connected to the Çöpler mine site. First one is the Çöpler stream with a drainage area of about 10 km^2 and bounds the mine site from the north-east and it is completely altered with mining operations. The second one is the Sabırlı stream which is located on south-east of the mine site. It drains the adjacent eastern basin of about 35 km^2 (Figure 2.1). The watersheds which represent the Çöpler and Sabırlı streams are shown in Figure 2.2 (Ekmekçi and Tezcan, 2007).

Figure 2.1. Topographical setting of the project area (from Ekmekçi et al., 2018)
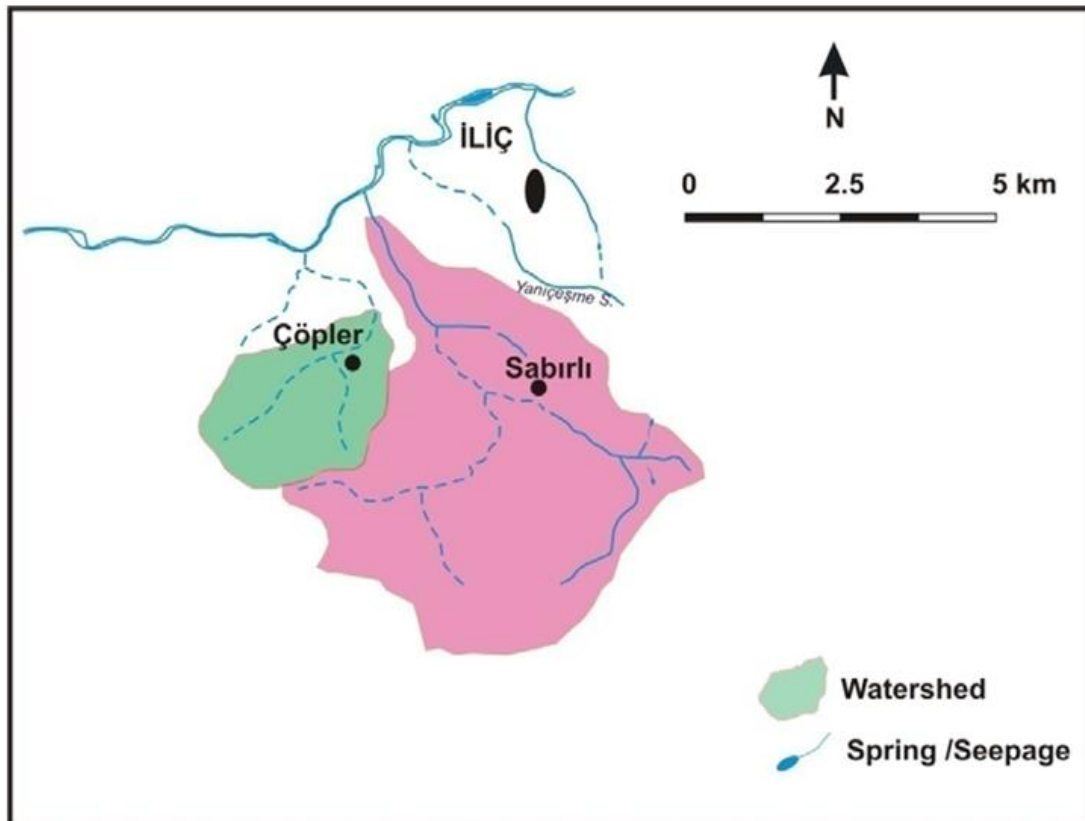
Figure 2.2. Watersheds of Çöpler and Sabırlı streams (from Ekmekçi and Tezcan, 2007)

2.2. Climate and Meteorology

The study area is in the Eastern Anatolia of Turkey. Generally, climate is cold and wet in winter, hot and dry in summers. The long-term meteorological data obtained from Divriği Meteorological Station is the most appropriate data for study area (Ekmekçi and Tezcan, 2007; SRK, 2015). Also, the mine has its own meteorological station onsite (WS05) but the data recorded on these station are not long enough for hydrometeorological analyses. Therefore, the onsite data was used in hydrological analysis for comparison between WS05 and Divriği stations.

Data recorded from the Divriği meteorological station between 1975 and 2016 show that average annual precipitation and air temperature is 383 mm and 12.8 °C, respectively. Precipitation is observed almost all along the year. The minimum precipitation observed in the months of July, August and September and average rainfall is less than 10 mm in these months. 30 mm and higher precipitation amounts occurred between October and May (Figure 2.3).

In WS05 meteorological station, only fifteen years' records exist. The fifteen years average of annual precipitation was calculated as 400 mm (2004-2019). The rainfall distribution is more uniform than the Divriği meteorological station data along the 8 months, October to May (Figure 2.4). Precipitation amounts almost similar in June to September in both data sets.

The long-term annual air temperature calculated for Divriği station is 12.8 °C. The monthly average maximum and minimum air temperature values are 25 °C (August) and -2.1 °C (January), respectively (Figure 2.5). The long-term annual air temperature calculated for WS05 station is 12 °C. The monthly average maximum and minimum air temperature varies 26.4 °C and 0 °C (Figure 2.6). Calculated values for both stations are nearly the same. The difference is likely caused by different recording periods of the stations.
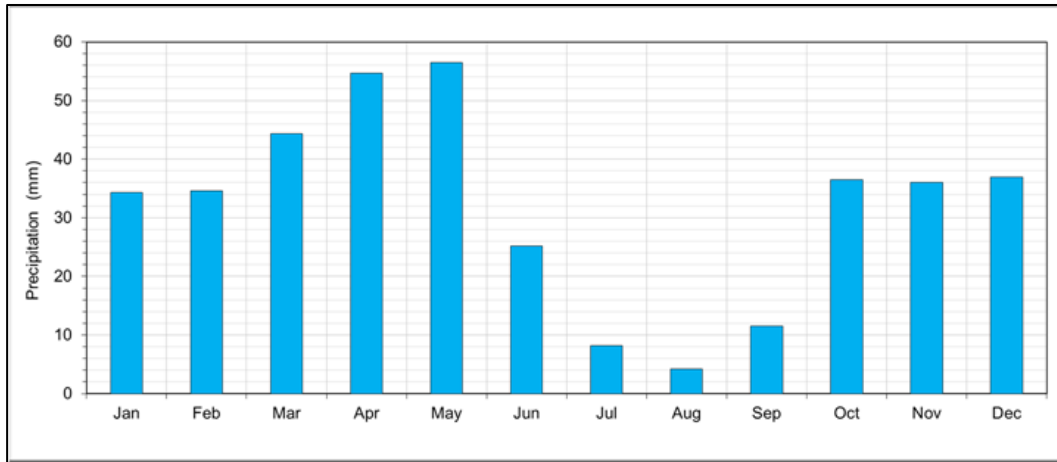
Figure 2.3. Long- term (1974- 2016) averages of monthly precipitation recorded at Divriği Meteorological Station (from Ekmekçi et al., 2018)
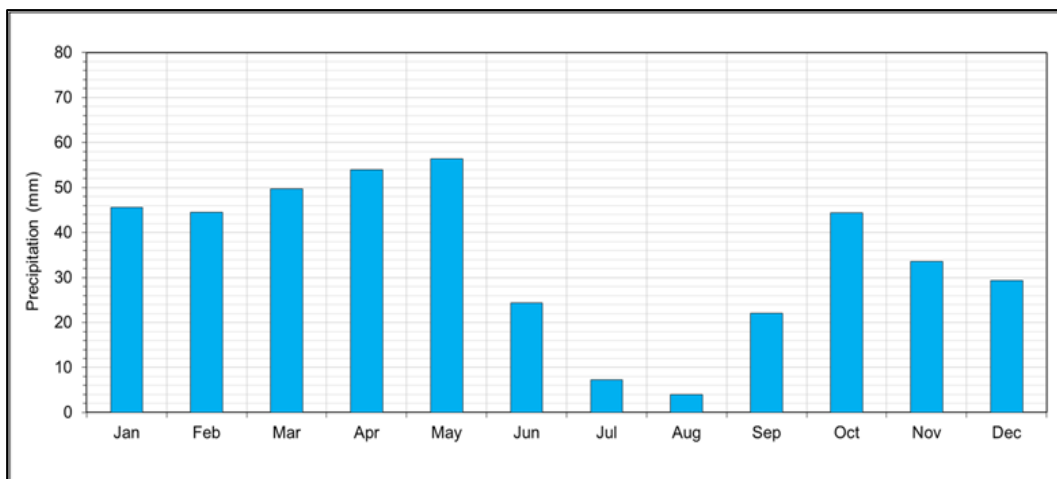
Figure 2.4. Fifteen- years (2004- 2019) averages of monthly precipitation recorded at WS05 Çöpler Meteorological Station (from Ekmekçi et al., 2018)
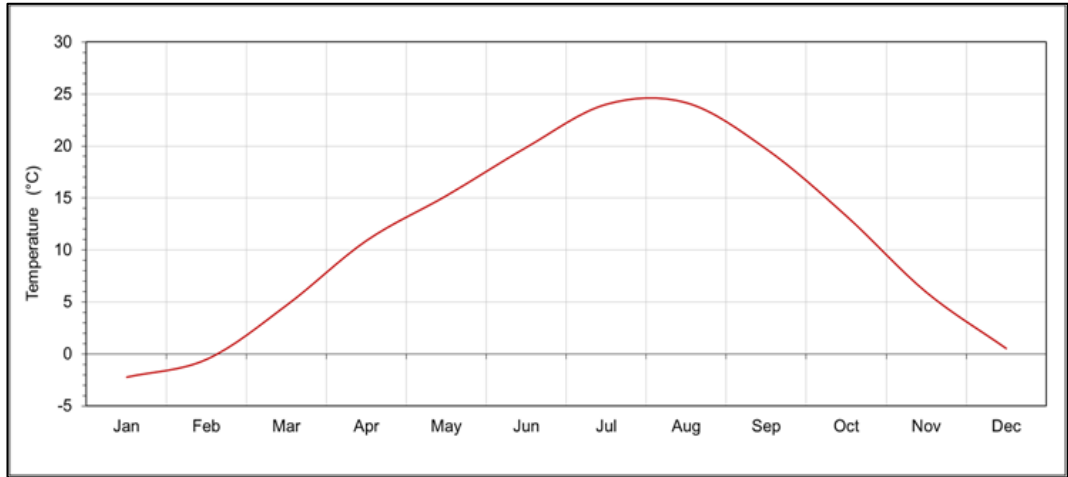
Figure 2.5. Long- term (1974- 2016) averages of monthly temperatures recorded at Divriği Meteorological Station (from Ekmekçi et al., 2018)
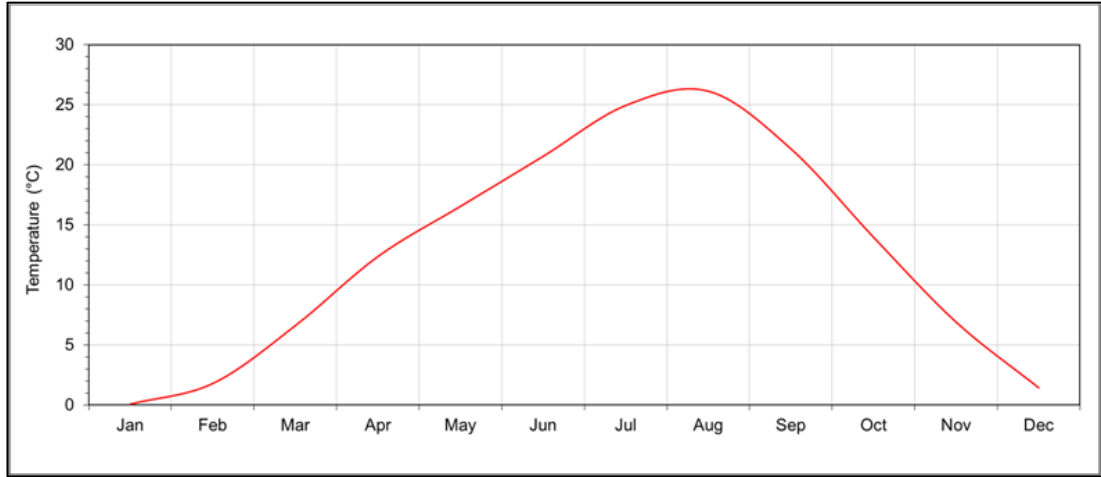
Figure 2.6. Fifteen- years (2004- 2019) averages of monthly precipitation recorded at WS5 Çöpler Meteorological Station (from Ekmekçi et al., 2018)

2.3. Geology

2.3.1. Regional Geology

The regional geological setting has been studied by Özgül et al (1981) at a 1/100000 scale. According to this study the regional geological setting can be described as three "structural units" overlain by post-tectonic deposits. Based on structure, stratigraphy and metamorphism, Özgül et al. (1981) have defined three structural units in the region, from bottom to top: Keban Unit, Munzur Dağı Unit (Munzur Limestone), and Ovacik Unit. The study site is mainly located within the Munzur Dağı Unit.

11

The 1/100000 scale map of the Çöpler site and surrounding is shown in Figure 2.7.

The metasediments that crop out at the mine site are not shown in the regional geological map. It has been described as a lithological unit of the Keban Unit which forms the basement in the region. The contact relations between the Munzur limestone, the metasediments and the diorite are not defined in detail.

A high-angle thrust fault defined as a tectonic contact that is marked by the Sabırlı stream. Normal faults developed in the Munzur limestone are the products of the post-Miocene tensional tectonic regime.
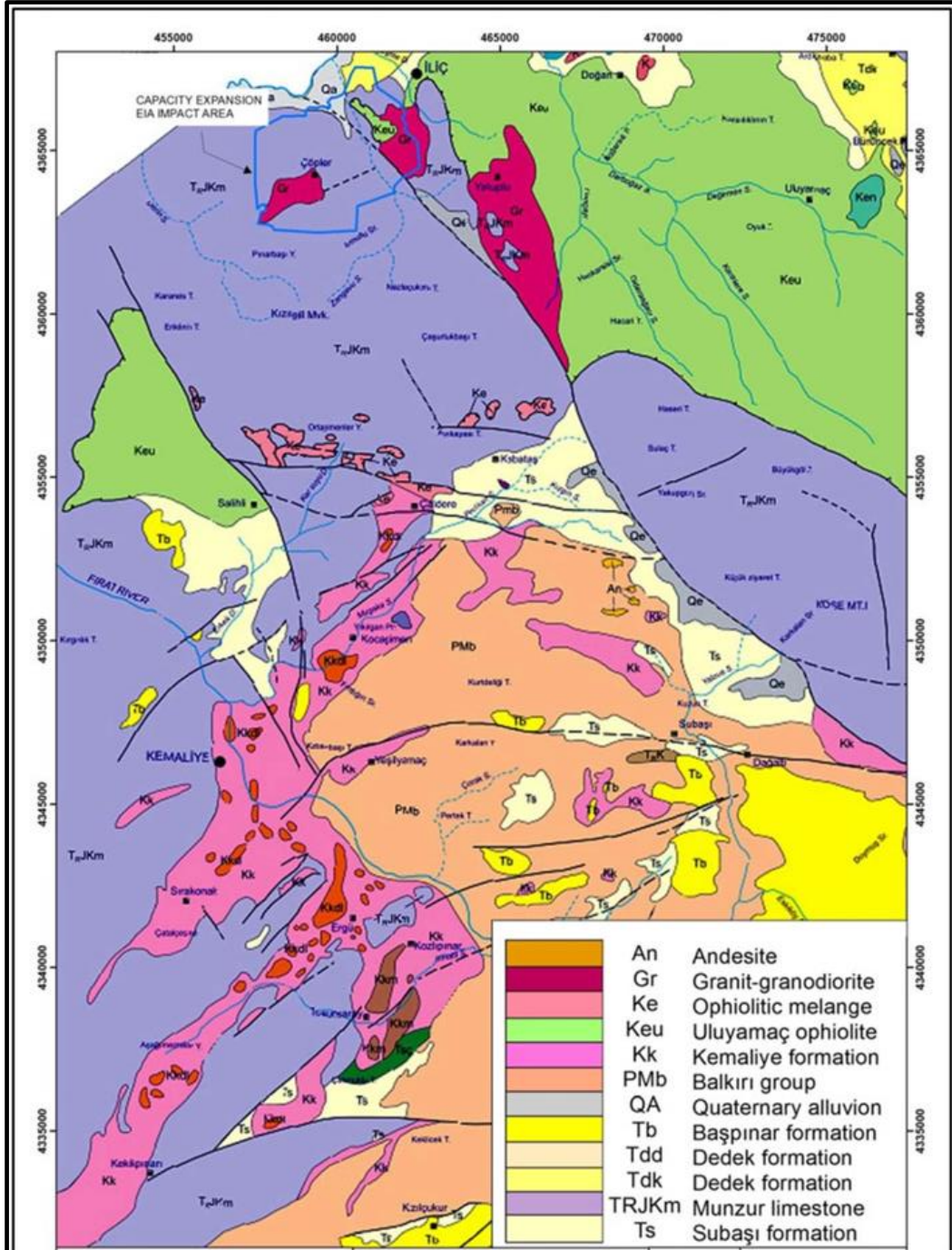
Figure 2.7. Geological map of the study area and its vicinity (Ekmekçi and Tezcan, 2007: Özgül et al., 1981)

13

2.3.2 Mine Site Geology

The geology of the mine site is consisting of three main lithology which are carbonate rocks (Munzur Limestone), metasediments and diorite and their alteration products. The mine site is surrounded by carbonate rocks, while the metasediments and diorite crop out at the central part. The carbonate rocks characterized by mainly shelf-type carbonates and it has been continuous without a significant change in facies. The metasediments described as metamorphic rocks which originated from mainly clastic and carbonate deposits. The diorite described as highly altered plutonic rock unit crop out at the mine site and generally caused contact metamorphism in the carbonate rocks (Alacer Gold, 2013). Metasediments and diorite are the main two lithological units where the mined ore exists. According the data obtained from drilling and surveying in excavations and pit walls, the geological model being updated by an appropriate software. However, there is still a gap of information on the shear zones. This gap partly filled with a detailed core description obtained from drill holes on the critical cross-sections. The geology of the critical cross-sections was produced by geologists of Anagold A.Ş. by using the LeapFrog™ software. The geological map of the mine site produced by geologist of Anagold A.Ş. is shown in Figure 2.8.

The study conducted by Terrane Geoscience Inc. in 2018 was about structural mapping and 3D fault modeling (Terrane, 2018). The study shows that there are series of major fault sets and several more minor sets that cover the mine site (Figure 2.9). The first major fault set is the South Çöpler Fault Zone and series of sub-parallel faults. The most recent seismic activities have divided the north and south of the mine into two principal structural domains. The second set is the North Çöpler Fault and study done by Terrane Geoscience Inc. shows that this fault zone is steeply-dipping, E-W trending and bisects the Manganese pit. The third one is the Northern Boundary Fault Zone which shows similar geometry with the South Çöpler Fault, but it has been offset in many places by NE-SW trending sinistral strike-slip faults. The last one is Marble Fault Zone which has offset the mineralization between the Marble and Manganese pits.
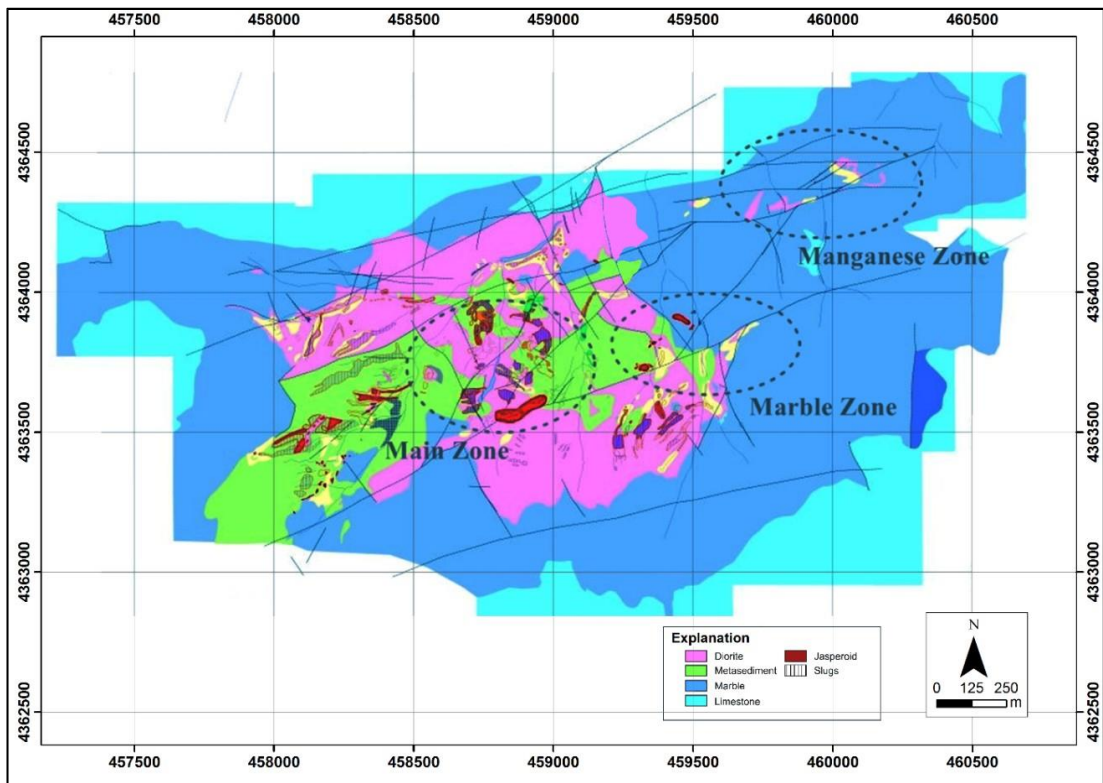
Figure 2.8. Geological map of the mine site
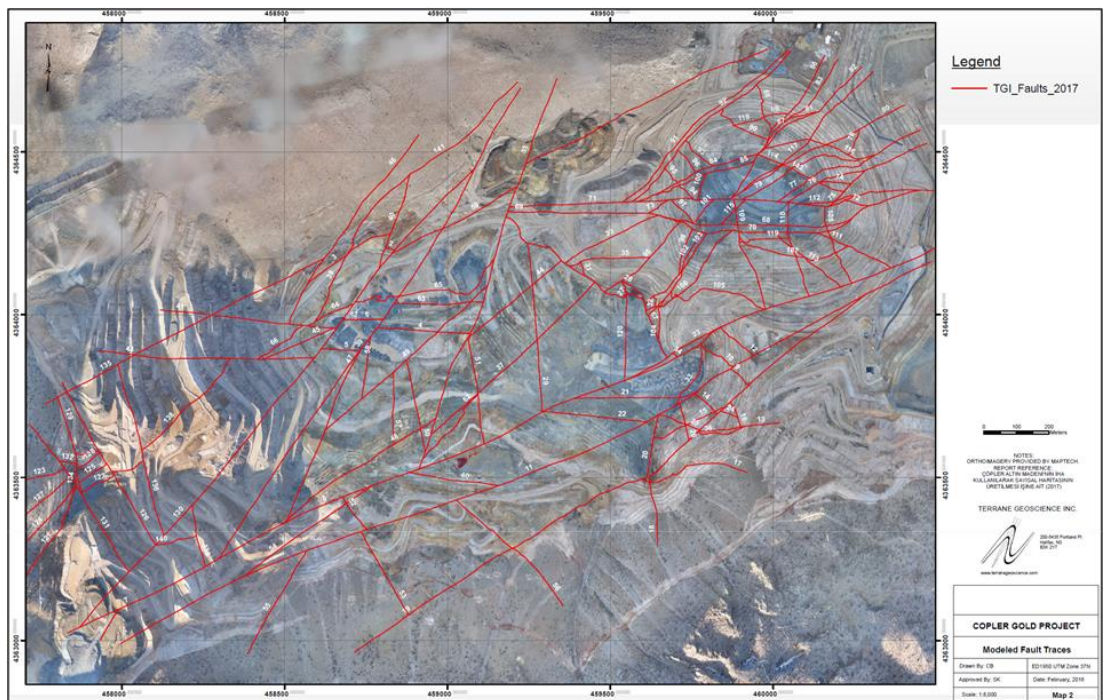
Figure 2.9. Fault map of the mine site by Terrane (2018)

2.4. Mining Operation and Current Site Conditions

The mine site is mainly divided into three main pits which are known as the Manganese pit, the Marble pit and the Main pit (Figure 2.8). The Marble pit also divided into two pits; the northern and southern pits. Mining operations change the site conditions very frequently, ore extraction has always been prior target so creating and maintaining observation network was very difficult. This is also true for temporary canal construction. The canals are placed along certain locations and they are not lined, causing the seepage of water into underground. The water collected in these canals has affected the pore water pressure at and around these locations (Figure 2.10).

Figure 2.10. Earth canals where surface and subsurface waters are collected and ponded (from Ekmekçi et al., 2018)

CHAPTER 3

HYDROLOGY

3.1. Regional Scale Precipitation and Temperature

The meteorological data was obtained from two stations for this study; Divriği Meteorological Station and WS05 (installed by Anagold A.Ş. at the mine site). In most previous studies, the Divriği station was used for sub-basin scale hydrological analysis. However, in this study, WS05 station is preferred because it is more representative of the site conditions.

The correlation analysis has been conducted between two stations by Ekmekçi et al. (2018). The results showed that the mine site receives more precipitation than the Divriği region. However, temperature data is more compatible between stations. In general, these two stations correlate well with each other. The histograms which show the long term average precipitation and the long term average temperature recorded by Divriği and WS05 stations for the common period of 2004-2016 are given in Figure 3.1 and Figure 3.2, respectively.
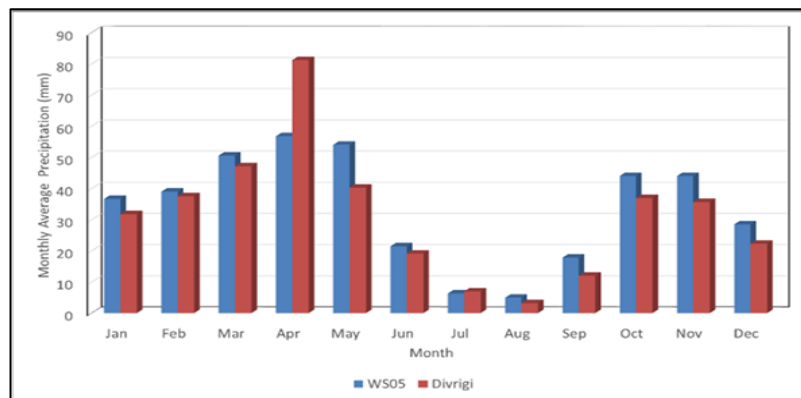
Figure 3.1. Long term averages of precipitation at Divriği and WS05 meteorological (from Ekmekçi et al., 2018)

17
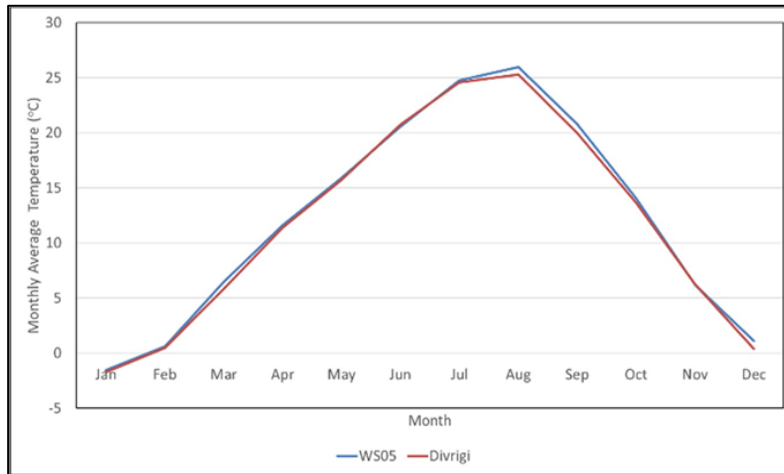
Figure 3.2. Long term averages of air temperature at Divriği and WS05 meteorological (from Ekmekçi et al., 2018)

3.2. Mine Site Water Balance

3.2.1. Precipitation

As the main input of water, the precipitation data was used in water balance calculations for the study site. The monthly average precipitation recorded at WS05 station for the period between 2004-2019 is summarized in Table 3.1. The data given in the table was calculated from daily records. The annual averages show that precipitation varies between 310 mm (in 2004) and 456 mm (in 2005) and a long term average precipitation is calculated as 400 mm. The histogram which shows the monthly variation of precipitation is given in Figure 3.3. An important detail is that the variability of monthly precipitation is high in summer seasons and while in winter seasons the monthly variability is low.

3.2.2. Evapotranspiration

Evapotranspiration is one of the important components of water balance and is commonly calculated using Thornthwaite model (McCabe and Markstrom,2007) based on monthly average air temperature and precipitation. The monthly mean air temperature data is given in Table 3.2. The potential evapotranspiration (PET) and the actual evapotranspiration (AET) was calculated using Thornthwaite-Mather equation for the study site (Figure 3.4). In the Figure 3.4, PET and AET values coincide during winter and spring months when the precipitation exceeds the potential

18

evapotranspiration. The annual potential evapotranspiration is calculated as 743 mm and the annual actual evapotranspiration which depends on the available water is calculated as 354 mm for the period of 2004-2019.

Table 3.1. Monthly average precipitation recorded at WS05 for the period between 2004- 2019

Average Precipitation (mm)													
Years	Jan	Feb	Mar	Apr	May	Jun	Jul	Aug	Sep	Oct	Nov	Dec	Total
2004	74.3	25.7	22.3	57.1	59.7	21.8	4.7	6.2	0	5	25.5	8.3	310.6
2005	41	55.8	60	64.8	51.2	16.1	1.7	8	11.8	61	54.4	30.4	456.2
2006	15	43	87.6	80.2	34.2	9.5	14	1	17.8	104.3	13	0.4	420
2007	14	32.3	61.7	60.6	35.7	16.2	0.4	17.2	0	35	74	70	417.1
2008	8.3	32	70	40.9	46.2	19.3	0	8.2	36.2	53.4	88	21.7	424.2
2009	28.1	42.3	27.2	51.9	29.9	17.4	16.8	0	28	29	70.5	40.2	381.3
2010	47.6	32.2	27.7	68	24.6	18.8	1.2	0	8	95.5	0	37.5	361.1
2011	24.4	53.2	47.8	89.2	71.6	50.6	22.4	3	7.4	3.6	28.8	7.6	409.6
2012	37.8	39.2	19.4	38.4	47.2	15.9	6.4	0.6	5	34.4	84.8	108.9	438
2013	31.9	48.5	56.8	57.4	51.2	10	7.8	0.4	36.4	27.6	32.6	11.5	372.1
2014	21.4	39	56.1	25.2	82.4	16.1	5.3	3.4	49.8	70.2	43.6	18.8	431.3
2015	94.6	30.8	87.5	65	54	14.4	0	1.2	12	70.4	18	4.8	452.7
2016	61.4	68.8	52.8	34.8	63.8	45	7.6	19	35.8	8.8	27.2	16.4	441.4
2017	13.4	2.8	31.2	61.2	104.4	29.4	0	1	1	18	55.6	22.4	340.4
2018	67.6	12	59.6	4.4	76.6	24.1	1.4	8.6	9.6	31.2	25.8	75.2	396.1
2019	25.4	15.8	24.6	75.2	36.8	-	-	-	-	-	-	-	177.8
Min	8.3	2.8	19.4	4.4	24.6	9.5	0	0	0	3.6	0	0.4	73.0
Max	94.6	68.8	87.6	89.2	104.4	50.6	22.4	19	49.8	104.3	88	108.9	887.6
Mean	37.9	35.8	49.5	54.6	54.3	21.6	6.0	5.2	17.3	43.2	42.8	31.6	399.8
Sx	25.0	16.9	22.2	21.6	21.4	11.8	6.9	6.1	15.9	31.6	27.1	30.8	237.2
CV(%)	66.0	47.2	44.7	39.5	39.4	54.4	114.8	117.7	92.3	73.1	63.4	97.3	8.5
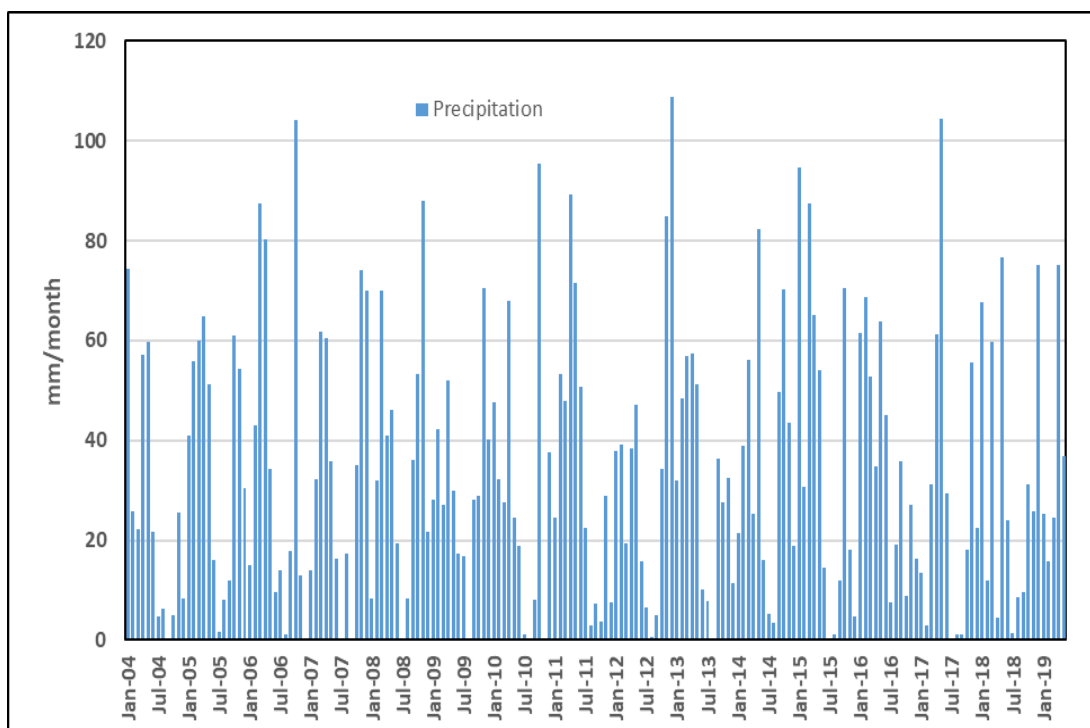
Figure 3.3. The histogram of monthly average precipitation recorded at WS05 for the period between 2004-2019

Table 3.2. Monthly average air temperature recorded at WS05 for the period between 2004- 2019

Years	Jan	Feb	Mar	Apr	May	Jun	Jul	Aug	Sep	Oct	Nov	Dec	
Average Temperature (°C)													
2004	-2.2	3.1	5.5	11.4	15.2	20	23.3	24	20.1	15	8.3	-2.4	
2005	-2.2	3.1	5.5	11.4	15.2	18.9	25.9	25.6	19.2	9.7	4.5	0.7	
2006	-4.6	-0.2	6.2	11.2	12	19	25	25.7	20.3	12.7	4.2	-1.3	
2007	-2.5	-0.6	5	6.9	18.7	21	24.5	25.9	21.6	15.7	1.8	-0.8	
2008	-8.4	-7.9	7.6	13.3	13.7	19.3	24	24.7	19.2	14.5	3.5	2	
2009	-3.4	-1	5.6	9.3	15	21.2	22.1	26	16	16.2	6.2	4.7	
2010	2.3	6.1	9	11.7	17	22.8	27	27.6	23.6	13.8	9	6.1	
2011	1.3	0.3	6.4	11.3	14.3	19.7	25.5	24.9	21	13.6	2.2	1.2	
2012	-2	-8.1	1.6	13.8	17.6	21.8	22	24.6	21.9	15.1	9	2.1	
2013	-1.9	3.5	7.2	13.1	17.5	21.5	23.4	24.2	18.7	12.1	8.7	-2.5	
2014	2.5	3.8	8.1	12.4	17	20.9	26.3	27.3	20.3	13.5	5.3	5.3	
2015	0.5	4.2	6.7	10.6	17.4	21	25.5	26.6	24.5	14.6	7.8	0.3	
2016	-2.2	2.9	7.4	14	15.4	17.3	25	27.7	19.3	15	6.3	-2.4	
2017	-1.5	0.3	7.6	11.9	16.1	21.9	27	28.2	24.6	14.1	6.9	3.4	
2018	3.25	6.02	10.63	15.23	17.83	22.32	26.9	26.34	22.43	16.05	8.27	3.81	
2019	0.45	4.22	7.06	10.44	18.96	-	-	-	-	-	-	-	
													Average
Min	-8.4	-8.1	1.6	6.9	12.0	17.3	22.0	24.0	16.0	9.7	1.8	-2.5	7.7
Max	3.3	6.1	10.6	15.2	19.0	22.8	27.0	28.2	24.6	16.2	9.0	6.1	15.7
Mean	-1.3	1.2	6.7	11.7	16.2	20.6	24.9	26.0	20.8	14.1	6.1	1.3	12.4
Sx	3.0	4.2	2.0	2.0	1.9	1.5	1.7	1.3	2.3	1.7	2.4	2.9	2.2
CV (%)	-230.1	342.9	29.5	16.9	11.8	7.3	6.7	5.1	11.2	12.0	39.9	214.3	39.0

20
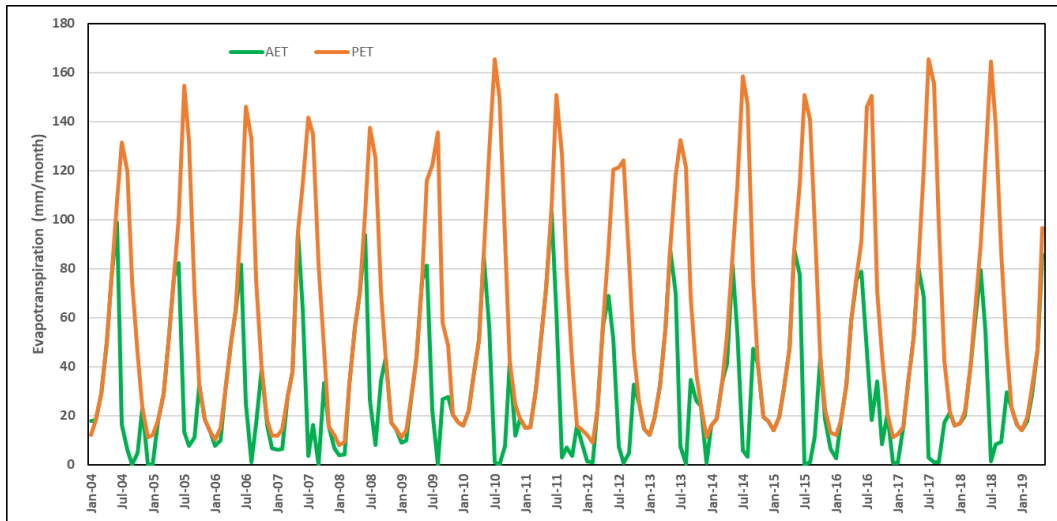
Figure 3.4. Monthly average potential (PET) and actual (AET) evapotranspiration calculated using the data recorded at WS05 for the period between 2004-2019

3.2.3. Runoff

The surface runoff was calculated from the Thornthwaite-Mather water balance approach, taking into account the direct and indirect runoff. The snow pack and the snow melt fractions were also considered for months when the air temperature is below 0 °C. Considering the topography and geology of study site, runoff coefficient is chosen as 0.5. The annual total runoff was calculated as 56.1 mm for the years between 2004 and 2019. The monthly average total runoff for the period of 2004-2019 is shown in Figure 3.5.
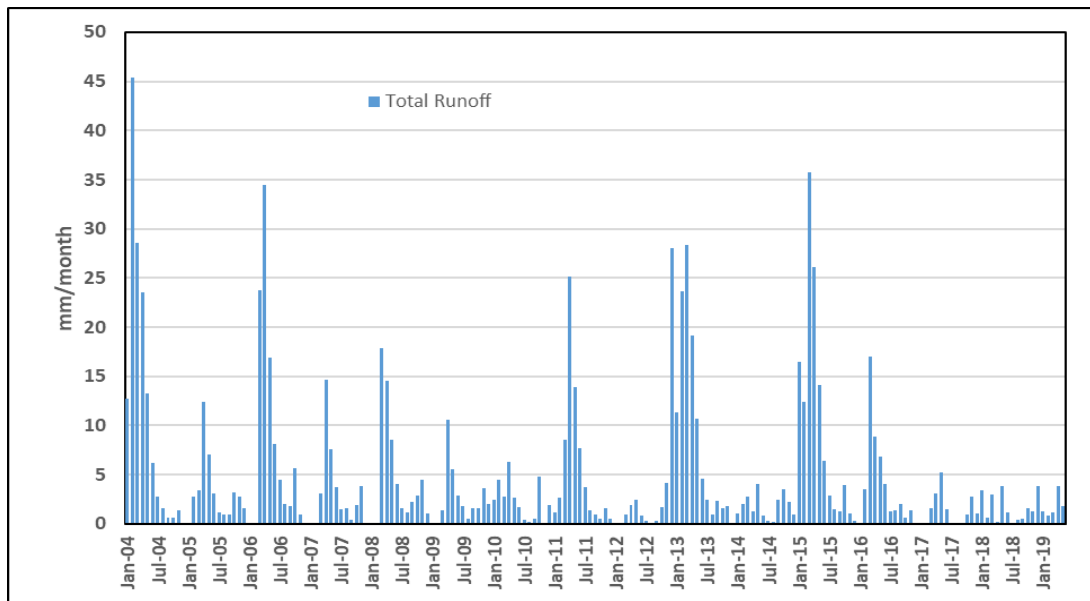
Figure 3.5. Monthly average total runoff, calculated using the data recorded at WS05 for the period between 2004-2019

3.2.4. Surplus Water and Infiltration

The surplus water was calculated using the Thornthwaite-Mather equation with an assumption of a soil storage capacity of 100 mm. The average annual surplus water was calculated as 36.3 mm for the study site. Figure 3.6 shows the monthly total surplus water for the period between 2004-2019. It should be noted that the surplus water occurred just in wet years' like 2004, 2006, 2013 and 2015. In dry years like 2012, 2014, 2017 and 2018 surplus water has not occurred.

3.2.5. Hydrologic Budget of Çöpler Stream Basin

As mentioned in Chapter 2, Çöpler stream watershed is about 10 km^2 and it has been completely altered by mining activities. Use and diversion of waters in the mine site does not allow a systematic monitoring of the elements of water cycle; therefore, calculation of water balance is difficult to achieve. Under natural pristine conditions and assuming that the surplus water infiltrates and recharge the groundwater system, the whole basin groundwater potential was calculated as 0.36×10^6 m^3/year. For the mine site it was found to be around 0.135×10^6 m^3/year. The water budget components (Figure 3.7) which was evaluated using Thornthwaite Water Balance Model by McCabe and Markstrom (2007) is summarized in Table 3.3.

22
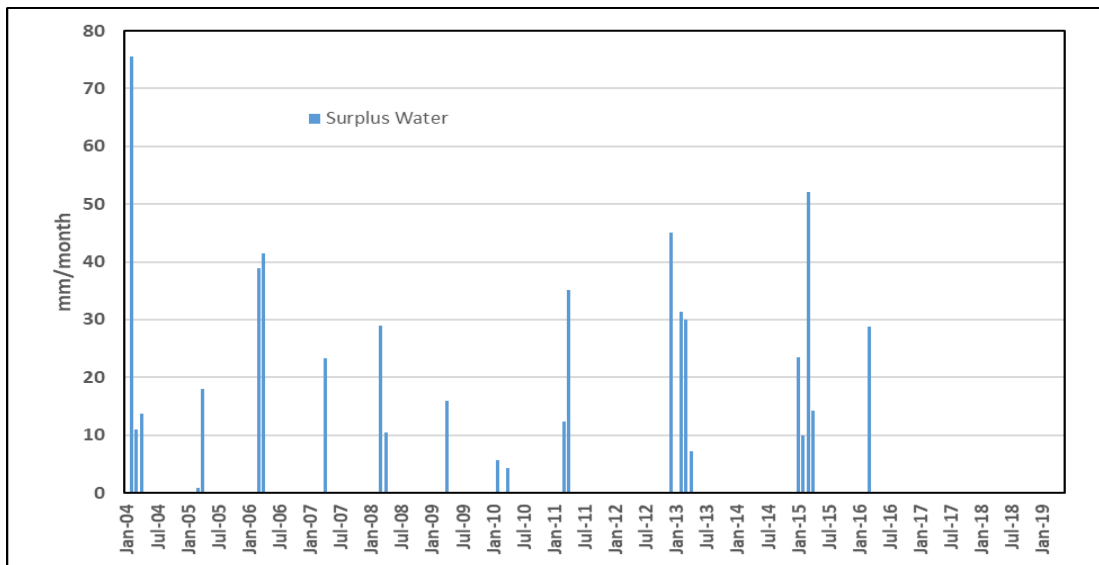
Figure 3.6. Monthly total surplus water, calculated using the data recorded at WS05 for the period between 2004-2019
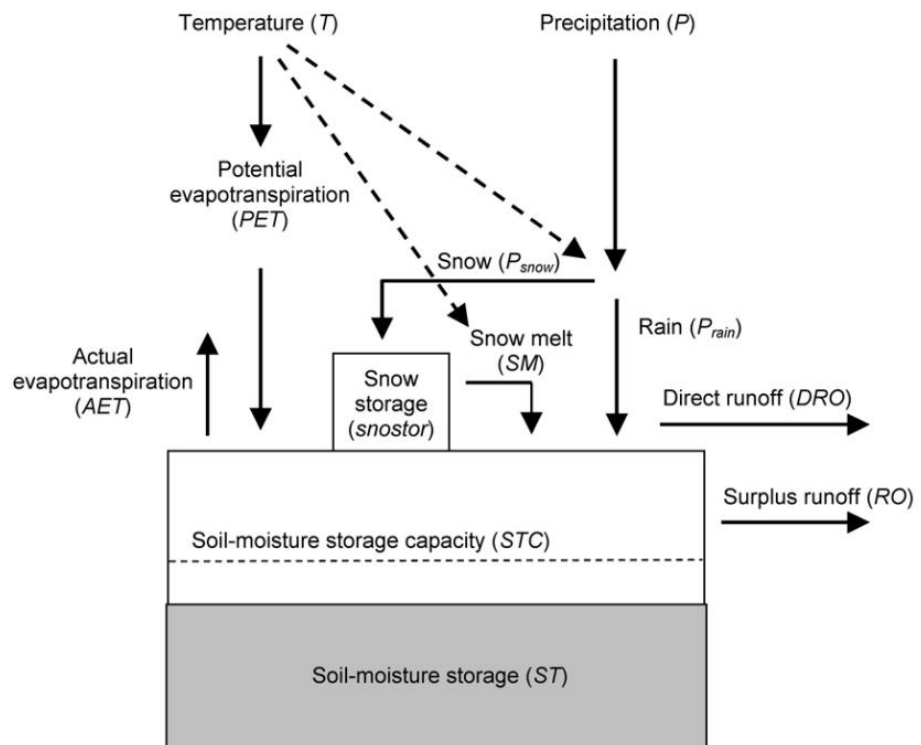
Figure 3.7. Diagram of Thornthwaite water balance model (McCabe and Markstrom, 2007)

Table 3.3. Long term averages of monthly water balance for Çöpler site

Month	PET (mm)	P (mm)	P-PET	Soil Moisture Storage	AET (mm)	PET-AET	Snow Storage (mm)	Surples Water (mm)	Total Runoff (mm)	Stream Flow (L/s)
Jan	12.9	37.9	4.2	56.5	9.5	3.3	26.6	1.5	3.1	8.8
Feb	16.6	35.8	14.3	65.2	14.5	2.1	30.4	7.7	6.2	24.2
Mar	31.3	49.5	30.9	83.7	31.1	0.2	15.2	12.7	11.3	54.2
Apr	51.3	54.6	8.7	82.0	50.2	1.1	7.1	11.5	12.9	61.5
May	81.7	54.3	-25.8	59.2	78.8	2.9	2.8	0.0	7.8	38.7
Jun	111.9	21.6	-88.8	9.8	74.2	37.7	0.5	0.0	3.8	17.2
Jul	145.9	6.0	-139.8	0.0	16.0	129.9	0.0	0.0	1.7	7.5
Aug	135.6	5.2	-130.6	0.0	4.9	130.6	0.0	0.0	0.9	4.1
Sep	78.8	17.3	-62.4	0.0	16.4	62.4	0.0	0.0	1.2	8.1
Oct	42.8	43.2	-1.8	12.7	28.3	14.5	0.0	0.0	2.3	19.6
Nov	20.5	42.8	20.1	34.1	19.3	1.3	0.0	0.0	2.2	16.4
Dec	14.2	31.6	9.1	43.8	10.5	3.7	7.1	3.0	2.8	1.0
Annual	743.4	399.8			353.7			36.3	56.1	21.8

CHAPTER 4

HYDROGEOLOGICAL CHARACTERIZATION

4.1. Characterization of Site Hydrogeology

4.1.1. Drill Holes and Wells

The hydrogeological characteristics of the lithological units in the field were obtained from drill holes and wells. A total of 11 small diameter (PQ) drill holes and a total of 10 large diameter wells were drilled to characterize the critical cross-sections (Figure 1.2). The small diameter wells have been cored to specify the geotechnical properties of lithological units by Golder Associates. Information about small diameter wells are summarized in Table 4.1. During the drilling process, at every 2 m, packer tests were applied to obtain permeability profile on the critical cross-sections. Details of the packer tests and the results obtained are reported in Chapter 4.2. After the packer tests completed, vibrating wire piezometers (VWP) were installed by ArtGeo, the supplier of the piezometers. The piezometers were installed in fully grouted borehole. The VWPs were all calibrated before installation. The VWPs were installed in boreholes at different levels to measure the pore water pressure at those zones. A total of 33 VWPs have been installed, 2 in shallow wells, 3 in intermediate wells and 4 in some deep wells. Details about the vibrating wire piezometers are shown in Table 4.2.

Besides the small diameter drill holes, 7 large diameter wells were drilled into the carbonate rocks and 3 large diameter wells into metasediments and diorite to characterize the groundwater conditions (Figure 1.2). The main purpose of the drilling large diameter wells was to determine the hydraulic head values at the both ends of the four critical cross-sections and to define the boundary conditions.

Table 4.1. Summary of revision of small diameter wells (Piezometers) (from Ekmekçi et al., 2018)

Section	Borehole_ID	X	Y	Z	Planned Depth(m)	Actual Depth (m)	Status
A	Pa1	459072.2	4364328	1177	167.00	168.00	Completed
A	Pa2	458989.6	4363997	1186	206.00	207.00	Completed
A	Pa3	458870.9	4363520	1275	135.00	136.00	Completed
A	Pa4	458793.8	4363211	1378	298.00	299.00	Completed
B	Pb1	458965	4364352	1204	124.00	125.00	Completed
B	Pb2	459055.7	4364061	1181	171.00	-	Cancelled
B	Pb3	459093.1	4363941	1205	255.00	256.00	Completed
B	Pb4	459166.5	4363734	1231	121.00	122.00	Completed
B	Pb5	459401.7	4363399	1309	134.00	136.30	Completed
C	Pc1	459154.4	4364266	1164	174.00	175.00	Completed
C	Pc2	459472	4363883	1146	76.00	-	Cancelled
E	Pe1	458693.8	4363966	1181	111.00	112.00	Completed
F	Pf3	459113.8	4364011	1195	-	206.00	Completed
				Total:	1972.00	1942.30	

Table 4.2. Details of piezometer boreholes (from Ekmekçi et al., 2018)

Borehole Code	Borehole Type	Coordinates (UTM - ED50 37N)		Ground Elevation	BH Bottom Elevation	BH Depth	VW Depths (m)	VW Lithology
		X	Y	Z	(m - asl)	(m)		
Pa1	Piezometer	459061.8	4364340.8	1177.3	1009.3	168	82 147	DIO MET
Pa2	Piezometer	459001.2	4363961.2	1191.1	984.1	207	31 75.5 160.5 181	MET MET MET MET
Pa3	Piezometer	458874.8	4363526.0	1275.3	1139.3	136	27 49 95 121	MET DIO CLY MET
Pa4	Piezometer	458816.0	4363210.9	1370.9	1071.9	299	33.3 109.3 249	DIO DIO MET
Pb1	Piezometer	459001.9	4364188.5	1170.2	1045.2	125	35.5 104	DIO DIO
Pb3	Piezometer	459093.0	4363949.4	1205.2	949.2	256	16 85 159 245	MET MET MET MET
Pb4	Piezometer	459173.3	4363742.2	1230.2	1108.2	122	19.3 56.3 101.3	MET MET MET
Pb5	Piezometer	459276.9	4363424.4	1295.5	1160.5	135	31.3 69.5 113.5	DIO DIO DIO
Pc1	Piezometer	459127.4	4364260.7	1166.8	991.8	175	9.5 30 96.3 158.2	MET DIO MET DIO
Pe1	Piezometer	458693.4	4363965.8	1182.5	1070.5	112	31 90.5	MET MET
Pf3	Piezometer	459111.4	4364014.8	1195.8	989.8	206	45.2 182.2	MET MET
MET: Metasediment			DIO: Diorite			CLY: Claystone		

Initially 8 large diameter wells were planned to be drilled at the both end of each cross-section to determine the boundary conditions. However, only 7 large diameter wells were drilled in carbonate rocks because the first large diameter well (Dwa-1) drilled at the northern part of the mine site showed that the carbonate rock in this section is dry and the groundwater level in the well represents the groundwater system in the metasediments and/or diorite. As a result, the wells planned to be drilled at the northern side of the mine were cancelled.

The detailed information about the wells such as coordinates, elevation, borehole bottom elevation, borehole depth and screen intervals are shown in Table 4.3. The wells have been screened close to the bottom while the upper sections were constructed with casing and sealed with cement following gravel packing. The upper sections were sealed to prevent entrance of surface water into the wells for more accurate groundwater level reading. An example large diameter well log is given in Figure 4.1. Other large diameter well logs can be found in Ekmekçi et al. (2018).

Table 4.3. Summary information about drilled large diameter wells (from Ekmekçi et al., 2018)

Borehole Code	Borehole Type	Coordinates (UTM - ED50 37N)		Ground Elevation	BH Bottom Elevation	BH Depth	Screen Interval (m)
		X	Y	Z	(m - asl)	(m)	
DWa1	Large Diameter Well	459099.9	4364475.4	1196.3	1004.3	192	96-184
DWa2	Large Diameter Well	458858.6	4363136.5	1412.8	1196.8	216	104-208
DWa3	Large Diameter Well	459065.6	4363143.1	1388.6	1196.6	192	56-184
DWb2	Large Diameter Well	459479.6	4363276.9	1312.7	1056.7	256	112-248
DWc2	Large Diameter Well	459778.5	4363467.5	1325.5	1036.5	289	96-280
DWe1	Large Diameter Well	457798.0	4363578.7	1433.5	1042.5	389	128-384
DWf1	Large Diameter Well	460233.6	4364538.0	1143.6	845.6	298	88-296
GSW1	Groundwater Sampling Well	459112.8	4363984.5	1197.0	1117.0	80	24-56
GSW2	Groundwater Sampling Well	459104.7	4364000.4	1196.8	988.8	208	136-200
GSW3	Groundwater Sampling Well	459121.9	4363998.6	1196.7	932.7	264	216-256

In the south part of the mine site, four large diameter wells were drilled to characterize the carbonate rock. The penetrated lithology was described as marble (carbonate rock) up to the certain depths. However, after certain depths, cuttings could not be obtained

due to loss of drilling mud. The rest of the lithologies were reported as "unknown" at Dwa-2, Dwb-2 and Dwc-2 wells. Only at Dwa-3, the boundary between marble and metasediments and/or diorite was determined. The groundwater level measurements in these wells show that ground water level is much lower than the expected bottom of the carbonate rock. Consequently, it can be concluded that the carbonate rock at the south part of the mine site is also dry and groundwater levels measured represents the groundwater level of metasediments and/or diorite.

Dwe-1 well, located in the southwestern part of the mine site, was drilled to a depth of 392 m from the surface. Up to 240 m depth from surface, lithology described as Marble, but after 240 m, due to complete loss of drilling mud, no cuttings have been obtained. The static groundwater level was measured at a depth of about 362 m. The boundary between carbonate rock and metasediments or diorite was not clear. However, reasonable assumption is that the groundwater level represents the hydraulic head in the metasediments or/and the diorite.

On the northeastern side of the mine site, Dwf-1 well was drilled up to the depth of 304 m. Up to 110 m, the lithology was described as marble (carbonate rock). However, between 110-304 m, lithology was reported as "unknown" due to the complete loss of drilling mud. The static groundwater level was measured about 261 m and also response of the well after pumping shows that groundwater level represents the metasediments or/and the diorite which means the carbonate rock in this part of the mine site is also dry.

The Groundwater Sampling Wells were drilled into the almost center of the mine and depth of these wells was decided by examining the packer test results of nearest piezometer Pf3. These wells aimed at tapping three different permeable zones in the metasediments. Also, water samples were analyzed from the sealed zones to determine the origin of groundwater in different depths. The hydrochemical information about these wells are given in the Chapter 5.

	Project Name:	**Optimization of Groundwater Control for Slope Stability at Çöpler Mine Site**	Well Name
HMT Hacettepe Mineral Technologies	Contracted by:	**Anagold Madencilik Tic. ve San. A.Ş.**	**Dwa-1**

Province/District:	Erzincan/İliç		**Well Depth (m):**	192
Well Location:	Northern Region of the Main Pit		**Drill Diameter:**	17.5 inch
Coordinates:	East (m):	459099.925	**Casing:**	Steel, 273 mm
	North (m):	4364475.415	**Screen Interval:** 96-112 m, 120-136 m, 144-160 m, 168-184 m	
Elevation (m):	1196.255			
Slope/Angle:	90°		**Gravel Filter:**	81-192 m, 7-15 mm gravel
Starting Date:	19.07.2017		**Sand Buffer/Bentonite Seal:**	80-81 m / 78-80 m
Ending Date:	10.09.2017		**Concrete:**	0-78 m
Type of Drilling:	Rotary		**Formation/Aquifer:**	Munzur Limestone (Metamorphic)
Drilling Fluid:	Mud		**Average Static Water Level:**	180.19 m
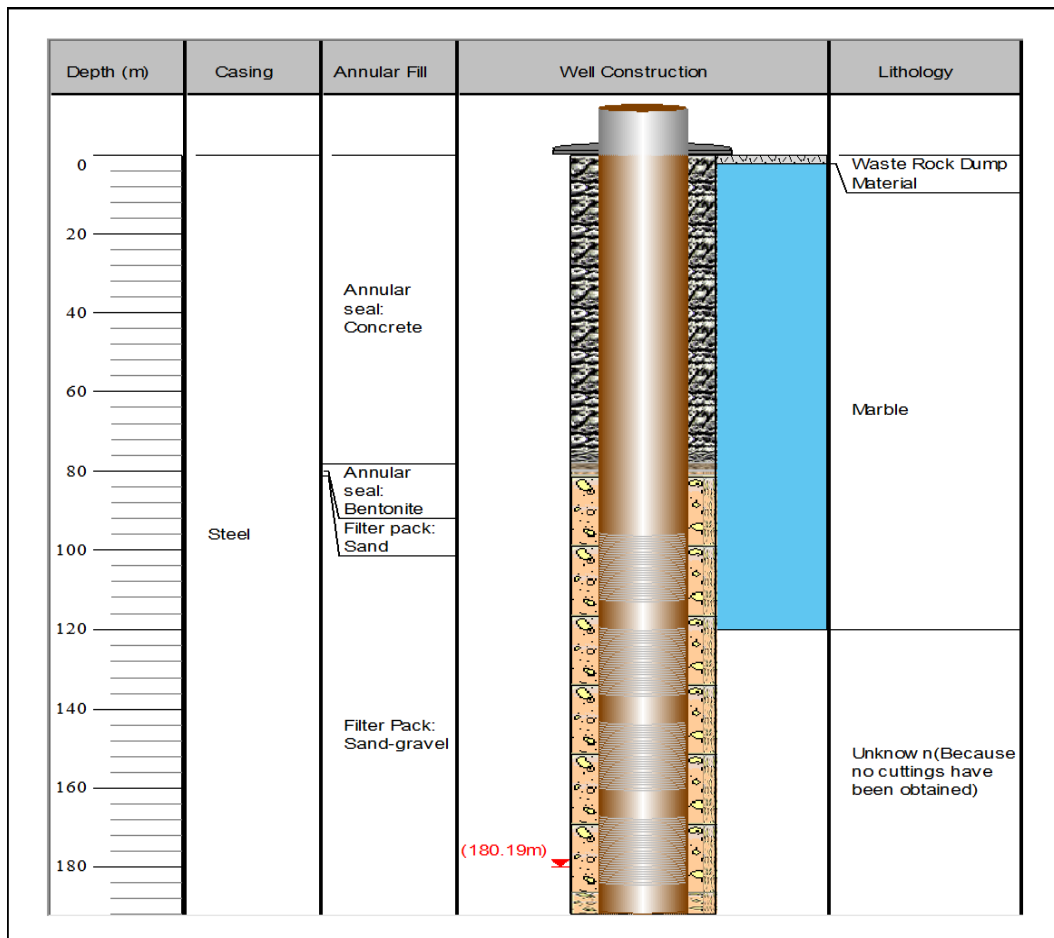
Figure 4.1. Large diameter well log (from Ekmekçi et al., 2018)

4.1.2. Fracture/Karstic Zones

To obtain the fracture and/or karst data, coring in the carbonate rocks is required. However, due to complete loss of drilling mud in almost all large diameter wells, the fracture and/or karst data could not be obtained except zones where the loss of drilling mud was occurred which indicates a well-developed karst at those zones.

In Dwa-1 (the northern part of the mine), complete loss of drilling mud was reported at section 39 meters below ground level (mbgl) to 192 mbgl. The southern part of the mine site shows different character from the northern part. In Dwa-2 well, almost no loss of mud was observed up to 198 mbgl. The complete loss of drilling mud reported in the driller log has been noted as 198 mbgl to 216 mbgl. In Dwa-3 well, there is no loss of drilling mud reported but the thickness of carbonate rock is much less than expected. The expected contact between carbonate rock and diorite is 385 mbgl. However, the drilling process has shown that the thickness of carbonate rock is 125 mbgl which means the diorite unit beneath the carbonate rock intruded irregularly. In Dwb-2 well, the complete loss of drilling mud has been reported at 64 mbgl to 256 mbgl. Another well drilled in southern part of the mine site, Dwc-2, loss of drilling mud has been reported at 83 mbgl to 289 mbgl. The complete loss of drilling mud has been reported at southwestern edge (Dwe-1) and northeastern edge (Dwf-1) of the mine site as well. In Dwe-1, the loss of drilling mud was started at 241 mbgl and in Dwf-1, the loss of drilling was mud started at 109 mbgl.

The information obtained from the depths where loss of drilling mud occurred, karstification levels can be interpreted. In the southern part, estimated karstic zone elevation is around 1250 masl (Dwa-2, Dwb-2, Dwc-2), while it is around 1200 masl in the western part of the mine (Dwe-1). In the eastern part, elevation of the karst estimated as 1050 masl (Dwf-1). Due to the irregular intrusion of diorite beneath carbonate rocks at the southern edge of the mine, estimated karst zone is not deep as the other areas. However, it is not clear that those zones indicate a productive karst aquifers or not.

4.1.3. Fractures on Cores

The geotechnical logging was conducted by Golder in 11 small diameter drill holes to characterize the metasediments and diorite units exposed in the mine site and its near vicinity. In the logs, detailed lithological description of metasediments and diorite is given with other information such as RQD, grain size, porosity and hydraulic conductivity values. The lithology is classified as faults, brecciated, foliated, sheared etc. The grain size ranged from very fine/aphanitic to very coarse. The RQD and the hydraulic conductivity values were plotted side by side to observe any relation between hydraulic conductivity and RQD. It is clear that the higher RQD values matched with lower hydraulic conductivity values. The porosity is classified from highly porous to none. An example geotechnical/hydrogeological log of VWPs well is shown in Figure 4.2. Other logs of the VWPs wells can be found in Ekmekçi et al. (2018).

Fractures defined by Golder in the geotechnical logs were used to calculate fracture frequency. Calculated fracture frequency was plotted as depth wise graphs for each piezometer well. An example depth wise fracture frequency graph is shown in Figure 4.3. The fracture frequency profiles of all piezometer wells are given in Appendix A. As can be seen in the figures, almost all fracture frequency profiles show significant decreases with depth.

The metasediments-diorite unit characterized by an average fracture frequency which is 15.24 fractures per run length in meters. The fracture frequency reaches the maximum level in the Pb1 drill hole as 83 fractures per meter. Descriptive statistics of fracture frequency per run length of each piezometer well is summarized in Table 4.4. It is noteworthy that all piezometer wells show similar characteristics except the Pb3. The coefficient of variations of overall data evaluated as almost 100 % which means the lithological unit is far from being homogenous.
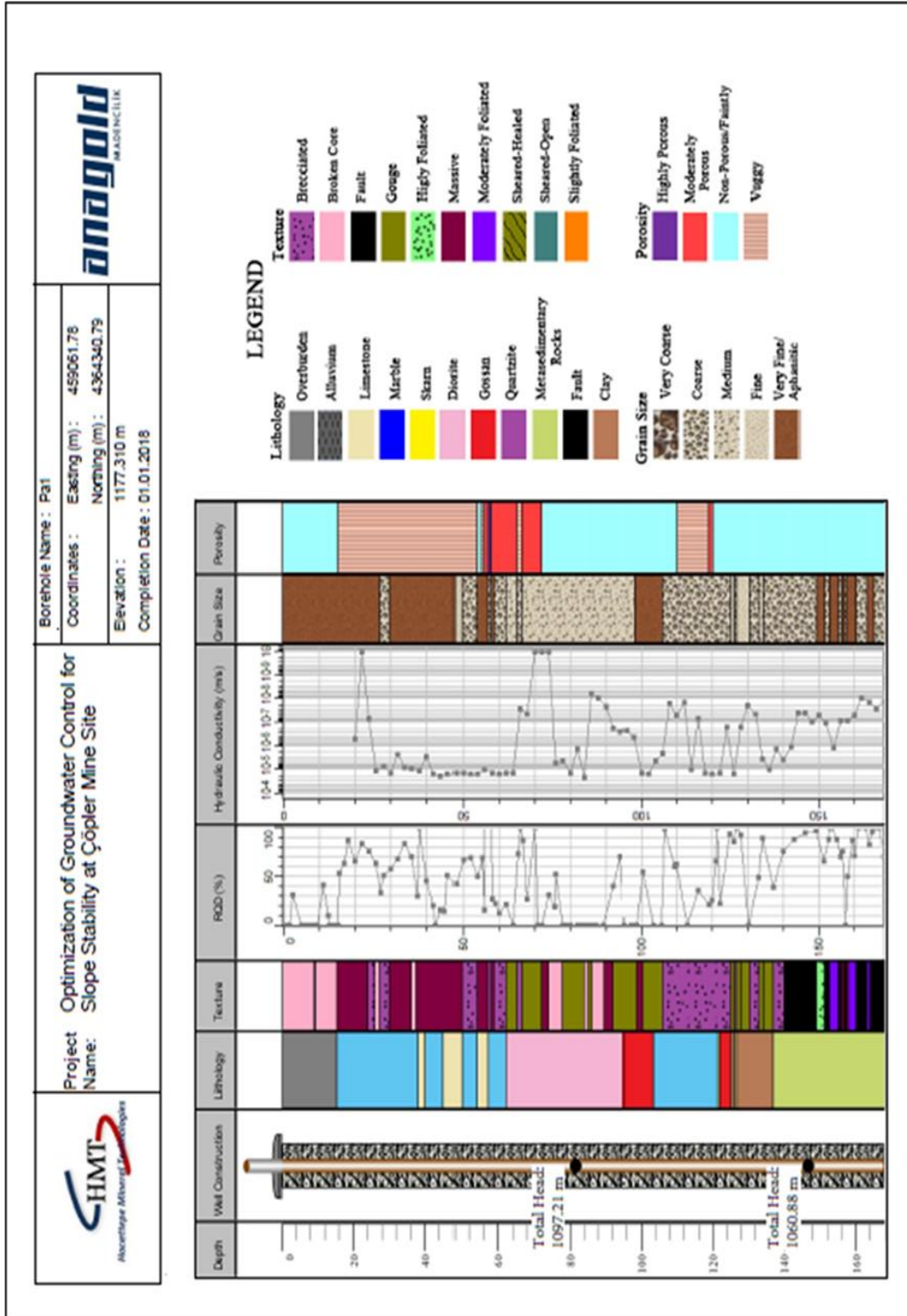
Figure 4.2. Geotechnical/hydrogeological log for well Pa1 (from Ekmekçi et al., 2018)
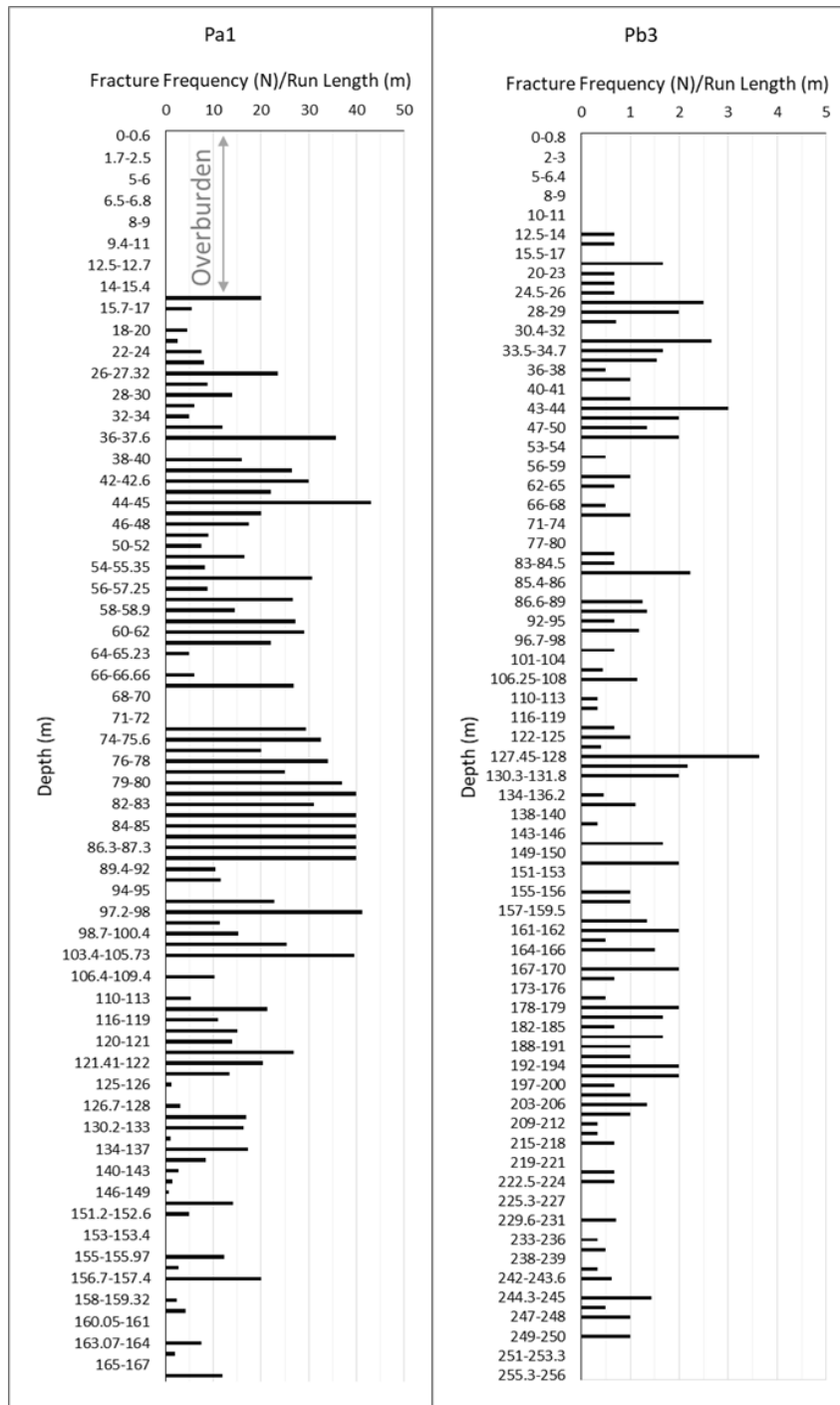
Figure 4.3. Fracture frequency profiles for two drill holes (from Ekmekçi et al., 2018)

Table 4.4. Descriptive statistics of fractures recorded in geotechnical logs (from Ekmekçi et al., 2018)

Descriptive Statistics of FF (N)/Run Length (m)					
Piezometer ID	Min	Max	Mean	Standard Dev.	Cv (%)
Pa1	0.0	43.0	14.7	13.0	88.4
Pa2	0.0	40.4	21.3	11.8	55.5
Pa3	0.0	40.0	26.3	16.0	60.8
Pa4	0.0	41.1	24.2	13.3	54.9
Pb1	0.0	83.0	21.0	15.5	73.7
Pb3	0.0	3.6	0.7	0.8	108.2
Pb4	0.0	64.0	10.6	14.1	132.2
Pb5	0.0	80.0	7.0	13.5	194.2
Pc1	0.0	79.0	3.4	8.7	255.3
Pe1	0.0	27.0	10.3	8.0	77.3
Pf3	0.0	43.3	17.1	15.3	89.8

Descriptive Statistics of FF (N)/Run Length (m)					
All Data	Min	Max	Mean	Standard Dev.	Cv (%)
	0	83.00	15.24	15.23	99.92

4.2. Packer Tests

Packer tests were conducted in 11 small diameter wells. The test range was set up to 2 m to obtain a high resolution characterization. The design and application of the test were completed according to Houlsby (1976). Five pressure stages were applied for at least 10 minutes at each test interval and water intake has been recorded every 5 minutes. If there was a significant difference in water intake records, the test was extended for another 5 minutes to ensure steady-state conditions. The permeability values were evaluated in Lugeon Units (Lu) for each one these five pressure stages using the formula:

$$L = \frac{10 \times Q}{P}$$

L= Lugeon value

Q= Water taken in test (liters/meters/minute)

P= Test pressure (bars)

10 as correction for standard test pressure of 10 bars

The Lugeon values were converted to hydraulic conductivity (m/s) values according to Houlsby (1990) and Roeper et al. (1992). A histogram of results has shown in depth-wise variation permeability in piezometer wells. The red mark was used for values which are greater than the 50 Lu. Example histograms are given in Figure 4.4. Other histograms are shown in Appendix B.

4.2.1. Basic Statistics of the Test Results

The packer test results showed that metasediments and the diorites have similar hydrogeological properties and can be accepted as a single hydrostratigraphic unit. The mean permeability is about 12 Lu, also the geometric and harmonic means were calculated as 0.96 Lu and 0.02 Lu, respectively. As a result, the medium is overall of very low permeability (Table 4.5). The coefficient of variation is 342 % which is a very high value, indicating a great heterogeneity. Hydraulic conductivity values also show the similar results with the Lu values. The arithmetic mean, geometric mean and harmonic mean values are; $1x10^{-6}$ m/s, $9.52x10^{-8}$ and $2.11x10^{-9}$, respectively. According to the results, the medium has low to very low permeability. The coefficient of variation values for all drill holes shows a heterogenic system overall. The packer-test result statistics of each piezometer well are listed in Table 4.6.

Table 4.5. Summary of basic statistics of permeability values of overall data (from Ekmekçi et al., 2018)

Descriptive Statistics of Lu Values							
All Data	Min	Max	Mean	Geomean	Harmonic Mean	Standard Dev.	Cv (%)
	0.001	521.64	11.55	0.96	0.02	39.58	342.64
Descriptive Statistics of K Values (m/s)							
All Data	Min	Max	Mean	Geomean	Harmonic Mean	Standard Dev.	Cv (%)
	1E-06	5.10E-05	1.01E-06	9.52E-08	2.11E-09	3.61E-06	358.98
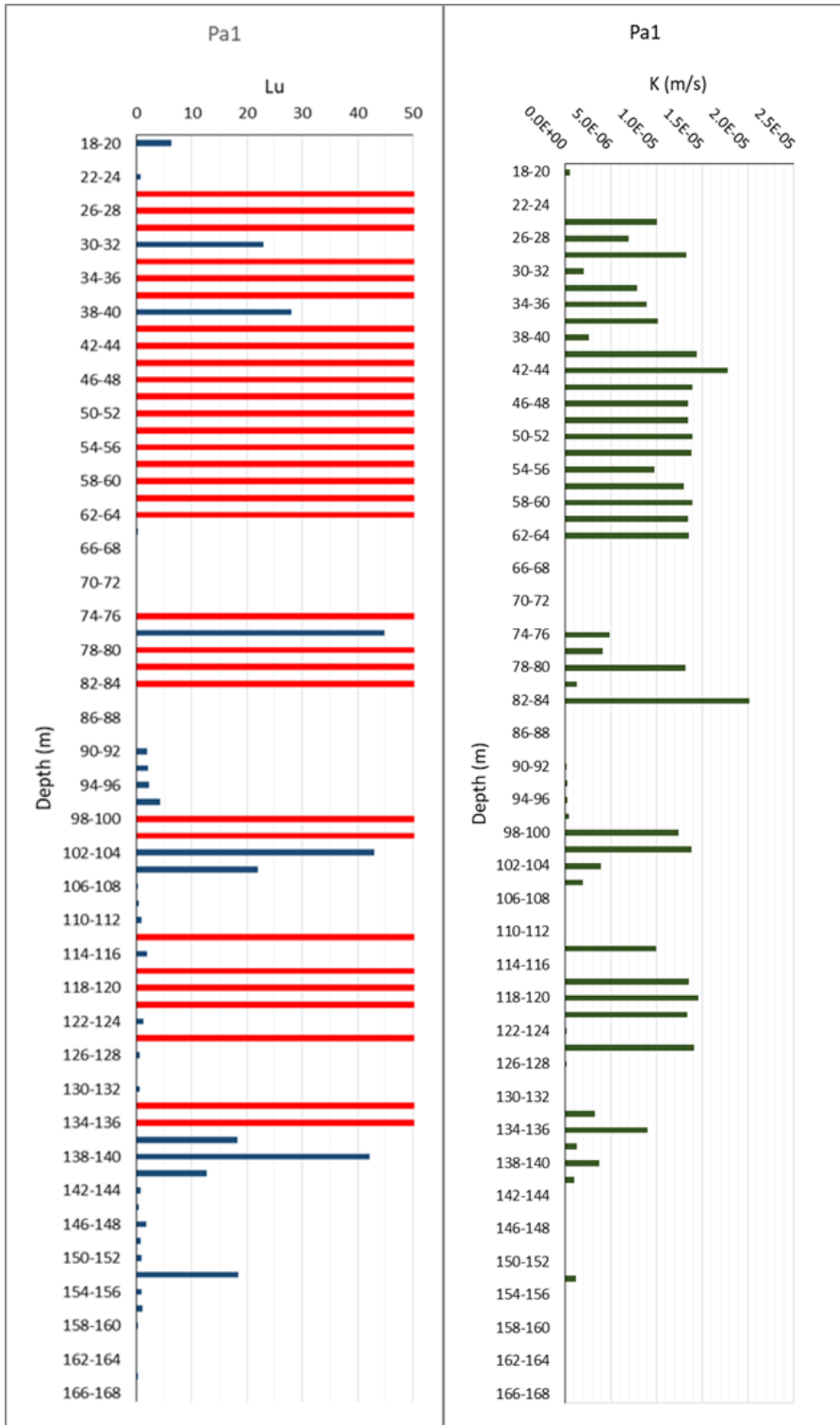
Figure 4.4. Depth- wise histograms of permeability (Lu) and hydraulic conductivity (m/s) of drill hole Pa1 (from Ekmekçi et al., 2018)

Table 4.6. Summary of basic statistics of permeability values obtained for each drill hole a) in Lu and b) in m/s units (from Ekmekçi et al., 2018)

Descriptive Statistics of Lu Values							
Piezometer ID	Min	Max	Mean	Geomean	Harmonic Mean	Standard Dev.	Cv (%)
Pa1	0.001	358.55	61.76	5.85	0.02	75.07	121.6
Pa2	0.001	160.43	10.89	1.14	0.03	34.19	314.1
Pa3	0.001	136.77	20.26	3.32	0.01	38.18	188.4
Pa4	0.001	76.46	6.97	0.91	0.02	14.13	202.7
Pb1	0.029	1.71	0.66	0.53	0.36	0.37	56.5
Pb3	0.001	3.71	0.71	0.32	0.04	0.79	111.0
Pb4	0.030	521.64	17.59	0.80	0.42	90.99	517.4
Pb5	0.427	3.15	1.41	1.33	1.26	0.51	36.1
Pc1	0.001	150.05	4.66	0.12	0.00	21.65	464.7
Pe1	0.001	52.96	2.22	0.62	0.01	7.17	322.8
Pf3	0.187	104.55	12.28	5.46	2.14	16.44	133.9

a

Descriptive Statistics of K Values (m/s)							
Piezometer ID	Min	Max	Mean	Geomean	Harmonic Mean	Standard Dev.	Cv (%)
Pa1	1.00E-10	2.02E-05	5.21E-06	5.08E-07	1.82E-09	6.18E-06	118.7
Pa2	1.00E-10	1.48E-05	1.07E-06	1.03E-07	3.25E-09	3.31E-06	310.3
Pa3	1.00E-10	1.21E-05	1.80E-06	2.92E-07	1.15E-09	3.24E-06	180.0
Pa4	1.00E-10	7.05E-06	6.28E-07	1.18E-07	1.55E-09	1.25E-06	199.2
Pb1	1.32E-08	1.44E-07	6.06E-08	5.18E-08	4.28E-08	3.22E-08	53.1
Pb3	1.00E-10	3.39E-07	6.54E-08	3.34E-08	4.77E-09	7.03E-08	107.5
Pb4	3.70E-09	5.10E-05	1.77E-06	7.33E-08	4.02E-08	9.14E-06	518.0
Pb5	3.82E-08	2.71E-07	1.28E-07	1.22E-07	1.15E-07	4.22E-08	33.0
Pc1	1.00E-10	1.37E-05	4.27E-07	1.38E-08	4.68E-10	1.96E-06	458.3
Pe1	1.00E-10	8.05E-06	2.89E-07	6.36E-08	1.35E-09	1.10E-06	378.7
Pf3	2.42E-08	9.64E-06	8.28E-07	3.93E-07	1.91E-07	1.34E-06	162.1

b

4.2.2. Permeability Distribution on Critical Cross-Sections

Packer test results were drawn on the critical cross-sections as hydraulic conductivities (m/s) for the hydrogeological characterization. The cross sections are given in Appendix C. Cross-section A is given as an example in Figure 4.5. Two large diameter wells drilled in the carbonate rocks at the both end of cross-section. On these wells, representative groundwater measurements were put as blue marks. At various depths, there are some permeable zones that can be observed. However, it is not clear that the permeable zones belong to the same extensive zone.
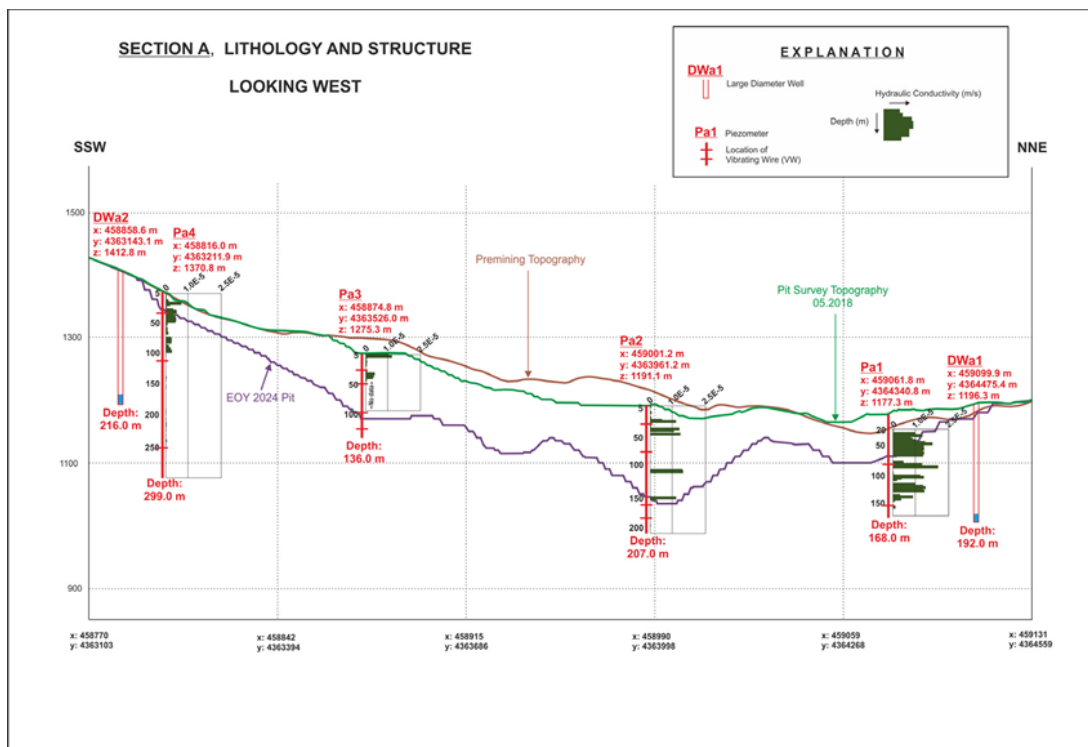
Figure 4.5. Permeability results plotted on drill holes for cross- section A (from Ekmekçi et al., 2018)

4.3. Pumping Tests

Pumping tests have been planned to obtain hydraulic properties (hydraulic conductivity and storage coefficient) of the carbonate rock aquifer and the metasediments-diorite units. Unfortunately, the carbonate rock was dry in most of the large diameter wells. Only hydraulic conductivity of metasediments and diorite could be obtained. Dwf-1, Dwb-2, Dwa-3, GSW-1, GSW-2 and GSW-3 large diameter wells subjected to a pumping test. Well locations on the mine map are shown in Figure 4.6. A list of the tests performed in the large diameter wells are summuraized in Table 4.7. As shown in the table, constant discharge has continued only couple of hours and a long recovery period has followed. The test data was evaluated to obtain the hydraulic characteristics of the metasediments-diorite units. Hydraulic conductivity values converted from transmissivity values indicate a low permability medium. The results obtained from pumping tests are lower than the packer tests. It is an expected result because packer test represent more local characterization. A fracture zone may give high permeability during the packer test time to time. Pumping tests are more representetive for the area of influence of the well.

38
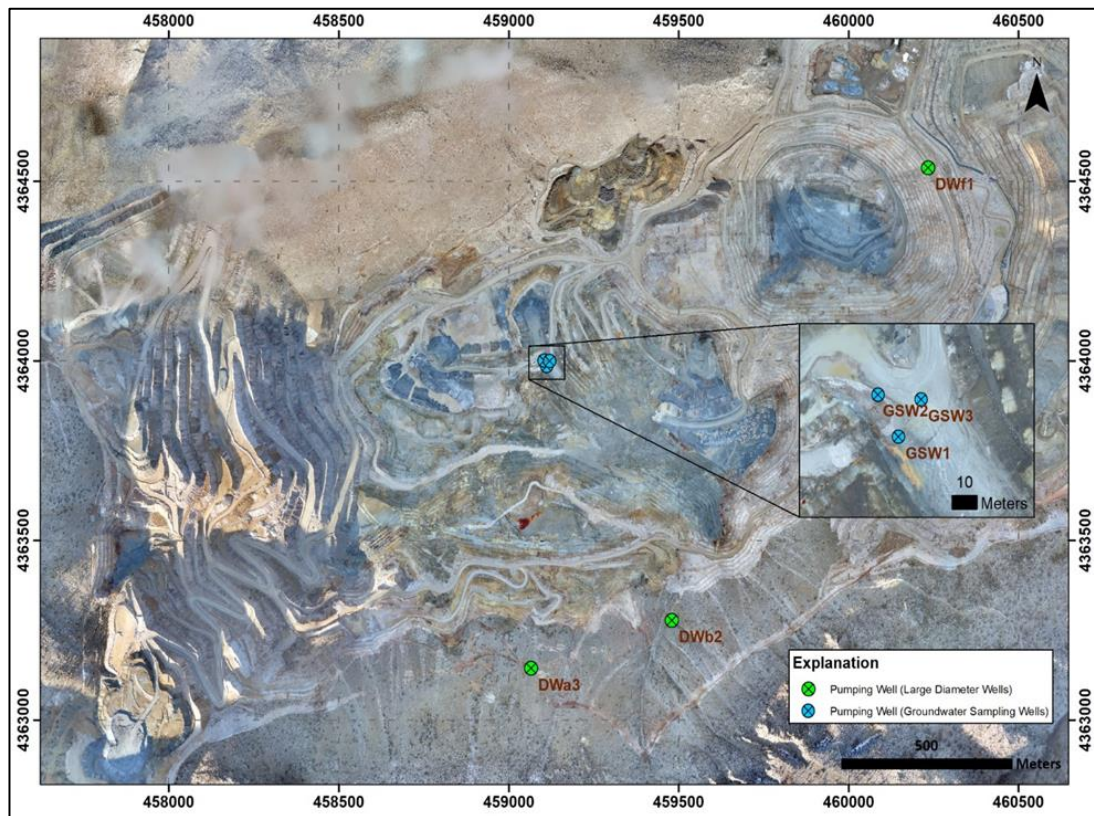
Figure 4.6. Location map of pumping wells (from Ekmekçi et al., 2018)

Table 4.7. Pumping test information and test results for large diameter wells (from Ekmekçi et al., 2018)

Well ID	Pumping Phase Duration	Total Duration of Test	Average Discharge Rate (L/s)	Methods	Aquifer Parameters		Geo. Mean of T and K	
					T (m2/s)	K (m/s)	T (m2/s)	K (m/s)
Dwf-1	2 h 30 min	8 days	0.62	Moench (1997)	4.15E-07	9.55E-09	4.15E-07	9.55E-09
Dwb-2	4 h 52 min	3 days	0.71	Cooper-Jacob	2.76E-06	3.39E-08	1.96E-06	2.42E-08
				Theis	2.18E-06	2.68E-08		
				Theis Recovery	1.26E-06	1.56E-08		
Dwa-3	45 min	30 days	0.44	Moench (1997)	8.31E-08	2.08E-09	8.31E-08	2.08E-09
GSW-1	2 h 27 min	12 days	0.58	Moench (1997)	5.67E-08	8.12E-10	6.69E-08	9.58E-10
				Moench (1985)	1.68E-08	2.40E-10		
				Theis Recovery	3.15E-07	4.51E-09		
GSW-2	4 h 45 min	6 days	0.58	Moench (1985)	8.40E-08	4.90E-10	6.47E-08	3.78E-10
				Theis Recovery	4.99E-08	2.91E-10		
GSW-3	1 h 35 min	14 days	0.63	Moench (1985)	1.54E-08	2.73E-10	8.86E-08	1.57E-09
				Theis Recovery	5.10E-07	9.05E-09		

As can be seen in Table 4.7, model types was fitted to the graphs represents the unconfined and/or leaky aquifers. This was also confirmed by geological and hydrogelogical field observations. The packer test results were shown that a permeable zone is underlined by a less permeable zone in the metasediments and diorite. Also hydraulic head measurements from VW piezometers prove that these sections are also unconfined in general. Similar results from different models for the same aquifer type have given similar results which confirms the interpretation above. The detail information about pumping tests and procedure can be found in Ekmekçi et al. (2018).

4.4. Groundwater Level and Pore Water Pressure Monitoring

The hydraulic head distribution along the critical cross-sections were monitored in both large diameter wells and small diameter drill holes. In all wells, contact gage was used for monitoring on weekly basis up to July 2018 then monthly basis monitoring was used. The VWPs installed in small diameter drill holes has a continuous record of hydrostatic pressure which is used to calculate the pore water pressure in kilopascal (kPa). Also pressure probes were inserted in some large diameter wells for continuous record of water level variations. In some large diameter wells, groundwater level measurements were taken by water level meter manually. The list of monitored wells, starting date of monitoring and the recording method are given in Table 4.8.

Table 4.8. Groundwater level monitoring wells (from Ekmekçi et al., 2018)

Section	Well No	Started From	Notes
A	Pa1	01.01.2018	Weekly by Contact Gage & VWPs installation on 01.01.2018 up to date
	Pa2	03.02.2018	Weekly by Contact Gage & VWPs installation on 03.02.2018 up to date
	Pa3	10.12.2017	Weekly by Contact Gage & VWPs installation on 10.12.2017 up to date
	Pa4*	18.01.2018	Weekly by Contact Gage & VWPs installation from 19.01.2018 to 08.05.2018
	Dwa1	09.09.2017	Weekly by Contact Gage & Pressure probe installed from 22.01.2018 to 30.04.2018
	Dwa2*	11.03.2018	Weekly by Contact Gage until 06.05.2018
	Dwa3	10.01.2018	Weekly by Contact Gage & Pressure probe installed from 25.03.2018 to ddate20.05.2018
B	Pb1	06.02.2018	Weekly by Contact Gage & VWPs installation on 07.02.2018 up to date
	Pb3	05.03.2018	Weekly by Contact Gage & VWPs installation on 05.03.2018 up to date
	Pb4	24.02.2018	Weekly by Contact Gage & VWPs installation on 24.02.2018 up to date
	Pb5	13.03.2018	Weekly by Contact Gage & VWPs installation on 14.03.2018 up to date
	Dwb2	11.02.2018	Weekly by Contact Gage & Pressure probe installed from 21.04.2018 to 20.05.2018
C	Pc1	25.03.2018	Weekly by Contact Gage & VWPs installation on 22.03.2018 up to date
	Dwc2	15.02.2018	Weekly by Contact Gage & Pressure probe installed from 31.03.2018 to 10.04.2018
E	Pe1	05.10.2017	Weekly by Contact Gage & VWPs installation on 04.10.2017 up to date
	Dwe1	17.12.2017	Weekly by Contact Gage & Pressure probe installed on 11.03.2018 up to date
F	Pf3	09.11.2017	Weekly by Contact Gage & VWPs installation on 09.11.2017 up to date
	Dwf1	14.11.2017	Weekly by Contact Gage & Pressure probe installed on 19.02.2018 up to date
Sampling Wells	GSW1	17.04.2018	Weekly by Contact Gage & Pressure probe installed on 05.06.2018 up to date
	GSW2	02.05.2018	Weekly by Contact Gage & Pressure probe installed on 22.05.2018 up to date
	GSW3	08.05.2018	Weekly by Contact Gage & Pressure probe installed on 22.05.2018 up to date

4.4.1. Instrumentation

The monitoring network consist of the pore water pressure measurements from VWPs at small diameter drill holes, the pressure probes which measures the hydrostatic pressure, installed in some large diameter wells (Dwb-2, Dwf-1, GSW-1, GSW-2, GSW-3) and manual measurements taken by water level meter from other large diameter wells. The vibrating wire piezometers were installed in fully grouted borehole. The vibrating wire piezometers were calibrated before installation (Figure 4.7). Conversion of pressure readings to pore water pressure was applied by using the equations provided by the manufacturer.

Figure 4.7. Vibrating wire piezometers installed in small diameter drill holes

4.4.2. Reading and Data Conversion

The VWPs measure the hydrostatic pressure which used to calculate the pore water pressure in kilopascal (kPa). After that the pore water pressure in kPa is converted to pressure head in meter. Finally, with the knowledge of the pressure head and elevation head, hydraulic head in meters above the sea level (masl) can be calculated easily.

The general equation used to make conversions is given below. The coefficients a, b and c have values specific to the VWP and obtained from the manufacturer's calibration sheets. The coefficients belong to each piezometer are given in Table 4.9.

$$L\,(kPa) = aR^2 + bR^2 + c$$

Where,

L, is the data converted to hydraulic pressure in kPa

R, is the reading downloaded from instrument

a, b and c are the coefficients specific to each piezometer

The hydrostatic pressure measured by pressure probes is used to calculate pressure head and the hydraulic head in meters above sea level (masl). The data sheet includes date, groundwater level depth from the surface in meter and groundwater elevation meters above sea level. The example data sheet is shown in Table 4.10 and also an example worksheet of vibrating wire piezometers is given in Table 4.11.

Table 4.9. Coefficients specific to vibrating wire piezometers

VWP NO	a	b	c
Pa1_82	3.33E-07	-0.38	2486.47
Pa1_147	-1.9E-08	-0.75	5027.84
Pa2_31	4.85E-07	-0.15	1001.20
Pa2_75	-1.3E-07	-0.38	2619.93
Pa2_160	-1.1E-07	-0.79	5153.99
Pa2_181	-1.2E-06	-0.76	5110.80
Pa3_27	4.09E-07	-0.14	901.62
Pa3_49	1.29E-06	-0.41	2618.76
Pa3_95	1.59E-07	-0.40	2608.17
Pa3_121	-2.8E-08	-0.67	3855.64
Pb1_35.5	-2.01E-07	-0.22	1284.67
Pb1_104	6.82E-07	-0.40	2635.78
Pb3_16	1.59E-07	-0.14	891.16
Pb3_85m	-1.5E-07	-0.39	2599.10
Pb3_159	-3.4E-07	-0.60	3827.25
Pb3_254	-1.9E-06	-1.41	8707.60
Pb4_19.3	1.41E-07	-0.10	567.91
Pb4_56.3	1.04E-06	-0.40	2671.88
Pb4_101.3	4.36E-08	-0.62	4030.21
Pb5_31.29	-2.4E-07	-0.22	1256.84
Pb5_69.5	3.66E-07	-0.38	2438.55
Pb5_113.51	2.32E-07	-0.60	3900.27
Pc1_9.5	4.8E-08	-0.10	702.79
Pc1_29.98	3.56E-07	-0.14	904.73
Pc1_96.31	-3.9E-07	-0.62	3950.32
Pc1_158.2	-1.1E-06	-0.59	3874.23
Pf3_45.2	2.71E-07	-0.23	1449.10
Pf3_182.2	1.86E-06	-0.79	5094.86

Table 4.10. An example worksheet recorded by pressure probes at large diameter wells

DWf1		
Date	GWL Depth (m)	GWL Elevation (m)
14.11.2017	285.93	857.64
15.11.2017	284.24	859.33
16.11.2017	281.93	861.64
17.11.2017	279.77	863.80
18.11.2017	277.88	865.69
19.11.2017	276.27	867.30
20.11.2017	275.17	868.40
21.11.2017	273.59	869.98
22.11.2017	272.50	871.07
23.11.2017	271.16	872.41
24.11.2017	270.40	873.17
25.11.2017	268.87	874.70
26.11.2017	267.66	875.91
27.11.2017	266.56	877.01
28.11.2017	265.82	877.75
29.11.2017	265.39	878.18
30.11.2017	265.00	878.57
1.12.2017	264.33	879.24
2.12.2017	263.83	879.74
3.12.2017	263.33	880.24
4.12.2017	262.92	880.65
5.12.2017	262.52	881.05
6.12.2017	262.07	881.50

Table 4.11. An example worksheet showing the data contained in the spreadsheets

Time (date)	Frequency (Hz)	L (digit)	Temperature (°C)	Pressure (kPa)	Pressure Head (m)	Elevation Head (m)	Total Head (m)
01-01-18 11:10		5871.9	16.1	256.50	26.16	1095.00	1121.16
01-01-18 11:15		5873.8	16.1	255.78	26.09		1121.09
01-01-18 11:20		5874.8	16.1	255.40	26.05		1121.05
01-01-18 11:25		5876.3	16.1	254.83	25.99		1120.99
01-01-18 11:30		5877.2	16.1	254.48	25.96		1120.96
01-01-18 11:35		5878.7	16.1	253.91	25.90		1120.90
01-01-18 11:40		5879.7	16.1	253.53	25.86		1120.86
01-01-18 11:45		5881.1	16.1	253.00	25.81		1120.81
01-01-18 11:50		5882.1	16.1	252.62	25.77		1120.77
01-01-18 11:55		5883.5	16.1	252.09	25.71		1120.71
01-01-18 12:00		5884.5	16.1	251.71	25.67		1120.67
01-01-18 12:05		5885.5	16.1	251.33	25.64		1120.64
01-01-18 12:10		5886.4	16.1	250.99	25.60		1120.60
01-01-18 12:15		5888.4	16.1	250.23	25.52		1120.52
01-01-18 12:20		5889.4	16.1	249.85	25.48		1120.48
01-01-18 12:25		5890.3	16.1	249.51	25.45		1120.45
01-01-18 12:30		5891.3	16.1	249.13	25.41		1120.41
01-01-18 12:35		5892.3	16.1	248.75	25.37		1120.37
01-01-18 12:40		5893.7	16.1	248.21	25.32		1120.32
01-01-18 12:45		5894.7	16.1	247.83	25.28		1120.28

### 4.4.3. Groundwater Level Monitoring in Carbonate Rocks

The measurements and tests applied in large diameter wells drilled in the carbonate rock unit that surrounds the mine site showed that the carbonate rock in the mine site is generally dry. The boundary between carbonate rock and metasediments and/or diorite unit could not be determined because no cuttings came out of the wells after a certain depth. Almost all wells drilled much deeper than the bottom of the carbonate rock, so the groundwater level measured from large diameter wells is most probably originates from the metasediments and diorite.

The groundwater level in large diameter wells have been measured by a contact gage on weekly basis until July 2018 and then have been continued with monthly basis manual measurements. The groundwater level hydrographs of large diameter wells are given in Figures 4.8 through 4.11.

The groundwater levels show that Dwa-1, Dwa-2, Dwc-2 and Dwe-1 wells were followed a decreasing trend; while an increasing trend have been observed in Dwa-3 and Dwf-1 wells. Dwb-2 almost became stable after pumping for an initial test. Dwa-1 well was the first completed well and it is the only well located on northern part of the mine site. The hydraulic head fluctuated between 1033.46 masl and 1011.85 masl. Dwa-2 showed similar behavior with Dwa-1 well. The hydraulic head changed from 1218.6 masl to 1207.3. In Dwa-3 well, hydraulic head showed an increasing trend. The measurements changed between 1232.81 masl and 1268.76 masl. Dwb-2 showed a stable profile except April and May 2019. In these months, fluctuations of water levels occurred between 1142 masl and 1152 masl. In Dwc-2, rapid decreasing of groundwater level was observed and afterwards it became stable around 1042 masl. The hydraulic head has measured as 1163.6 masl and it decreased up to two months and then stabilized at 1072 masl in Dwe-1. In Dwf-1, the hydraulic head was measured as 856.71 masl at the end of drilling and the two months after the end of drilling phase, the hydraulic head stabilized around 881.59 masl.
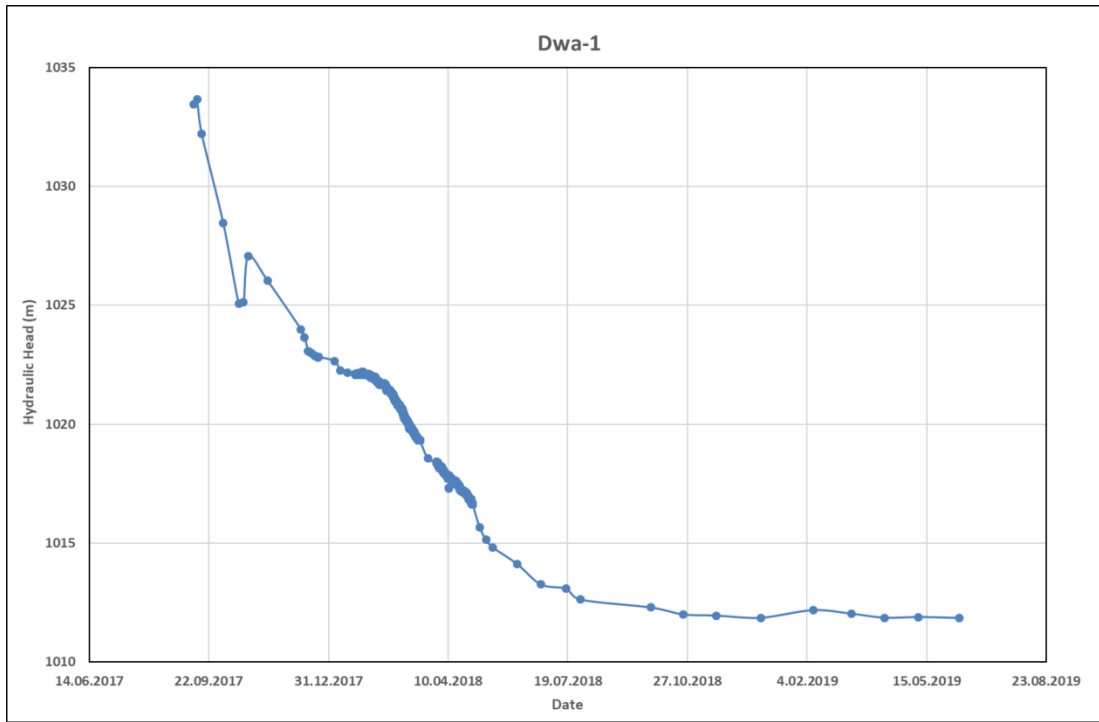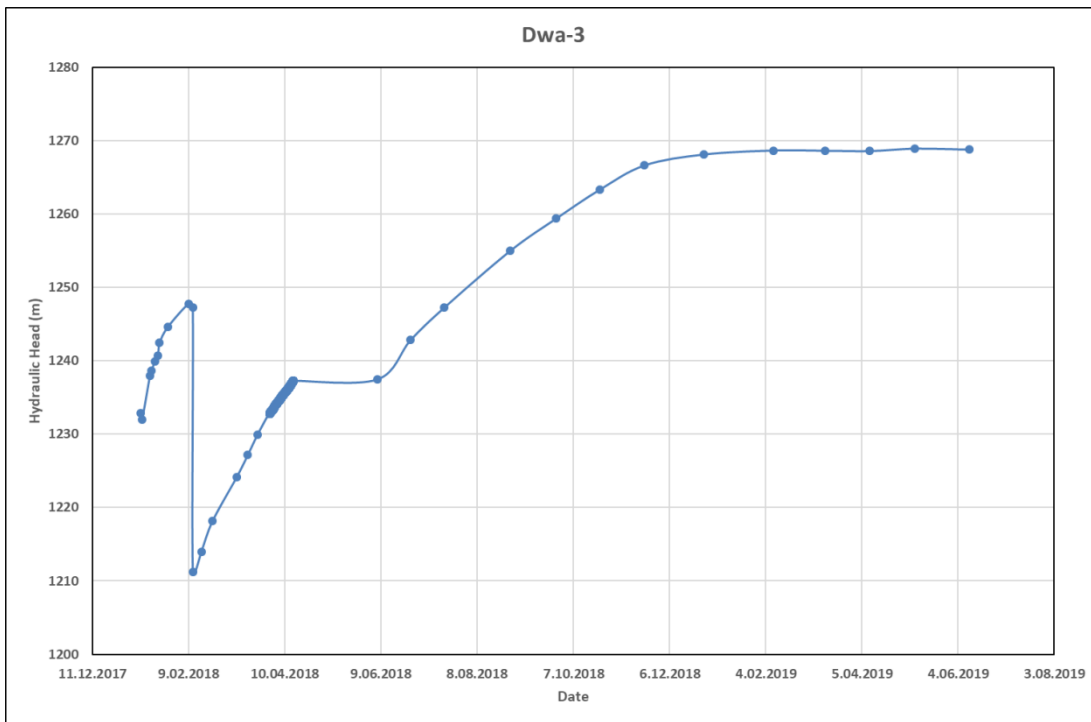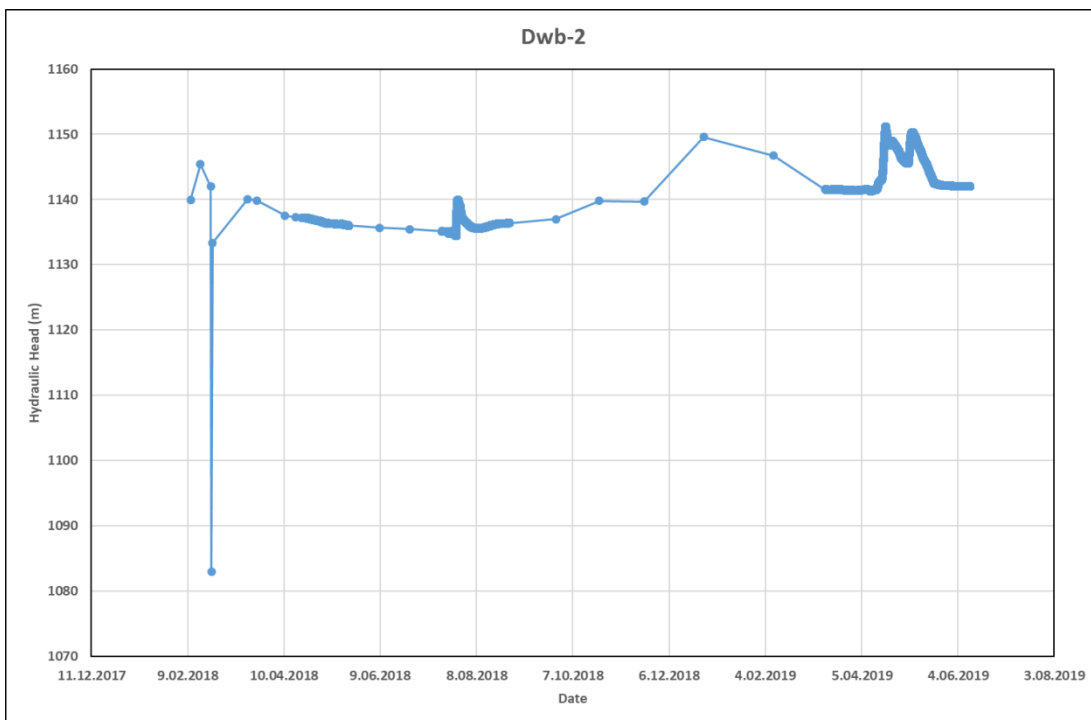
a
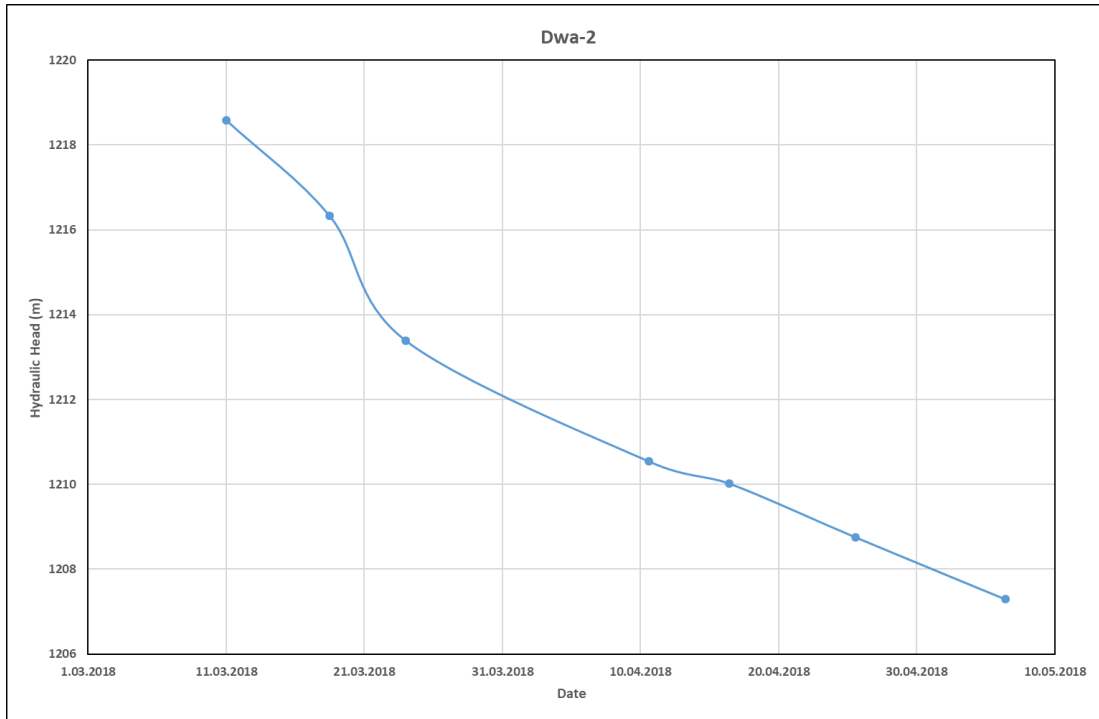
b

Figure 4.8. Groundwater level hydrographs of a. Dwa-1 and b. Dwa-2

45

a

b

Figure 4.9. Groundwater level hydrographs of a. Dwa-3 and b. Dwb-2

a

b

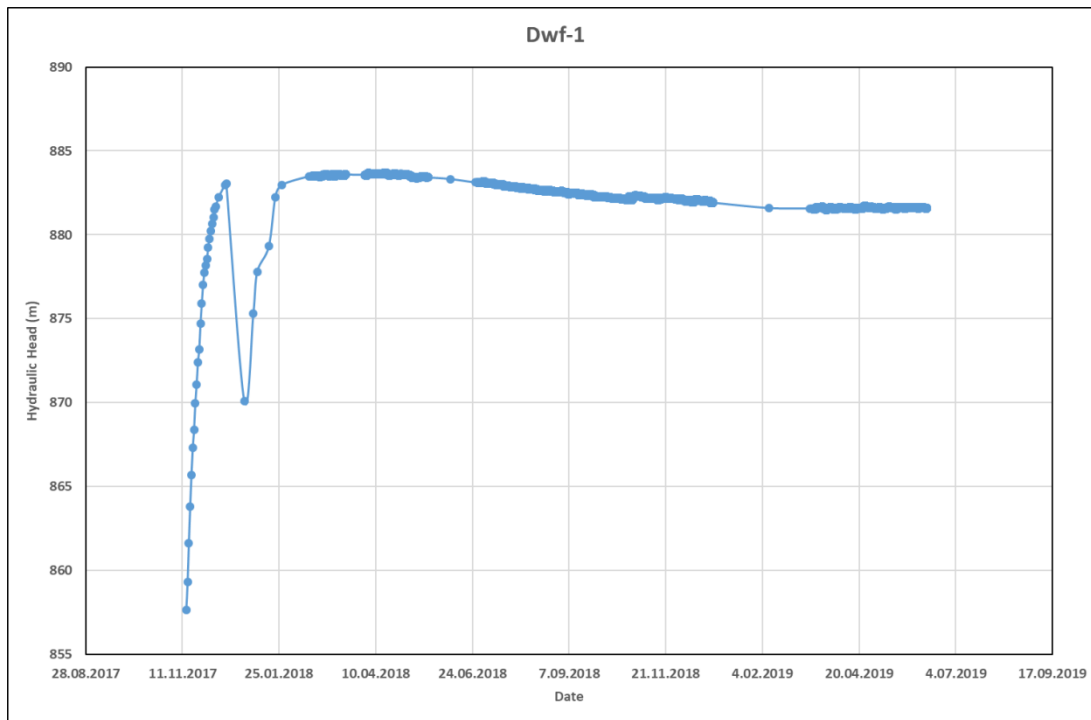Figure 4.10. Groundwater level hydrographs of a. Dwc-2 and b. Dwe-1

Figure 4.11. Groundwater level hydrographs of Dwf-1

4.4.4. Pore Water Pressure Monitoring in Diorite and Metasediments

The GSW wells and the vibrating wire piezometer wells were drilled into metasediments and diorite units to characterize them. Monitoring was continued on those wells until 11.06.2019. The hydraulic head values measured from GSW wells which screened at different depths showed a downward hydraulic gradient (Figure 4.12). In GSW-1 well, the hydraulic head was stabilized at around 1189 masl while GSW-2 well was stabilized at around 1159 masl and about 960 masl at GSW-3 well. The head difference between GSW-1 and GSW-2 is about 30 m, the head difference between GSW-2 and GSW-3 is about 199 m. The screen intervals of GSW wells are 24-56 mbgl, 136-200 mbgl and 216-256 mbgl for GSW-1, GSW-2 and GSW-3, respectively. Assuming that the hydraulic head represents the middle of the screen intervals, the hydraulic gradient calculated as 0.23 between GSW-1 and GSW-2 and 2.93 between GSW-2 and GSW-3. Results show that the medium is heterogeneous and upper sections has higher hydraulic conductivities than lower sections. Another observation supports this interpretation is that groundwater level at GSW-1 was affected during pumping at GSW-2 but no response was recorded at GSW-1 and GSW-2 during pumping at GSW-3 for pumping test (Figure 4.12).
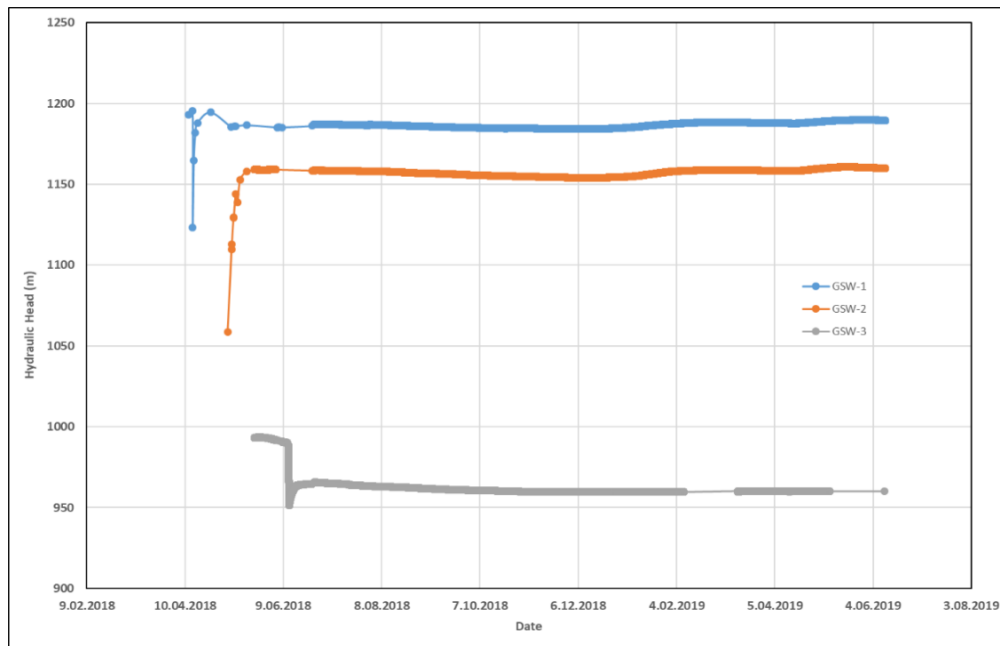
48

Figure 4.12. Hydraulic head vs time at GSW wells

The vertical change in hydraulic head in metasediments-diorite were also recorded by the VWPs installed at different depths in drill holes. The temporal variations in hydraulic head, pressure head and pore water pressures were plotted. Examples of these graphs for Pa1 well are given in Figure 4.13. Same graphs were also drawn for other piezometer wells which can be found in Ekmekçi et al. (2018). In almost all piezometer wells a downward gradient observed similar with GSW wells.
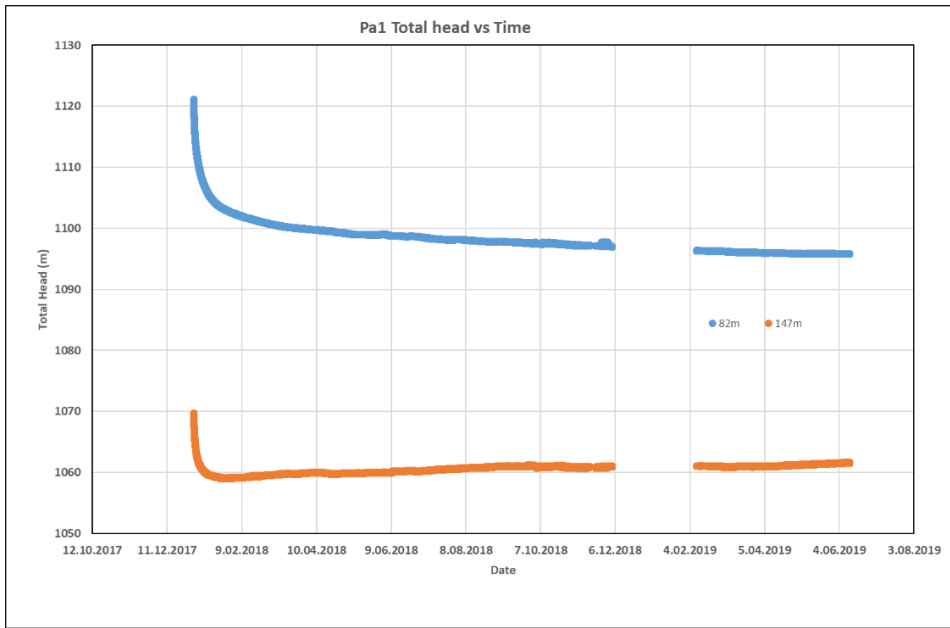
a
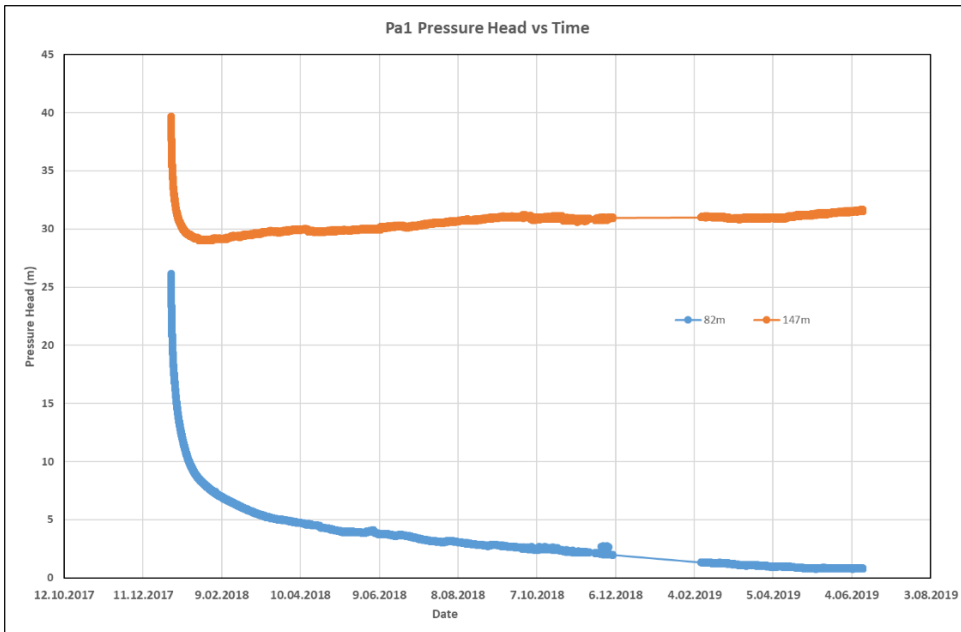
b
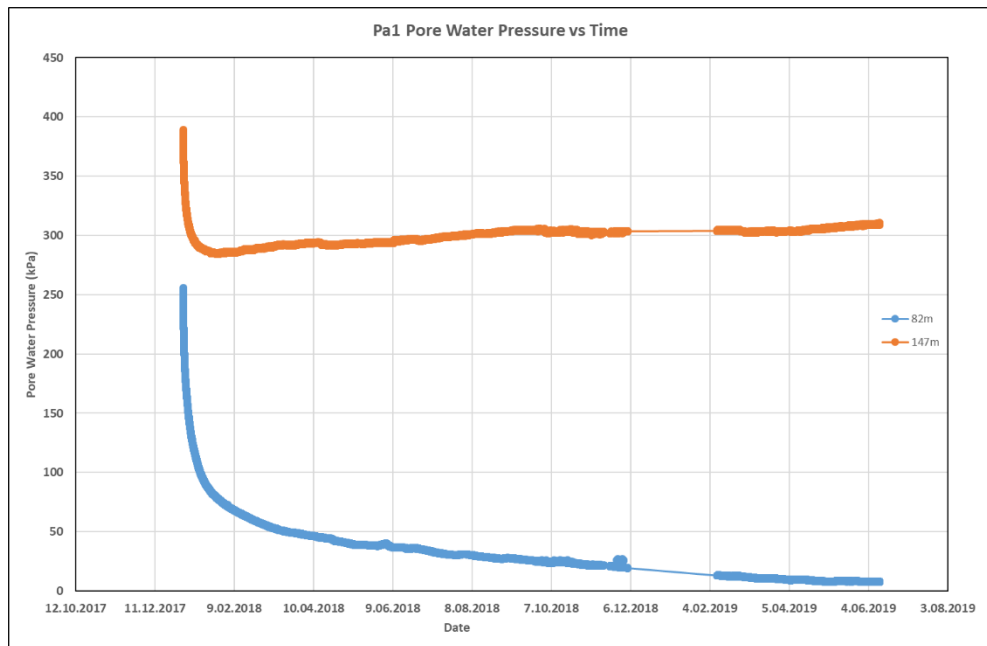
c

Figure 4.13. Temporal variation of a) hydraulic head, b) pressure head, and c) pore water pressure at VWPs in drill hole Pa1

4.4.5. Temporal Change of Hydraulic Head on Critical Cross-Sections

The readings of pressure probes inserted in large diameter wells and the VWPs inserted in small diameter drill holes have been evaluated to determine the hydraulic head distribution and hydraulic gradient on the critical cross-sections. The hydraulic heads calculated using the pore water pressure readings are shown in graphs for each critical cross-section. The graphs for cross-section A are given in Figure 4.14. The gradient is downward in Pa1 and Pa4 wells. However, in other piezometer wells, the hydraulic gradient shows different patterns between vibrating wire piezometers. For example, in Pa2, the hydraulic gradient is upward between VWP3 and VWP4 only. Same situation is also observed in Pa3. The hydraulic gradient is upward between VWP1 and VWP2 only. Different hydraulic gradients in vertical profile of small diameter wells confirms the heterogenity of the medium. Dwa-2 and Pa4 wells were later removed from the monitoring network due to mining activities.

51

In section B, the downward hydraulic gradient is observed in Pb3 and Pb4. However, in Pb1, readings showed an upward gradient. In Pb5, until May 2019, the downward gradient can be seen between three VWPs. After May, the hydraulic gradient was changed reversly between VWP1 and VWP2 (Figure 4.15). Similar with section A, vertical hydraulic gradient profile is not uniform indicating heterogeneous medium.
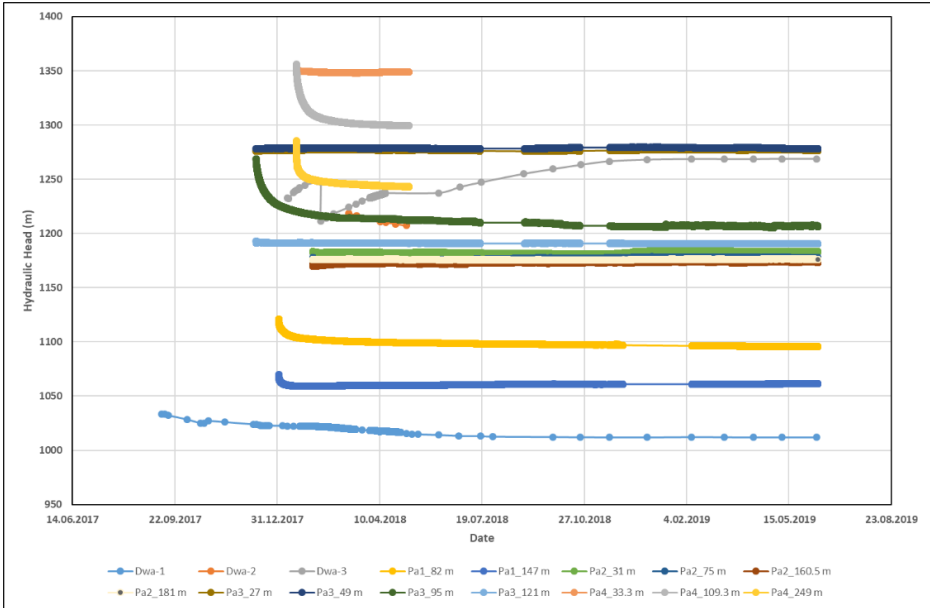

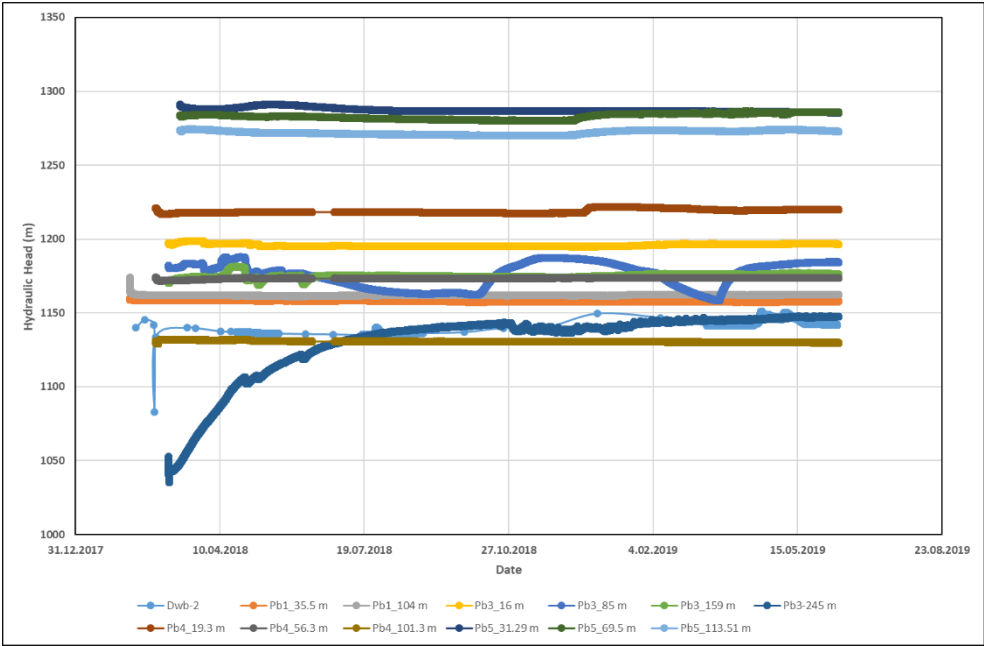Figure 4.14. Hydraulic head distribution at cross- section A

Figure 4.15. Hydraulic head distribution at cross- section B

52

There is only one drill hole equipped with VWPs on cross section C, E and F. In section C, shallow piezometers have almost the same hydraulic head but it is clear that the downward hydraulic gradient is increasing with depth (Figure 4.16). Sections E and F have showed quite similar characteristics. Each well equipped with two VWPs and readings indicated a downward gradient (Figure 4.17 and Figure 4.18).
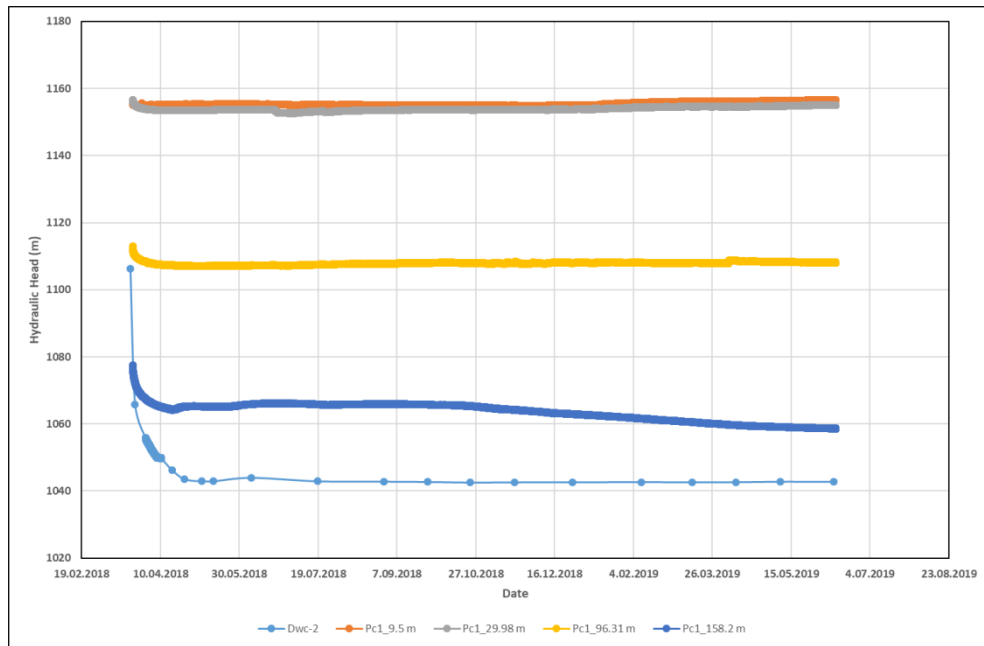

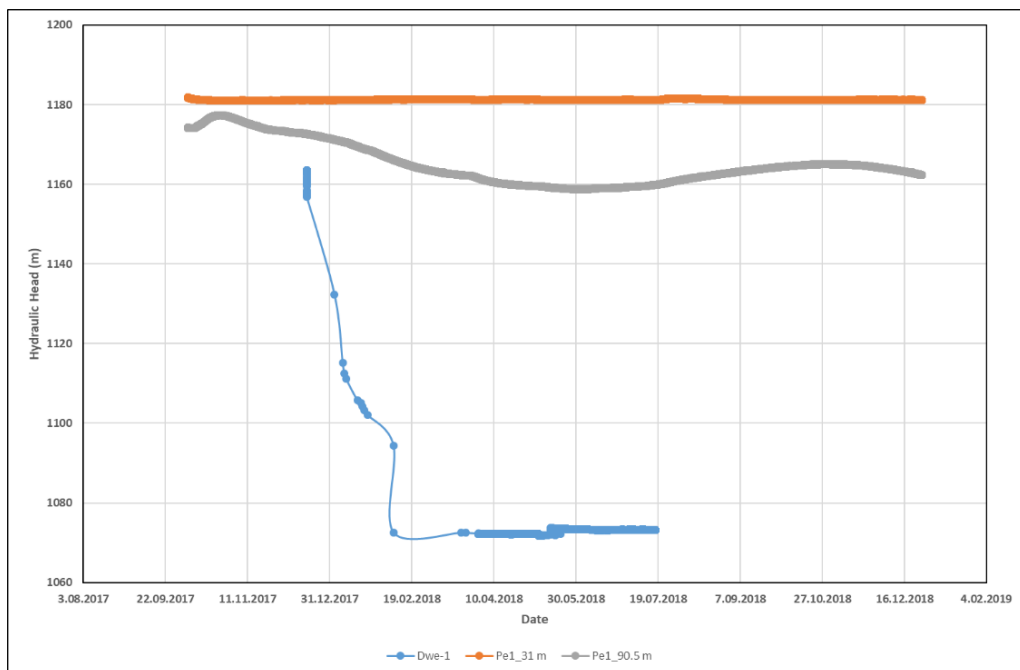Figure 4.16. Hydraulic head distribution at cross- section C

Figure 4.17. Hydraulic head distribution at cross- section E
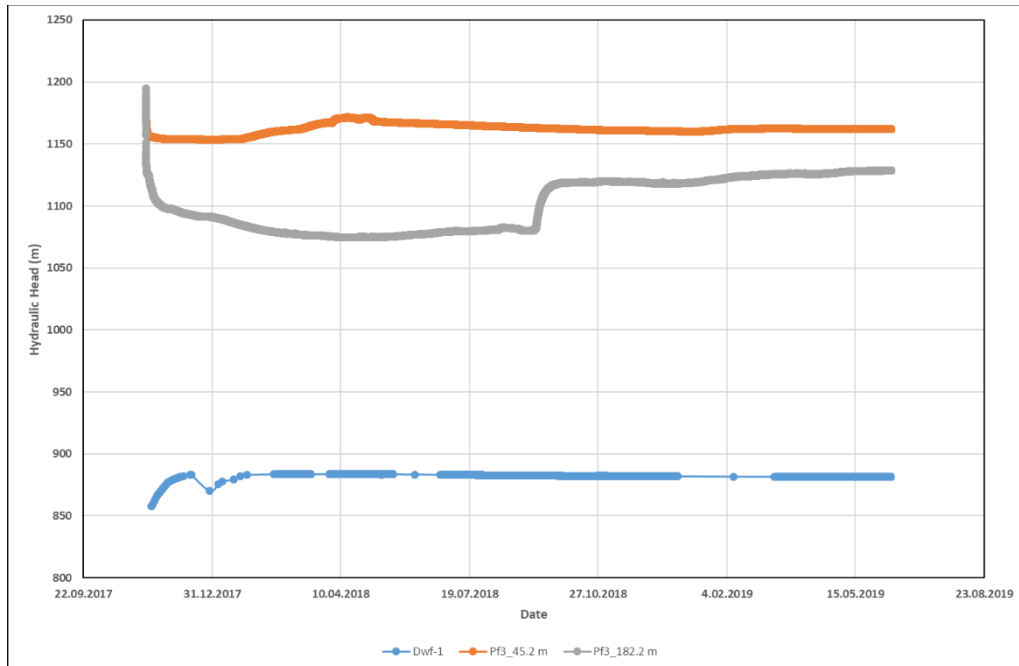
Figure 4.18. Hydraulic head distribution at cross- section F

The pressure head values measured from piezometer wells are plotted on each critical cross-section as light blue bars to understand the pore water distribution with respect to the current situation and the ultimate pit bottom topography (Figure 4.19 to Figure 4.23). The large diameter wells placed both ends of cross-sections. Representative groundwater levels illustrated as dark blue marks.

The cross-section A, B and C passed through the mine site approximately south-north direction and intersect the deepest part of the main pit. On the other hand, cross-section E and F passed through the mine site approximately east-west direction, to illustrate the longitudinal extension of the mine site.

Figure 4.19. Pressure heads recorded at VWPs on cross- section A (from Ekmekçi et al., 2018)

Figure 4.20. Pressure heads recorded at VWPs on cross- section B (from Ekmekçi et al., 2018)
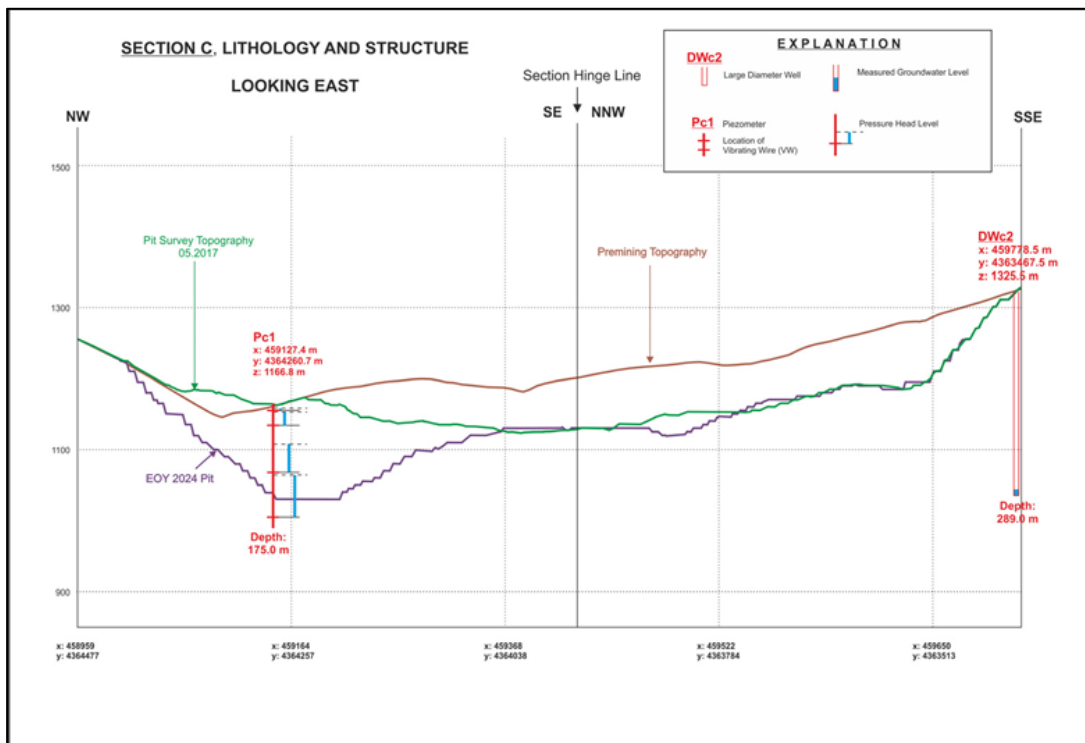
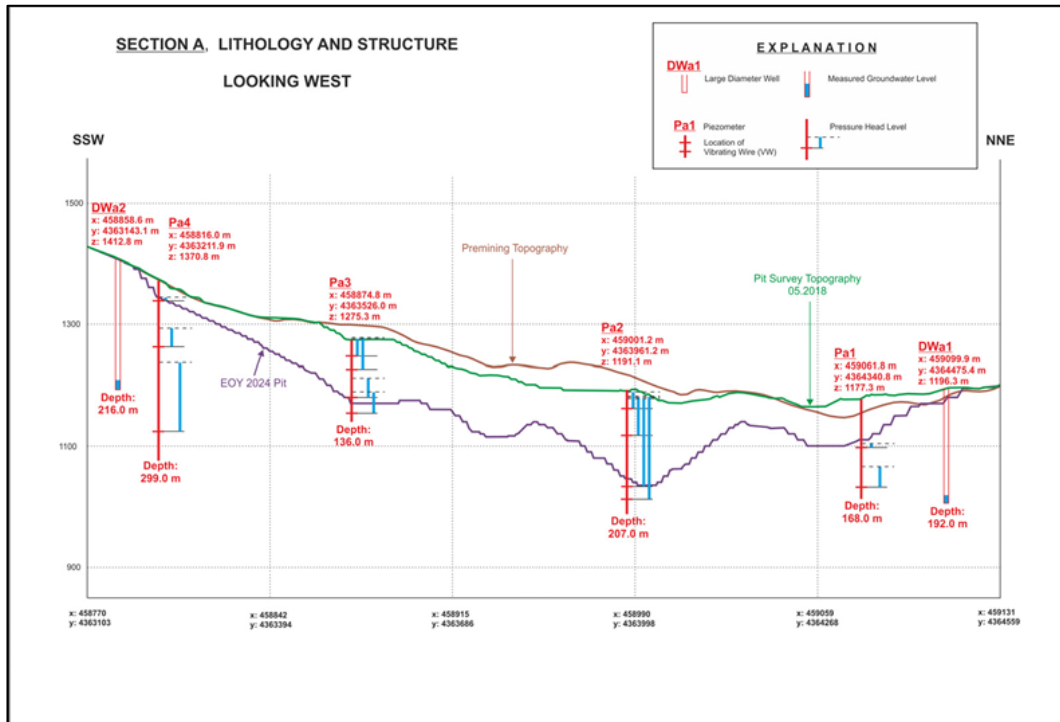Figure 4.21. Pressure heads recorded at VWPs on cross- section C (from Ekmekçi et al., 2018)
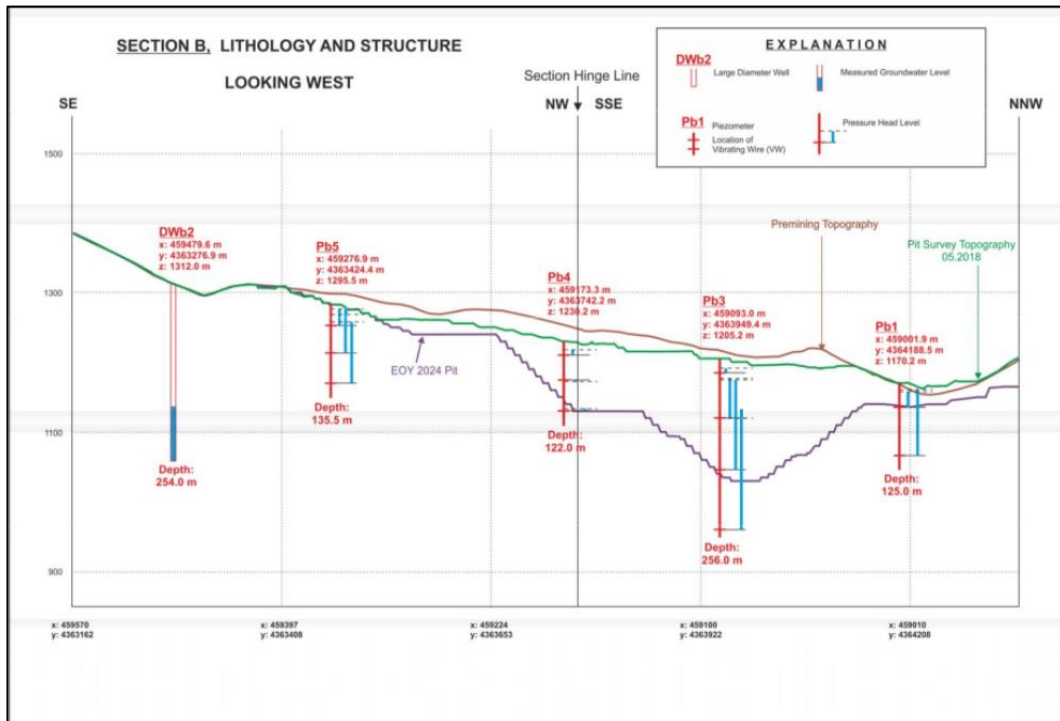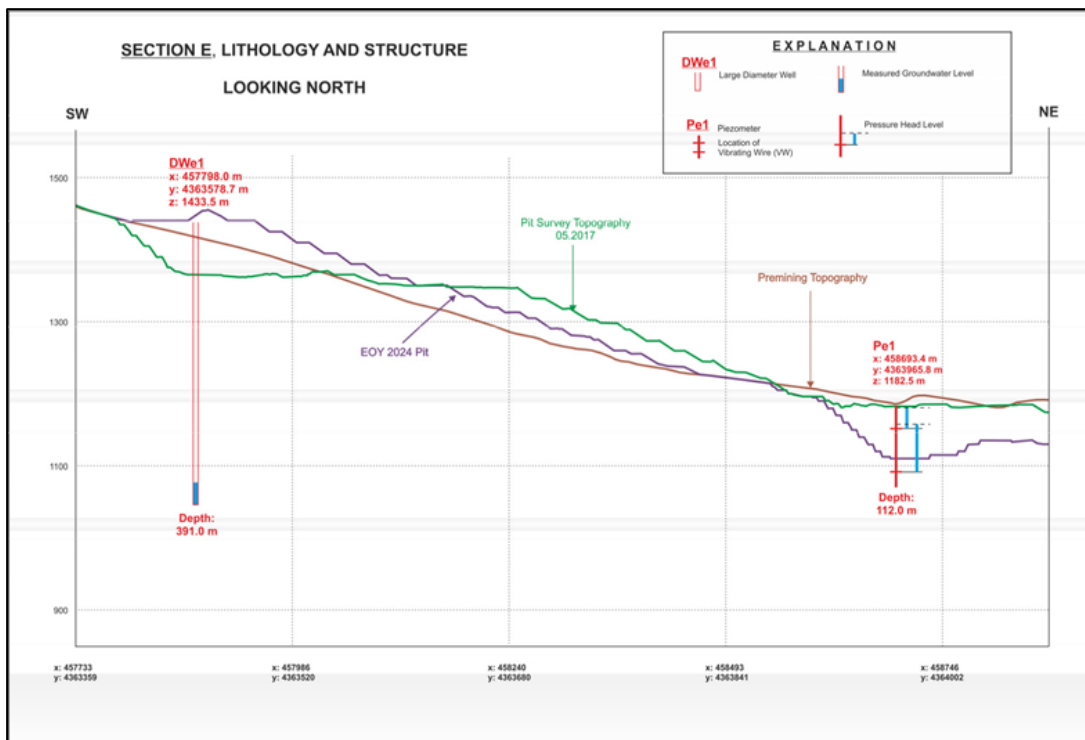

Figure 4.22. Pressure heads recorded at VWPs on cross- section E (from Ekmekçi et al., 2018)
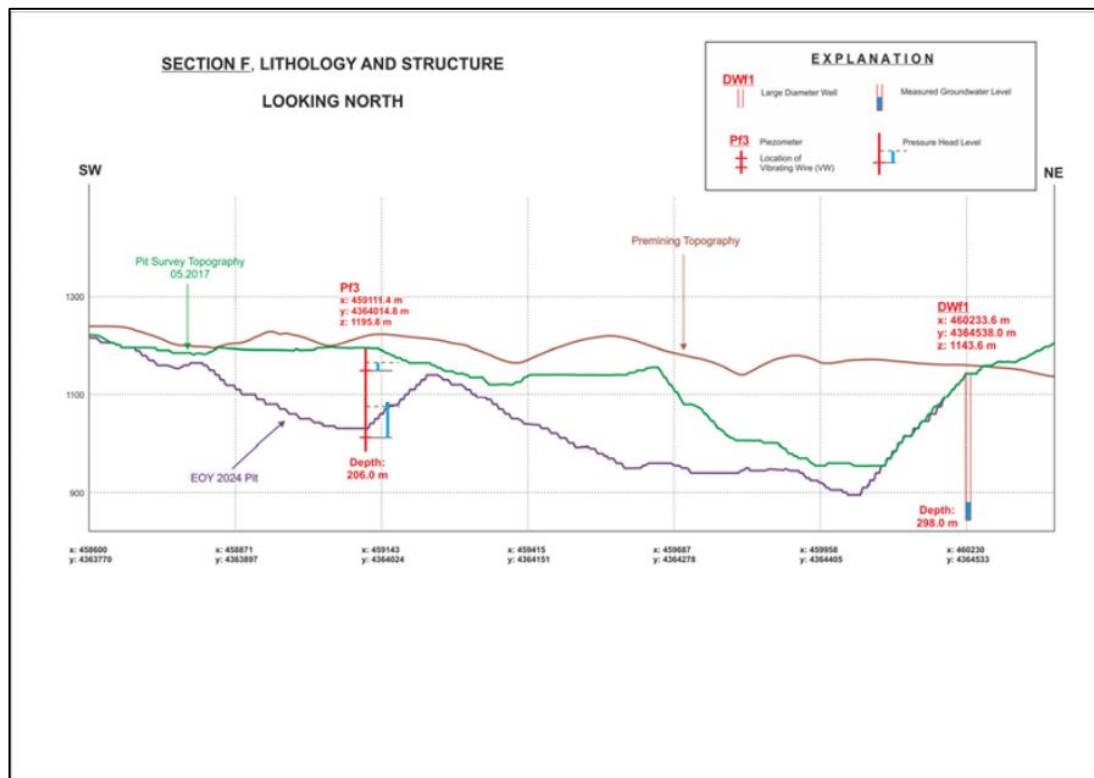
Figure 4.23. Pressure heads recorded at VWPs on cross- section F (from Ekmekçi et al., 2018)

4.5. Effects of Precipitation on Hydraulic Head Distribution

The readings obtained from pressure probes and VWPs were plotted as hydraulic head to graphs with precipitation to understand effect of precipitation on hydraulic heads at each well. On some graphs, scale was enlarged to catch the response of hydraulic heads in detail.

An example hydrograph and hyetograph of Pa1_82 was plotted with precipitation recorded at weather station at the site in Figure 4.24. The hydraulic head did not show any response to precipitation at this piezometer. However, at enlarged view, it can be observed that there were slight changes in hydraulic head response to precipitation (Figure 4.25). Other hydrographs and hyetographs can be found in Ekmekçi et al. (2019).

With hydrographs and hyetographs, the relationship between hydraulic head and precipitation has been proven especially in metasediments and diorite. The time lag varies from 0 day to 30 days and can be related with depth of the VWPs. The shallow VWPs response to precipitation were in shorter time than the deeper ones.

The rainfall infiltration breakthrough (RIB) method was used to simulate variations of hydraulic head in response to precipitation. The RIB method (Xu and Beekman, 2003) based on cumulative rainfall departure (CRD) method found by Xu and Van Tonder (2001) used for calculating the recharge in drill holes (Figure 4.25). The simulations obtained from RIB and CRD methods plotted as graphs, similar to ones shown in Figure 4.26.

The dark blue and light blue bars in these graphs indicate precipitation and recharge, respectively. Observed water levels plotted as solid dark blue lines, simulated groundwater level by RIB method plotted as solid red line and simulated groundwater level by CRD method plotted as solid green line (Figure 4.26).
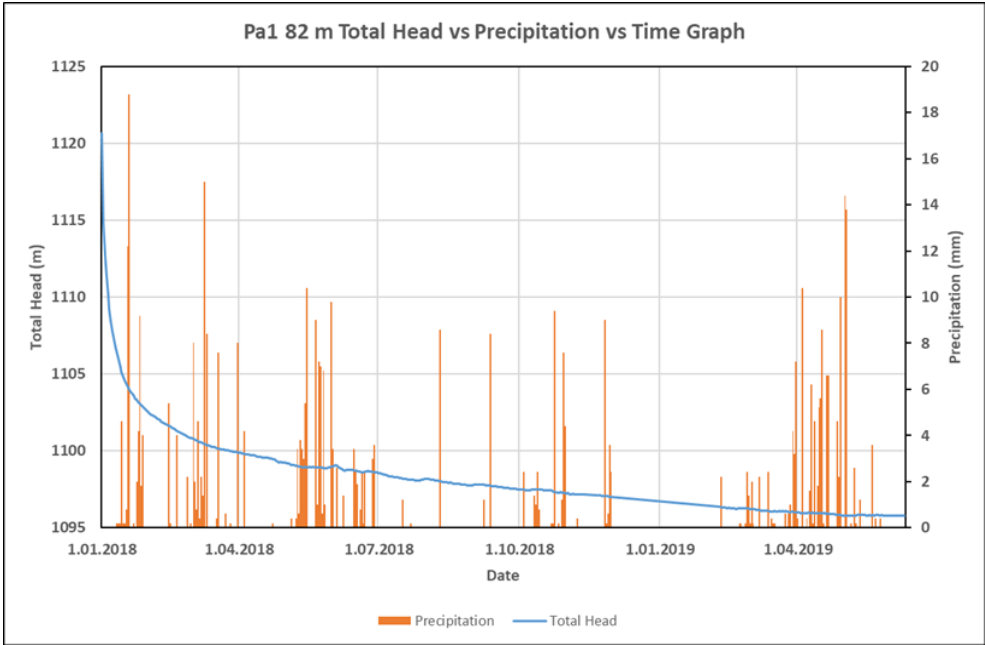
Figure 4.24. Hyetograph and hydrograph of VWP no Pa1_82 (from Ekmekçi et al., 2019)

58
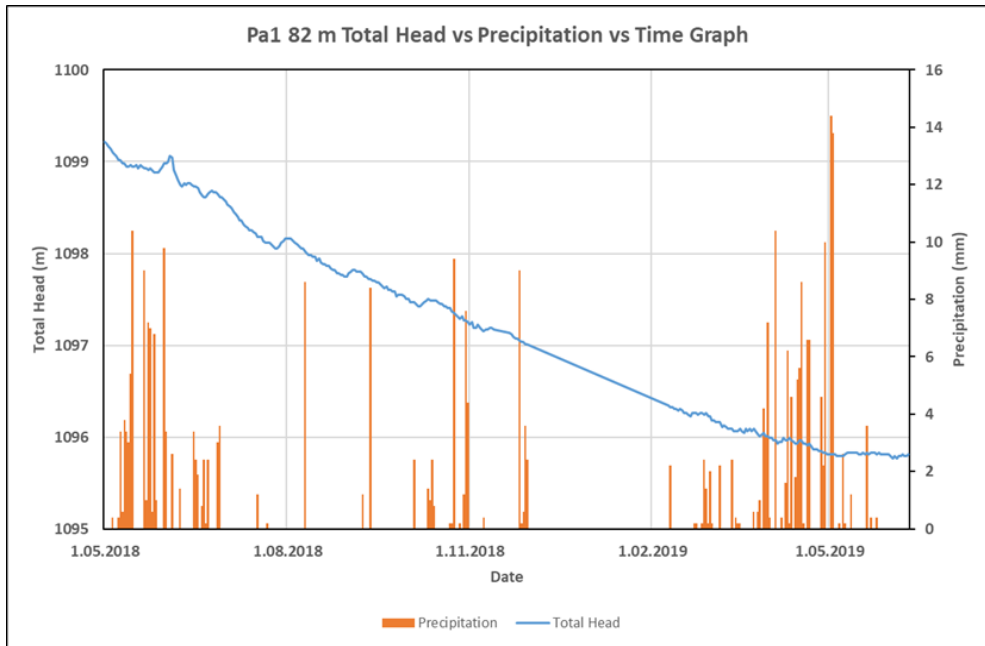
Figure 4.25. Hyetograph and hydrograph of VWP no Pa1_82 (enlarged view) (from Ekmekçi et al., 2019)
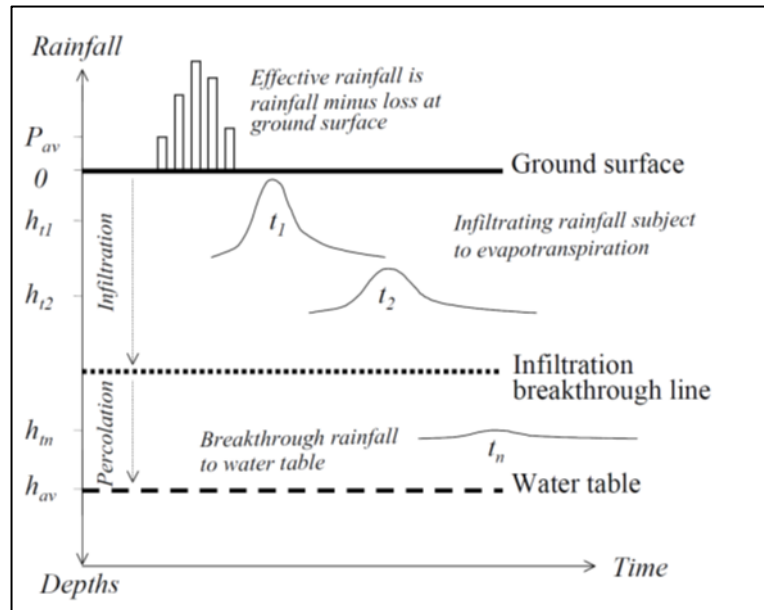
Figure 4.26. Rainfall infiltration breakthrough process (after Xu and Beekman, 2003)

An example simulation results produced by Ekmekçi et al. (2019) for Pa1_82 where the time lag was 14 days and the cumulative recharge period was 90 days are given in Figure 4.27. The annual recharge calculated as 70 mm and adjusted specific yield was 0.006 for the best fit.
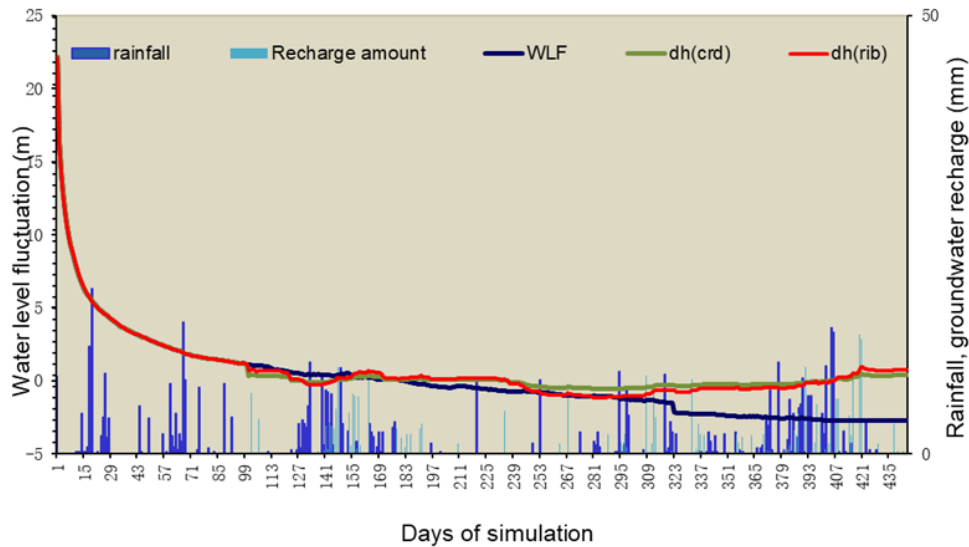
Figure 4.27. Results of simulation of VWP no Pa1_82 (from Ekmekçi et al., 2019)

The simulation results suggest that metasediments and diorite are hydrogeologically heterogeneous. Shallow sections have high permeability and respond to recharge is very fast. On the other hand, deep sections have lower permeability and time lag was observed in response to recharge on those sections and it increases with depth.

The estimated recharges values varied from 2 mm to 146 mm/year. In most piezometers the recharge rate is calculated to be around 35 mm/year. The specific yield adjusted to obtain the best fit has higher values at the shallow zones than the deeper zones. Its values ranges between 0.001 and 0.1 with a rough average of 0.05 at the shallow zones. This value decreases with greater depths down to 0.001. The specific yield values are obtained as a fitting parameter and they depend on the time series of the measured pore water pressure. The reliability of the estimated results depends on short stabilization period of VWPs. To accomplish more accurate evaluations, monitoring of the pore water should be continued for at least another year.

CHAPTER 5

HYDROCHEMISTRY

Hydrochemical sampling and analysis is an important part of characterization of groundwater, especially for determining the origin of groundwater and interaction with other water bodies. The groundwater sampling and physical and chemical field parameter measurements such as pH and electrical conductivity are conducted regularly by Anagold engineers from environment department. The groundwater samples have been collected from drill holes after completion of the construction of wells.

A total of six water samples were collected from large and small diameter drill holes. Three samples were collected from small diameter drill holes and other three were collected from large diameter wells. The well locations where the water samples were collected is shown in Figure 5.1. From the remaining wells, measurements could not be taken because wells could not be emptied completely to assure collected water samples belong to groundwater. The initial evaluations were performed using Piper Diagram by Ekmekçi et al. (2018) as shown in Figure 5.2. General distribution on the piper diagram shows that samples plot in Ca-Na-Cl-SO$_4$ hydrochemical facies, except Dwb-2 and GSW-2 wells. Dwb-2 has only fresh water among all six water samples with hydrochemical facies of Ca-Mg-HCO$_3$. GSW-2, which taps the groundwater in the metasediments at the intermediate depth, plots in the Ca-Mg-SO$_4$-HCO$_3$ facies meaning that the groundwater might be affected by the sulfide in the ore. The point to be considered is that the groundwater sample collected from large diameter wells in the carbonate rock is probably originated from the metasediments or/and the diorite.
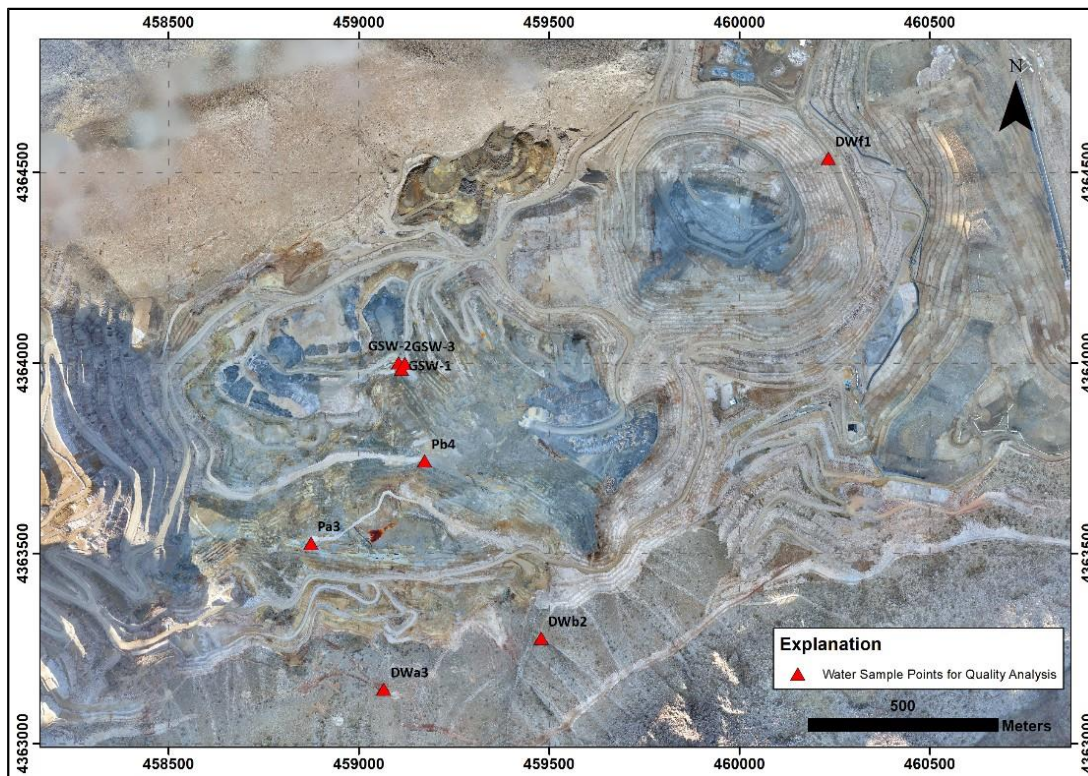
Figure 5.1. Location map of sampling points for water quality (from Ekmekçi et al., 2018)
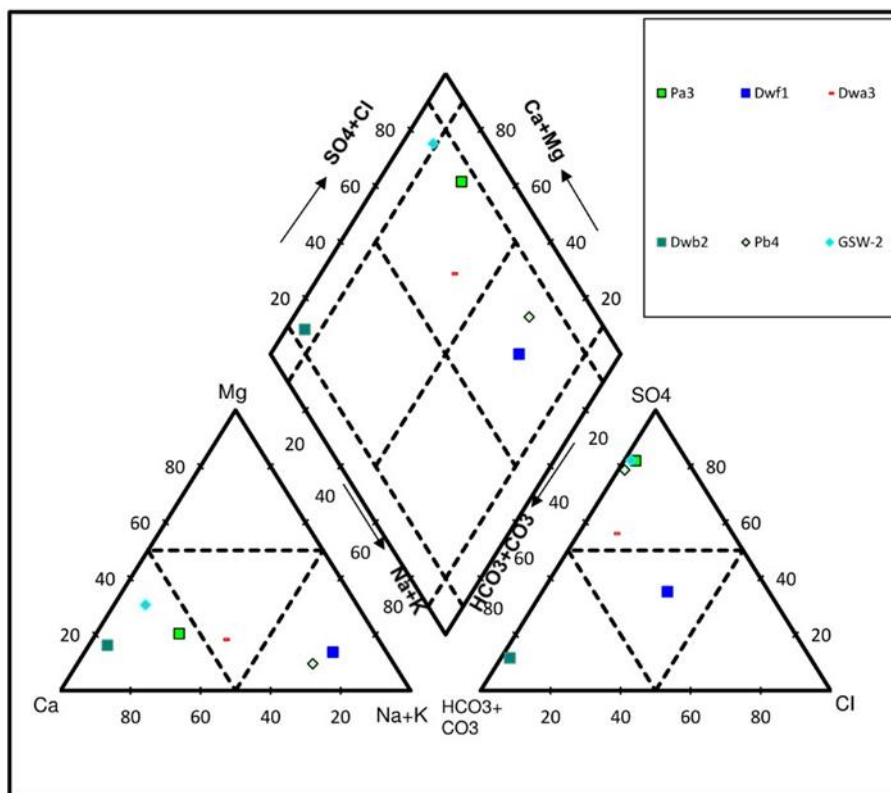
Figure 5.2. Plot of water samples on Piper diagram (from Ekmekçi et al., 2018)

5.1. Isotope Hydrology

The stable isotope analysis is a useful tool for determining recharge elevation and origin of groundwater in the system. Having dry carbonate rock surrounding the mine site, the origin of the groundwater in the metasediments and the diorite became a serious issue to be explained. A comprehensive stable isotope study was conducted to achieve this.

A total of 78 water samples were collected from water points such as rain water, surface waters, springs, groundwater in monitoring wells, pumping wells and piezometer wells. The sampling locations are shown in Figure 5.3. As can be seen from the figure, samples were not only collected from the mine site but it was performed in regional scale to obtain wide isotope variation with respect to elevation. Analysis were carried out in the Stable Isotope Laboratory of Hacettepe University by Liquid Laser Analyzer of Gatos Inc.[TM]. The result of analysis is given in Table 5.1.

Figure 5.3. Location of water points sampled for stable isotopes (from Ekmekçi et al., 2018)

Table 5.1. Results of stable isotope analyses a) rain waters, b) surface and groundwater 'ʰqo ʿƓᴏ gᴍᴋⱴʹcꞎ'423: +"

a)

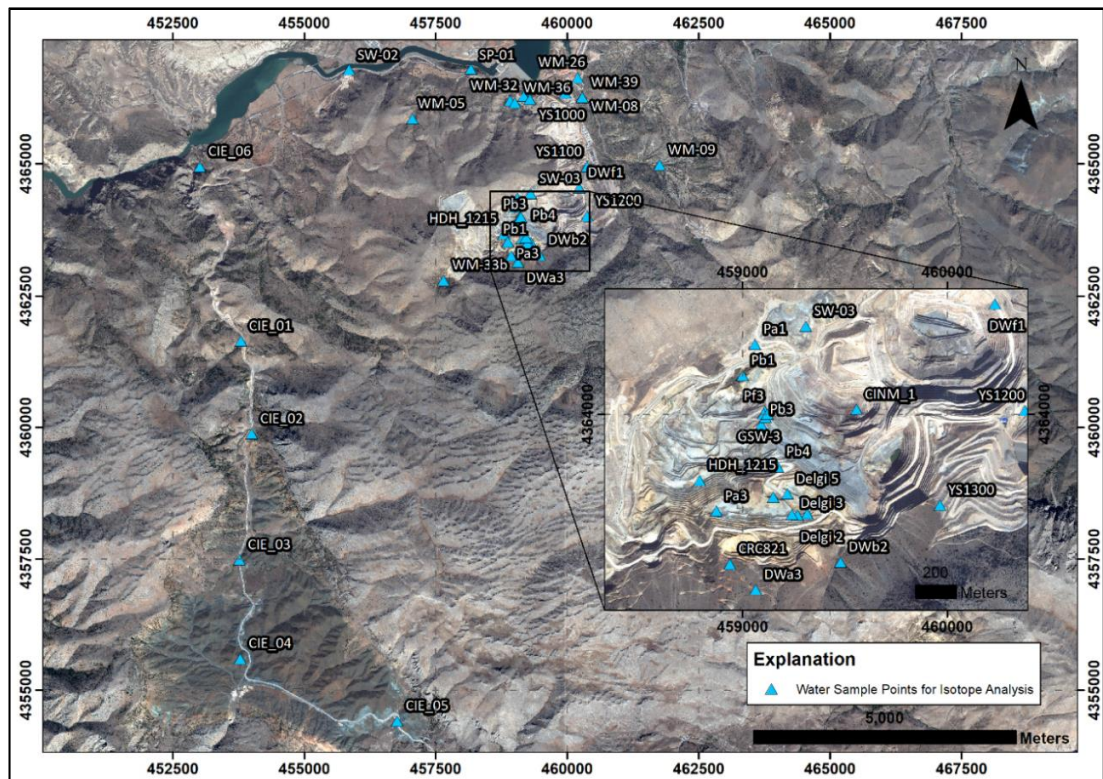| Sample ID	Date	Type	Latitude	Longitude	Elevation (m)	Temp. (°C)	pH	DO (mg/l)	Conductivity (us/cm)25°C	TDS (mg/l)	GWL (amsl)	Hydro-chemistry	δ 18O (‰)	δ 2H (‰)	D-Excess
YS1000-April-2017	April	Rain	459960.4	4366343.7	1000	N/A	N/A	N/A	N/A	N/A	N/A	+	-5.64±0.16	-36.39±1.08	8.76
YS1100-April-2017	April	Rain	460381.3	4364942.6	1100	N/A	N/A	N/A	N/A	N/A	N/A	+	-5.50±0.07	-34.92±0.64	9.06
YS1300-April-2017	April	Rain	459965.7	4363556	1300	N/A	N/A	N/A	N/A	N/A	N/A	+	-6.02±0.12	-37.93±0.36	10.26
YS1000-May-2017	May	Rain	459960.4	4366343.7	1000	N/A	N/A	N/A	N/A	N/A	N/A	+	-5.25±0.16	-32.69±1.48	9.33
YS1100-May-2017	May	Rain	460381.3	4364942.6	1100	N/A	N/A	N/A	N/A	N/A	N/A	+	-5.55±0.07	-34.08±1.05	10.33
YS1200-May-2017	May	Rain	460380.6	4364017.5	1200	N/A	N/A	N/A	N/A	N/A	N/A	+	-5.87±0.18	-36.56±1.40	10.4
YS1300-May-2017	May	Rain	459965.7	4363556	1300	N/A	N/A	N/A	N/A	N/A	N/A	+	-5.99±0.19	-36.39±0.59	11.54
YS1000-June-2017	June	Rain	459960.4	4366343.7	1000	N/A	N/A	N/A	N/A	N/A	N/A	?	-5.04±0.00	-35.32±0.00	4.98
YS1100-June-2017	June	Rain	460381.3	4364942.6	1100	N/A	N/A	N/A	N/A	N/A	N/A	?	-5.26±0.00	-35.39±0.00	6.65
YS1200-June-2017	June	Rain	460381.3	4364942.6	1200	N/A	N/A	N/A	N/A	N/A	N/A	?	-5.64±0.00	-37.95±0.00	7.15
YS1300-June-2017	June	Rain	459965.7	4363556	1300	N/A	N/A	N/A	N/A	N/A	N/A	?	-5.72±0.00	-39.06±0.00	6.68
YS1000-October-2017	October	Rain	459960.4	4366343.7	1000	N/A	N/A	N/A	N/A	N/A	N/A	?	-3.69±0.06	-15.57±0.30	13.99
YS1100-October-2017	October	Rain	460381.3	4364942.6	1100	N/A	N/A	N/A	N/A	N/A	N/A	?	-3.88±0.06	-13.23±0.40	17.82
YS1200-October-2017	October	Rain	460380.6	4364017.5	1200	N/A	N/A	N/A	N/A	N/A	N/A	?	-3.92±0.09	-14.60±0.52	16.75
YS1300-October-2017	October	Rain	459965.7	4363556	1300	N/A	N/A	N/A	N/A	N/A	N/A	?	-3.63±0.05	-13.18±0.13	15.85
YS1000-November-2017	November	Rain	459960.4	4366343.7	1000	N/A	N/A	N/A	N/A	N/A	N/A	?	-6.88±0.05	-44.96±0.46	10.1
YS1100-November-2017	November	Rain	460381.3	4364942.6	1100	N/A	N/A	N/A	N/A	N/A	N/A	?	-7.09±0.02	-44.33±0.51	12.31
YS1200-November-2017	November	Rain	460380.6	4364017.5	1200	N/A	N/A	N/A	N/A	N/A	N/A	?	-6.99±0.03	-41.38±0.24	14.55
YS1300-November-2017	November	Rain	459965.7	4363556	1300	N/A	N/A	N/A	N/A	N/A	N/A	?	-7.76±0.01	-45.06±0.24	17.03
YS1000-December-2017	December	Rain	459960.4	4366343.7	1000	N/A	N/A	N/A	N/A	N/A	N/A	?	-7.52±0.04	-45.52±0.28	14.61
YS1100-December-2017	December	Rain	460381.3	4364942.6	1100	N/A	N/A	N/A	N/A	N/A	N/A	?	-8.04±0.03	-49.10±0.15	15.25
YS1200-December-2017	December	Rain	460380.6	4364017.5	1200	N/A	N/A	N/A	N/A	N/A	N/A	?	-8.93±0.06	-55.71±0.60	15.69
YS1300-December-2017	December	Rain	459965.7	4363556	1300	N/A	N/A	N/A	N/A	N/A	N/A	?	-8.24±0.02	-51.32±0.21	14.6
YS1000-January-2017	January	Rain	459960.4	4366343.7	1000	N/A	N/A	N/A	N/A	N/A	N/A	?	-14.05±0.12	-97.46±0.41	14.95
YS1100-January-2017	January	Rain	460381.3	4364942.6	1100	N/A	N/A	N/A	N/A	N/A	N/A	?	-14.31±0.04	-100.78±0.29	13.67
YS1200-January-2017	January	Rain	460380.6	4364017.5	1200	N/A	N/A	N/A	N/A	N/A	N/A	?	-14.00±0.06	-98.96±0.16	13.02
YS1300-January-2017	January	Rain	459965.7	4363556	1300	N/A	N/A	N/A	N/A	N/A	N/A	?	-13.89±0.08	-97.94±0.04	13.22
YS1000-February-2018	February	Rain	459960.4	4366343.7	1000	N/A	N/A	N/A	N/A	N/A	N/A	?	-8.82±0.05	-57.01±0.31	13.55
YS1100-February-2018	February	Rain	460381.3	4364942.6	1100	N/A	N/A	N/A	N/A	N/A	N/A	?	-8.99±0.08	-57.62±0.27	14.29
YS1200-February-2018	February	Rain	460380.6	4364017.5	1200	N/A	N/A	N/A	N/A	N/A	N/A	?	-9.57±0.05	-61.38±0.20	15.16
YS1300-February-2018	February	Rain	459965.7	4363556	1300	N/A	N/A	N/A	N/A	N/A	N/A	?	-9.91±0.06	-64.45±0.26	14.84
YS1000-March-2018	March	Rain	459960.4	4366343.7	1000	N/A	N/A	N/A	N/A	N/A	N/A	?	-5.04±0.07	-33.84±1.63	6.52
YS1100-March-2018	March	Rain	460381.3	4364942.6	1100	N/A	N/A	N/A	N/A	N/A	N/A	?	-6.27±0.13	-42.11±1.44	8.02
YS1200-March-2018	March	Rain	460380.6	4364017.5	1200	N/A	N/A	N/A	N/A	N/A	N/A	?	-6.42±0.07	-45.55±0.77	5.79
YS1300-March-2018	March	Rain	459965.7	4363556	1300	N/A	N/A	N/A	N/A	N/A	N/A	?	-6.60±0.10	-44.24±0.32	8.6
N/A	N/A	N/A	N/A	N/A	N/A	N/A	N/A	N/A	N/A	N/A	N/A	N/A	N/A	N/A	N/A
YS1000-May-2018	May	Rain	459960.4	4366343.7	1000	N/A	N/A	N/A	N/A	N/A	N/A	+	-6.62±0.16	-36.83±1.21	16.15
YS1100-May-2018	May	Rain	460381.3	4364942.6	1100	N/A	N/A	N/A	N/A	N/A	N/A	+	-6.90±0.12	-35.19±1.58	20.04
YS1300-May-2018	May	Rain	459965.7	4363556	1300	N/A	N/A	N/A	N/A	N/A	N/A	+	-6.61±0.11	-38.98±1.22	13.91

Sample ID	Date	Type	Latitude	Longitude	Elevation (m)	Field Parameters						Hydro- chemistry	Stable Isotopes		
						Temp. (°C)	pH	DO (mg/l)	Conductivity (μs/cm)25°C	TDS (mg/l)	GWL (amsl)		δ 18O (‰)	δ 2H (‰)	D-Excess
CIE_03	25-02-17	Fountain	453769	4357481.3	1435	5.88	7.53	12.8	190	123	N/A	?	-11.65 ± 0.10	-76.85 ± 0.77	16.42
CIE_04	25-02-17	Fountain	453781.8	4355600.7	1465	0.3	8.28	12.3	130	94	N/A	?	-09.65 ± 0.06	-60.24 ± 0.35	16.95
CIE_05	25-02-17	Fountain	456767.2	4354412	1340	8.12	8.62	11.3	199	129	N/A	?	-12.04 ± 0.19	-78.18 ± 0.87	18.17
CIE_06	25-02-17	Fountain	453012.7	4364944.4	930	8.52	7.91	11.1	165	107	N/A	?	-09.01 ± 0.09	-60.22 ± 1.00	11.82
CINM_1	27-02-17	Seepage	459558.1	4364022.4	1097.4	-	-	-	-	-	-	?	-09.57 ± 0.10	-65.71 ± 0.67	10.85
HDH_C_S_1260_23	27-02-17	Drain	459151.4	4363594.2	1259.8	-	-	-	-	-	-	?	-09.43 ± 0.08	-64.69 ± 0.88	10.75
HDH_1215	27-02-17	Drain	458793	4363677	1215	-	-	-	-	-	-	?	-09.65 ± 0.11	-66.51 ± 0.99	10.7
Delgi 1	28-02-17	Monitoring Well	459317.5	4363513.5	1267.3	12.8	7.05	2.7	-	-	1262.7	?	-10.14 ± 0.08	-69.99 ± 0.61	11.16
Delgi 2	28-02-17	Monitoring Well	459270.4	4363507.2	1267.9	9.9	7.07	7.92	-	-	1264.5	?	-12.39 ± 0.07	-85.27 ± 0.91	13.89
Delgi 3	28-02-17	Monitoring Well	459243.5	4363509.5	1266.4	10.3	6.92	2.5	-	-	1264.1	?	-10.34 ± 0.03	-70.80 ± 0.52	11.91
Delgi 5	28-02-17	Monitoring Well	459221.2	4363610.2	1262.2	10.9	6.71	2.2	-	-	1261.5	?	-10.20 ± 0.11	-70.71 ± 0.89	10.9
CRC821 or 19	01-03-17	Monitoring Well	458939.5	4363267.8	1366.7	10.5	7.27	2.31	-	-	1347.6	?	-08.56 ± 0.07	-54.27 ± 0.58	14.24
WM-05	03-03-17	Monitoring Well	457063.7	4365854.5	1020	15	7.46	2.76	935	458	901	?	-10.13 ± 0.14	-69.68 ± 0.96	11.37
WM-08	03-03-17	Monitoring Well	460291	4366260	962	13.7	7.27	2.9	786	390	946.6	?	-09.58 ± 0.13	-66.03 ± 0.22	10.6
WM-09	03-03-17	Monitoring Well	461760	4364977	897	15.4	7.54	4.74	1104	570	883.3	?	-10.41 ± 0.05	-75.12 ± 0.36	8.17
WM-26	03-03-17	Monitoring Well	460203	4366637	937	15.4	7.85	2.47	561	275	904.9	?	-09.97 ± 0.19	-70.89 ± 0.82	8.87
WM-32	03-03-17	Monitoring Well	458917.4	4366200	898.7	14	7.9	8.81	503	245	870.3	?	-09.97 ± 0.16	-68.96 ± 0.72	10.76
WM-33b	03-03-17	Monitoring Well	457652	4362796	1454	11.2	7.48	4.5	339	164	1308.7	?	-11.78 ± 0.14	-79.67 ± 1.00	14.58
WM-36	03-03-17	Monitoring Well	459009.1	4366157.1	904.1	13.6	8.07	9.04	375	182.7	862.4	?	-10.07 ± 0.06	-68.41 ± 0.62	12.19
WM-39	03-03-17	Monitoring Well	460292	4366263	962	13.7	7.34	5.17	749	369	873	?	-09.77 ± 0.12	-66.97 ± 1.05	11.15
ADR (WM-17,WM-41, WM-42)	03-03-17		N/A	N/A	N/A	13.5	7.46	8.93	377	184	N/A	?	-10.55 ± 0.18	-69.73 ± 1.73	14.69
WM-17	03-03-17	Pumping Well	459208.9	4366268	979.8	N/A	N/A	N/A	N/A	N/A	N/A	?	N/A	N/A	N/A
WM-41	03-03-17	Pumping Well	459177.6	4366284	983.9	N/A	N/A	N/A	N/A	N/A	N/A	?	N/A	N/A	N/A
WM-42	03-03-17	Pumping Well	459297.8	4366221.5	992.1	N/A	N/A	N/A	N/A	N/A	N/A	?	N/A	N/A	N/A
SW-02	03-03-17	Surface Water	455851.6	4366794.9	870	8.5	8.04	11.12	570	271	N/A	?	-10.83 ± 0.13	-72.44 ± 0.80	14.2
SW-03	03-03-17	Surface Water	459310.7	4364428.7	N/A	8.5	7.1	9.42	1481	738	N/A	?	-09.49 ± 0.12	-67.66 ± 0.90	8.26
SP-01	03-03-17	Spring	458170.4	4366796.8	869	12.7	7.62	7.37	514	251	N/A	?	-10.69 ± 0.09	-71.27 ± 0.85	14.22
Pf3_1	28-10-17	Groundwater	459111.4	4364014.8	1195.8	17.2	8.06	N/A	720	N/A	N/A	?	-10.51 ± 0.06	-68.20 ± 0.48	15.91
Pf3_2	28-10-17	Groundwater	459111.4	4364014.8	1195.8	16.8	8.32	N/A	618	N/A	N/A	?	-10.45 ± 0.04	-69.53 ± 0.17	14.06
DWf1	10-11-17	Groundwater	460233.6	4364538	1143.6	15.8	7.89	N/A	757	N/A	N/A	?	-10.49 ± 0.05	-68.16 ± 0.34	15.75
Pa3	06-12-17	Groundwater	458874.8	4363526	1275.3	14.1	7.08	N/A	2010	N/A	N/A	?	-10.23 ± 0.03	-70.50 ± 0.19	11.32
Dwf1_20dk	10-11-17	Groundwater	460233.6	4364538	1143.6	15.8	7.89	N/A	757	N/A	N/A	?	-10.40 ± 0.08	-69.00 ± 1.14	14.19
Dwf1_40dk	10-11-17	Groundwater	N/A	N/A	N/A	N/A	N/A	N/A	N/A	N/A	N/A	?	-10.35 ± 0.10	-70.33 ± 0.57	12.47
Dwf1_75dk	10-11-17	Groundwater	N/A	N/A	N/A	N/A	N/A	N/A	N/A	N/A	N/A	?	-10.42 ± 0.04	-70.88 ± 0.57	12.47
Pa1	31-12-17	Groundwater	459061.8	4364340.8	1177.3	N/A	N/A	N/A	N/A	N/A	N/A	?	-10.63 ± 0.04	-71.78 ± 0.41	13.24
Pb1	05-02-18	Groundwater	459001.9	4364188.5	1170.2	13.5	7.84	N/A	1593	N/A	N/A	?	-10.89 ± 0.05	-76.34 ± 0.89	10.75
PB3	03-03-18	Groundwater	459093	4363949.4	1205.2	15.3	7.75	1.86	644				-10.21 ± 0.08	-70.26 ± 0.18	11.44
Pb4	22-02-18	Groundwater	459173.3	4363742.2	1230.2	13.5	8.41	2.4	2653	N/A	N/A	?	-9.89 ± 0.09	-69.37 ± 0.30	9.77
DWb2	28-03-18	Groundwater	459479.6	4363276.9	1312.7	18.4	8.26	N/A	283	N/A	N/A	?	-9.89 ± 0.14	-65.03 ± 0.65	14.09
DWa3	16-04-18	Groundwater	459065.6	4363143.1	1388.6	N/A	N/A	N/A	N/A	N/A	N/A	?	-10.77 ± 0.08	-74.00 ± 0.36	0
GSW-1		Groundwater	459112.8	4363984.5	1197								-10.11 ± 0.08	-80.57 ±1.21	0.35
GSW-1 3v		Groundwater	459112.8	4363984.5	1197								-10.62 ± 0.06	-78.18 ± 0.89	6.8
GSW-2 (1)	05-06-18	Well	459104.7	4364000.4	1196.8	21.4	8.58	0.84	886				-10.39 ± 0.05	-81.34 ± 0.81	1.82
GSW-2 (2)	05-06-18	Well	459104.7	4364000.4	1196.8	21.6	8.23	0.51	860				-10.54 ± 0.05	-82.67 ± 0.35	1.62
GSW-3	12-06-18	Well	459121.9	4363998.6	1196.7	N/A	N/A	N/A	N/A				-10.48 ± 0.08	-83.83 ± 0.66	0.03

5.2. Isotopic Characteristics of Waters in Çöpler Area

The results of the stable isotope analysis showed that the deuterium and oxygen -18 is characterized by a deuterium excess of 14 (Ekmekçi et al., 2018). The local meteorological line obtained from the equation of D=8O-18+14. The graph of oxygen-18 vs deuterium is given in Figure 5.4. The plots of rain water were shown as green dots and the groundwater were shown as blue dots. The rain water plots over a wide range. Rain may be quite rich with respect to heavy isotopes which indicates the summer rain and while the winter rain is much depleted and forms one of the end members. As can be seen in the figure, the groundwater plots between winter rain and the warmer period rain suggesting that groundwater is mainly recharged by spring rains.
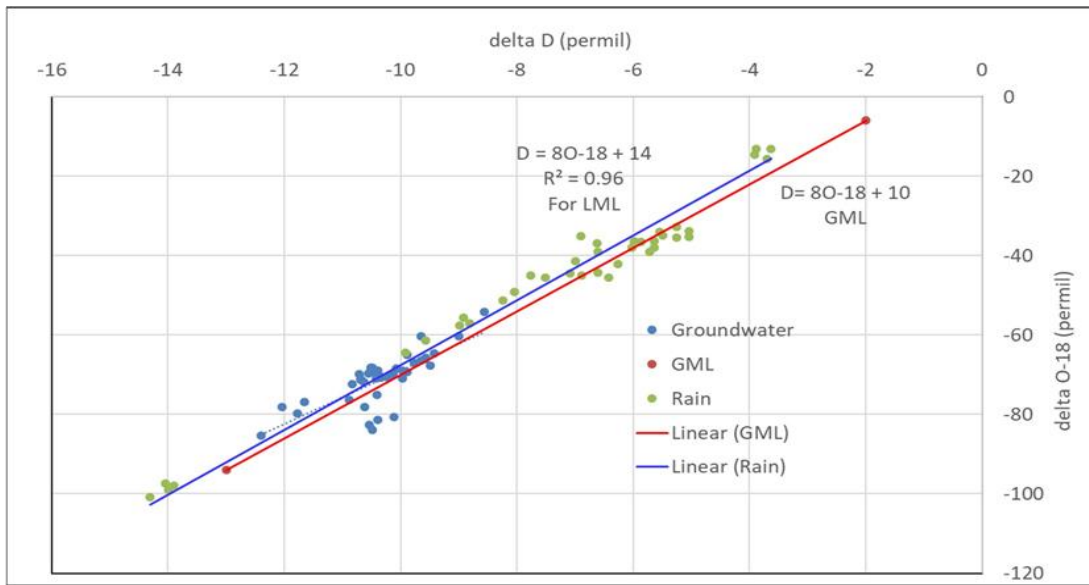
Figure 5.4. Plot of D- O- 18 and the meteorological line for the Çöpler site (from Ekmekçi et al., 2018)

5.3. Estimation of Recharge Area Elevations

The elevation–stable isotope equations and regression equations were established for both oxygen-18 and deuterium by Ekmekçi et al. (2018) (Figure 5.5). The recharge elevations estimated for groundwater in the mine site are given in Table 5.2. From both equations, different elevation estimations were obtained. The results show that the metasediments and diorite are recharged from between 1250 masl and 1400 masl on

66

the average. Even with the highest area considered, the recharge area falls within the slopes of the carbonate rocks surrounding the mine site.
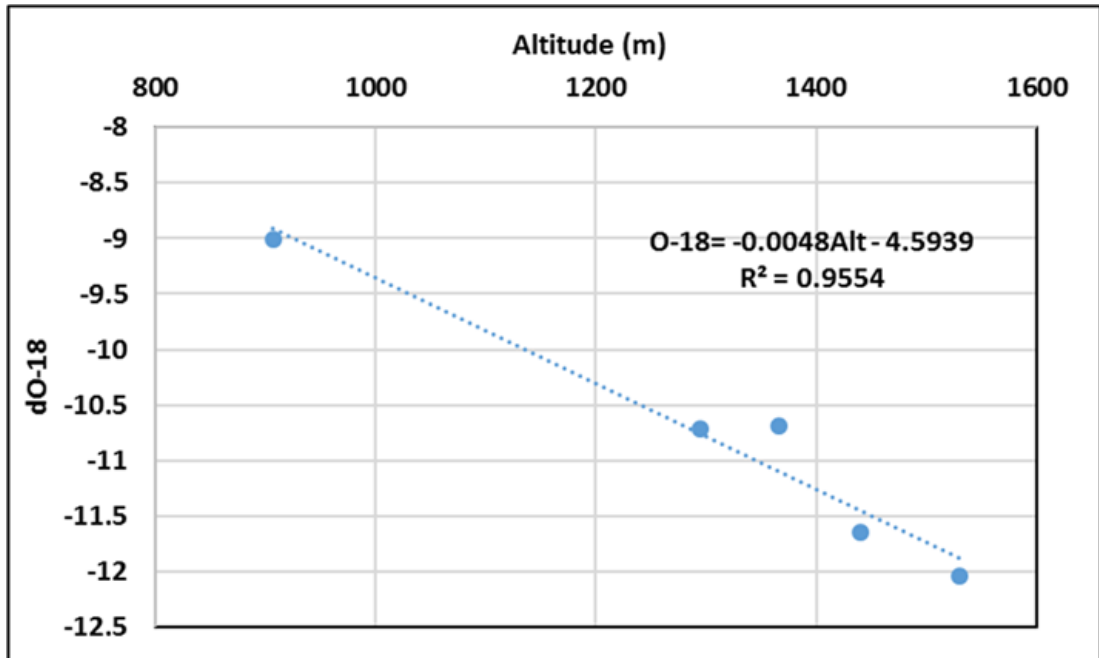
a
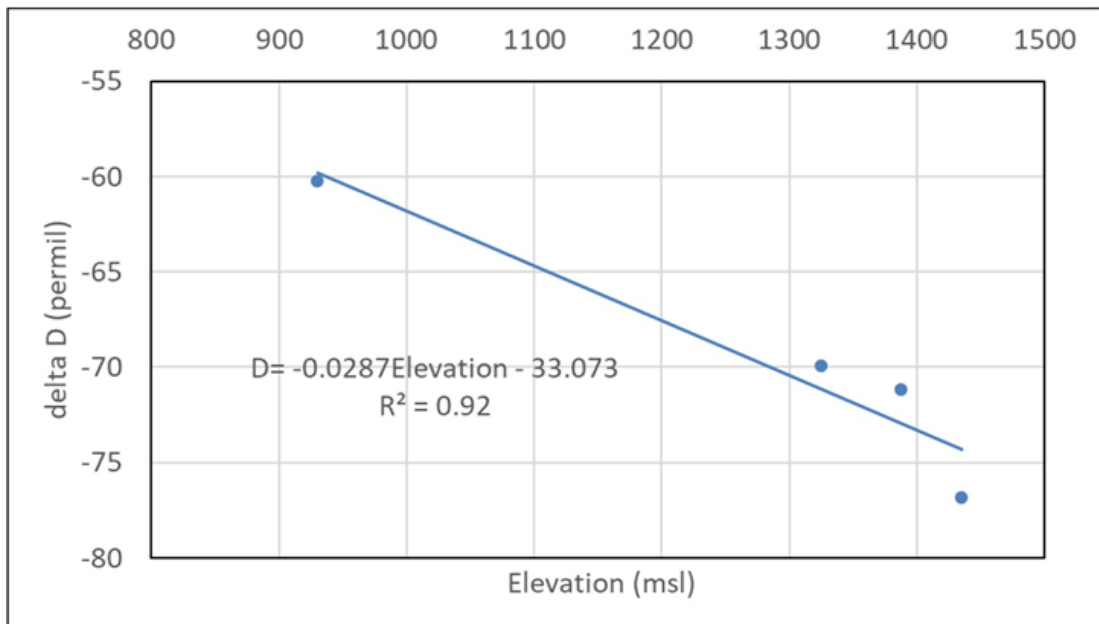
b

Figure 5.5. Regression between elevation and stable isotope a) oxygen- 18, b) deuterium (from Ekmekçi et al., 2018)

Table 5.2. Estimated recharge areas for groundwater in the mine site using O- 18 and D (from Ekmekçi et al., 2018)

Sample	Date	d O-18 (permil)	dD (permil)	Recharge Elevation (m)	
				O-18	D
Pf3_1	28-10-17	-10.51	-68.20	1267	1225
Pf3_2	28-10-17	-10.45	-69.53	1253	1272
DWf1	10-11-17	-10.49	-68.16	1262	1224
Pa3	06-12-17	-10.23	-70.50	1205	1305
Dwf1_20min	10-11-17	-10.40	-69.00	1242	1253
Dwf1_40min	10-11-17	-10.35	-70.33	1232	1300
Dwf1_75min	10-11-17	-10.42	-70.88	1247	1319
Pa1	31-12-17	-10.63	-71.78	1292	1350
Pb1	05-02-18	-10.89	-76.34	1348	1509
PB3	03-03-18	-10.21	-70.26	1202	1297
Pb4	22-02-18	-9.89	-69.37	1132	1266
DWb2	28-03-18	-9.89	-65.03	1132	1115
DWa3	16-04-18				
GSW-1		-10.11	-80.57	1181	1656
GSW-1 3v		-10.62	-78.18	1291	1573
GSW-2 (1)	05-06-18	-10.39	-81.34	1241	1683
GSW-2 (2)	05-06-18	-10.54	-82.67	1272	1729
GSW-3	12-06-18	-10.48	-83.83	1260	1770

CHAPTER 6

HYDROGEOLOGICAL CONCEPTUAL MODEL

The main objective of this study is to develop a representative conceptual hydrogeological model of the mine site. Data obtained from the field are evaluated in developing a conceptual model of the mine site. Field studies have been completed in June 26, 2018. However, monitoring of groundwater level and pore water pressure were continued until June 12, 2019.

6.1. Çöpler Groundwater System

The Çöpler groundwater system consist of the carbonate rocks surrounding, metasediments and diorite units at the center of the mine site and the Çöpler stream basin. At certain depths of the carbonate rock mass, karstified zones was observed which may indicate an aquifer. The metasediments and diorite units hydrogeologically act as single unit and has low permeability compared to carbonate rocks. In normal conditions, the expectation is that the carbonate rocks supply inflow toward the Çöpler groundwater system but ore drillings in the depression-like Zangardere and Uzundere areas have showed that a diorite intrusion act like a barrier against groundwater flow through the Çöpler groundwater system. According to the conceptual model illustrated in Figure 6.3, the carbonate rock mass divided into two parts. The larger part forming the main carbonate rock aquifer and the small part between the diorite intrusion and the metasediments has small area for recharge. The thin saturated zone is seem to be discharged towards the west to Karasu River and partly to the east to Sabırlı Creek.
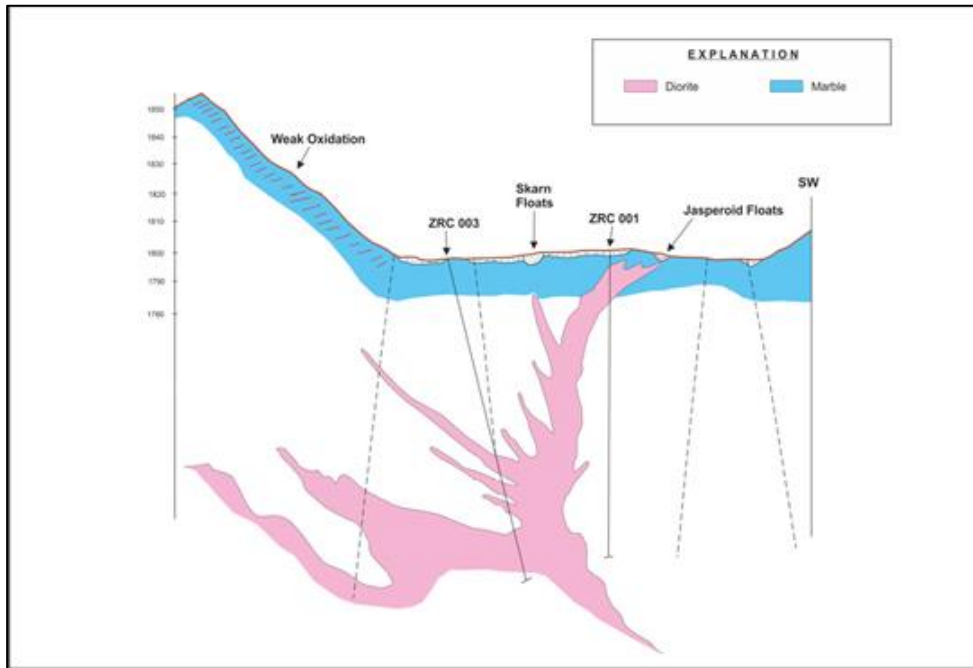
Figure 6.1. Geological cross-section at the Zangadere depression-like feature (by D. Yavuz)
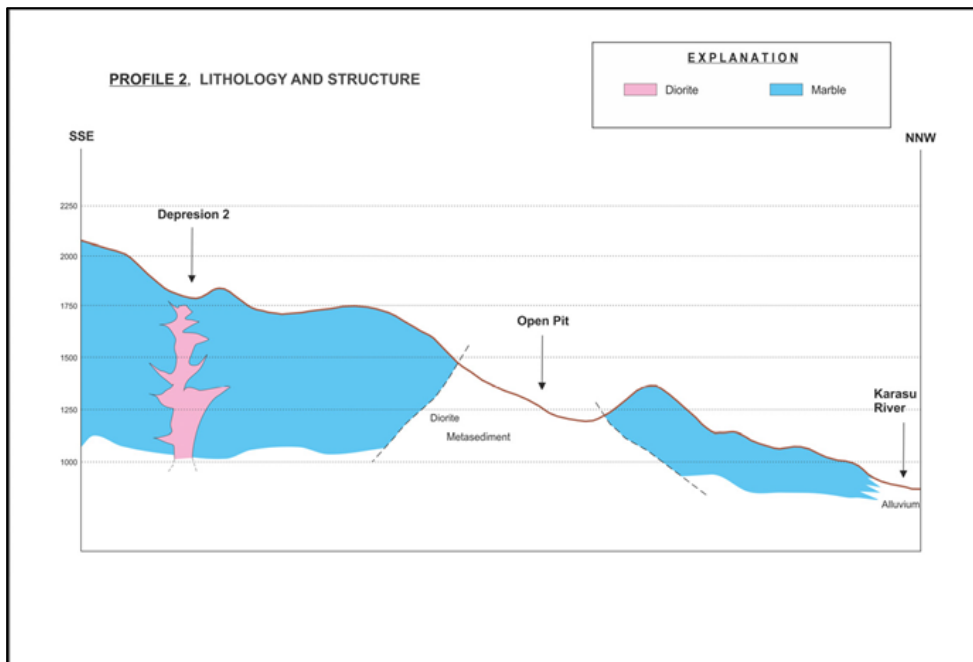
a
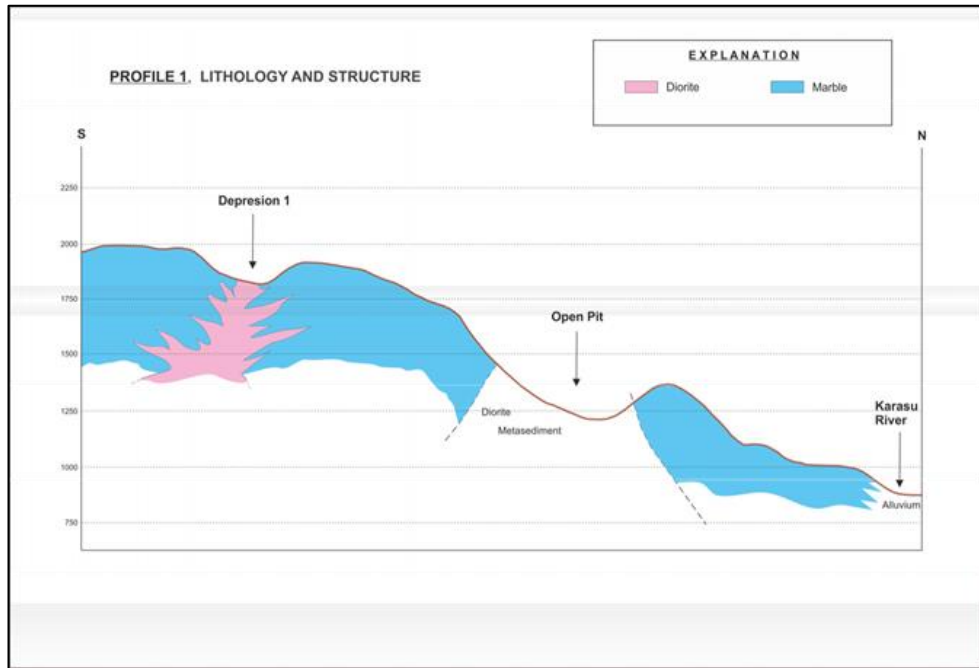
b

Figure 6.2. Geological cross-sections extending from depression-like features in the south to Karasu River in the north, traversing the mine area a) Zangadere, b) Uzundere (from Ekmekçi et al., 2018)
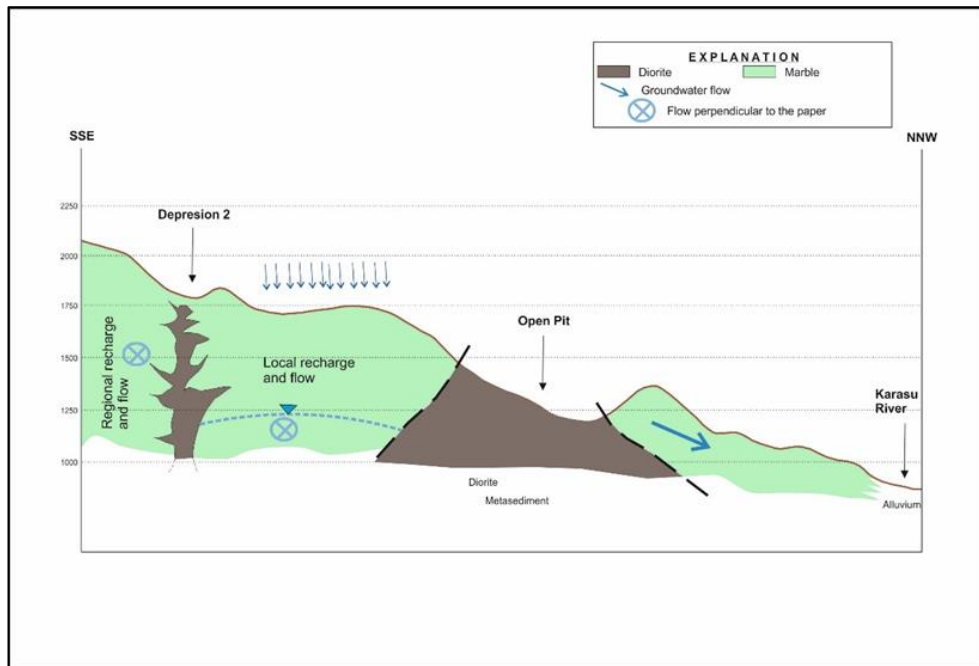
Figure 6.3. Hydrogeological cross-section demonstrating the role of diorite intrusion in regional groundwater flow (from Ekmekçi et al., 2018)

6.2. Conceptual Model of Site Hydrogeology

Hydrogeological conceptual model of the mine site was developed from available and obtained data of geology, insitu tests, hydrochemical and isotopic data to represents the mine site. The metasediments and diorite units act as a single hydrogeologic unit. Groundwater level measurements have showed that the metasediments and diorite are saturated almost all along the year. A total of 6 springs discharging from different elevations were sampled for stable isotope analysis. This information is used to estimate the altitude of the area recharging the flow domain. The analyses results showed that water samples collected from drill holes at elevation of about 1260 m were found to be recharged by infiltration from local precipitation, which means there is no evidence of groundwater contribution from distant highlands. The deuterium excess value of the highland springs is about 16 while it is about 10 at the mine site. Furthermore, the downward hydraulic gradient measured at the VWPs supports this finding.

The metasediments and diorite have high total porosity and low specific yield indicating that the pore water is retained by electrostatic forces in the medium and it resists to flow due to low hydraulic conductivity. The system is recharged by infiltration from direct local precipitation and outflow seems to occur by evapotranspiration. An important part of the surface runoff was observed to accumulate in topographical depressions and mainly in unlined ponds and canals excavated around the site. These features form a kind of artificial infiltration ponds. The vertical change in the hydraulic conductivity values suggests that the medium is heterogeneous. Hydrogeological conceptualization made for cross-section A is given as an example in Figure 6.4. According to the conceptual model given in Figure 6.4, the medium consist of different water bearing levels. The shallow layers are in under unconfined conditions and deeper layers are in leaky conditions. The conceptual model, which demonstrates the general working system of the mine site is given in Figure 6.5 (Ekmekçi et al., 2018).
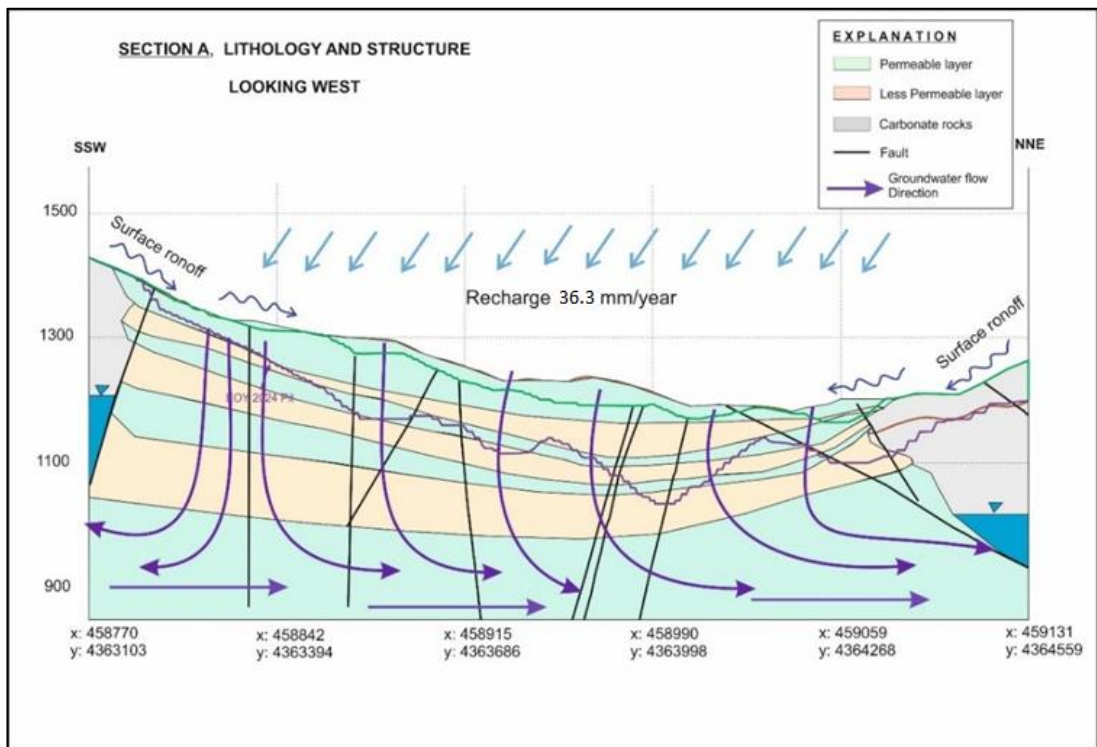
Figure 6.4. Hydrogeological conceptual model for the flow domain on cross-section A (from Ekmekçi et al., 2018)
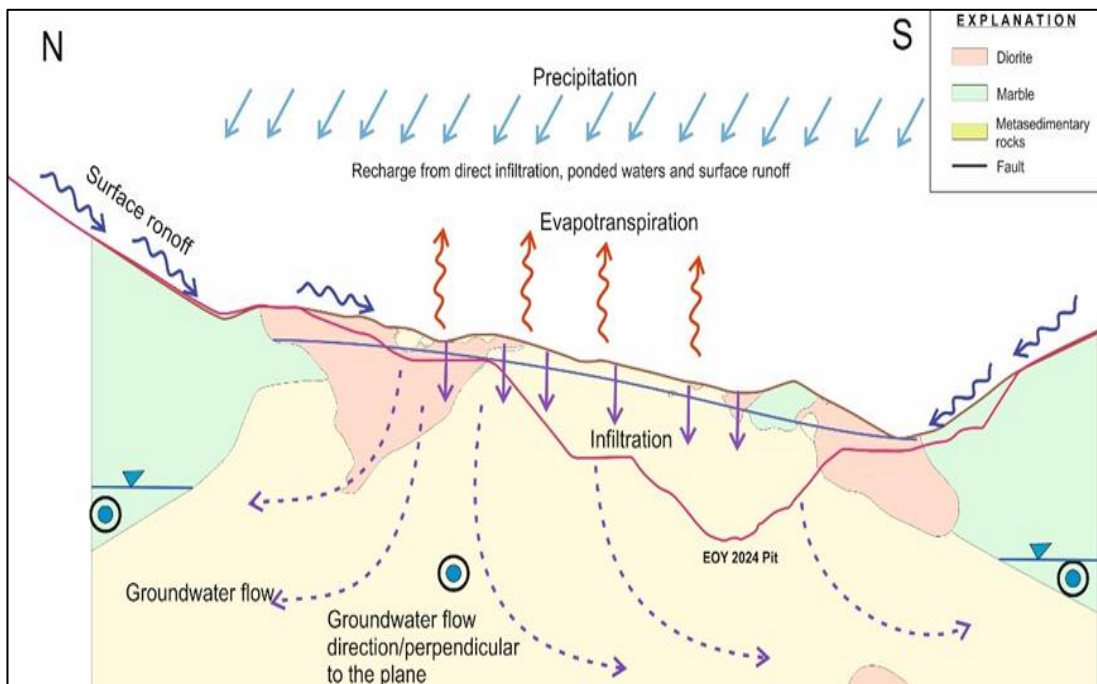
Figure 6.5. Hydrogeological conceptual model of the mine site (from Ekmekçi et al., 2018)

CHAPTER 7

CONCLUSIONS AND RECOMMENDATIONS

7.1. Conclusions

The mine site consists of three major lithological units: Carbonate rocks, metasediments and diorite. The metasediments and diorite shows similar hydrogeological characteristics, so these two units act as one single hydrostratigraphic unit.

The carbonate rock thought as major aquifer in the mine site. However, research results have showed that the carbonate unit does not contain groundwater in significant amount because of diorite intrusion at the Uzundere-Zangardere area where the highland in the south of the mine site. The intrusion acts like a hydrogeological barrier to groundwater flow and also it explains the dry carbonate rock mass surrounding the mine site.

Packer test results suggest the metasediments and diorite has heterogeneous medium. Therefore, it is presumable that they are subdivided into layers of different hydraulic conductivities as seen in the vertical profiles. Also, downward hydraulic gradient was observed in almost all piezometers drilled in the metasediments and diorite and it generally increases with depth.

The total porosity of metasediments and diorite units was found as 23 % and effective porosity was found as 5 %, meaning that the metasediments and diorite unit holds pore water against gravity. Upper sections of metasediments and diorite has higher permeability than lower sections. Decreasing permeability profile can be observed with depth which indicates a sort of perched aquifer formation in the site.
Complicated fault systems have an impact on flow of groundwater in the mine site. The hydrogeological characterization of faults could not be determined but the pore

water pressure obtained from vibrating wire piezometers suggest that faults generally act as an impermeable barrier in the site.

Stable isotope analysis has indicated that the metasediments-diorite are recharged by infiltration from local precipitation and there is no any sign of contribution to recharge from distant highlands. Recharge from precipitation was calculated as 36 mm/year.

Infiltration from surface runoff from the small watershed around the mine site contributes only in small amounts to recharge. Water ponded in canals act as artificial recharge sites whose contribution to groundwater are more significant than the infiltration from surface runoff.

7.2. Recommendations

The monitoring should continue at least one more year. The vibrating wire piezometer and large diameter wells should be protected against any kind of damage.

Sampling of groundwater from GSW wells on monthly basis for hydrochemical and stable isotope analysis has a great importance on hydrogeological conceptual model of the mine site. Pumps should be equipped in those wells to easily collect the samples.

The seepage faces which encountered in the mine site should be marked on map and coordinates of seepage faces should be noted. The canals dug on benches of the mine should be lined with impervious liners and ponding of water should not be allowed.

Hydrogeological characterization of the metasediments-diorite unit was achieved by packer testing. However, the data represents a small section of the material. There should be a direct test on the faults in the mine site to assess their nature.

Development of 3D Groundwater model of mine site is necessary for predicting pore water distribution and groundwater conditions precisely.

REFERENCES

Alacer Gold, 2013, Technical Report on the Çöpler Mineral Resource Update, Erzincan Province, Turkey, March 2013, 171p.

Alacer Gold, 2016. Çöpler Mine NI 43- 101 Technical Report, Erzincan Province, Turkey, June 2016, 384p.

Ekmekçi, M. and Tezcan, L., 2007. Hydrogeological Appraisal of The Çöpler Site (İliç-Erzincan), Hacettepe University International Research & Application Center for Karst Water Resources, 88p.

Ekmekçi, M., Yazıcıgil, H., Argunhan Atalay, Ç., Tayyar, D. and Kalkan, F., 2018. Optimization of Groundwater Control for Slope Stability at Çöpler Mine Site. Final Report, Ankara

Ekmekçi, M., Yazıcıgil, H. and Tayyar, D., 2019. Optimization of Groundwater Control for Slope Stability at Çöpler Mine Site. Monitoring Report, Ankara

Golder, 2013. Numerical Seepage Modeling for Leach Pad, Tailings Storage Facilities and Waste Rock Dumps at Çöpler Sulphide Project, Eastern Turkey, Turkey

Golder, 2014. Çöpler Mine Pit Slope Design Review, April 2014 Golder Associates, Reno

Golder, 2015. Çöpler Mine Sulfide Expansion Project, Slope Design Recommendations for Pit Slope Optimization Report, April 2015 Golder Associates, Reno

Golder, 2016. Site- Wide Surface Water Management Plan Update, Çöpler Mine Complex, April 2016 Golder Associates, Ankara

Houlsby, A.C. (1976). Routine interpretation of the Lugeon water-test. Quarterly Journal of Engineering Geology, 9, 303313.

Houlsby, A. C. 1990. Construction and Design of Cement Grouting: A guide to grouting in Rock Foundations. Volume 67 of Wiley Series of Practical Construction Guides, ISSN 0271-6011, John Wiley & Sons, Inc., 442p.

INR, 2017. Çöpler Gold Mine Surface Water Management Preliminary Design Report, INR Mühendislik ve Müşavirlik A.Ş., Ankara, 25p.

McCabe, G. L., and S. L. Markstrom, 2007: A monthly water-balance model driven by a graphical user interface. U.S. Geological Survey Open-File Rep. 2007-1088, 6 pp.

Özgül, N., Tursucu, A., Özyardimci, N., Senol, M., Bingöl, I. and Uysal, S. 1981. Munzur Dağlari'nın Jeolojisi, 136Ankara: Min. Res. Exptor. Inst. Turkey. Report. No. 6995, 136 p.

Roeper, T.R., Soukup, W. G & O'Neill, R. L. 1992. The Applicability of the Lugeon Methods of Packer Test Analysis to Hydrogeologic Investigation. Focus Conference on Eastern Regional Groundwater Issue, National Groundwater Association, Dublin, 8(3):29-36.

SE, 2010. Çöpler Sulfide Expansion Project Prefeasibility Study for Çukurdere Madencilik San. ve Tic. Ltd. Şti., 365p.

SWS, 2010. Hydrogeological Conceptual Model for The Çöpler Project, Schlumberger Water Services, Turkey, 23p.

SRK, 2015. "Volume 1: ESIA Report on the Çöpler Gold Mine Sulfide Expansion Project, Appendices., report prepared for Anagold Madecilik San. ve Tic. A.Ş., SRK Danışmanlık ve Mühendislik A.Ş., Report/Project Number: 941003. September 2015, Ankara, 262p.

Terrane, 2018. Report on Structural Mapping and 3D Fault Modeling.

Xu, Y., and Van Tonder, G.J. 2001. Estimation of recharge using a revised CRD method. Water SA 27 (3) 341–344.

Xu, Y. and Beekman H.E., 2003. Groundwater Recharge Estimation in Southern Africa. UNESCO IHP Series No. 64. UNESCO, Paris.

APPENDICES

APPENDIX A

Fracture Frequency Profiles for Drill Holes
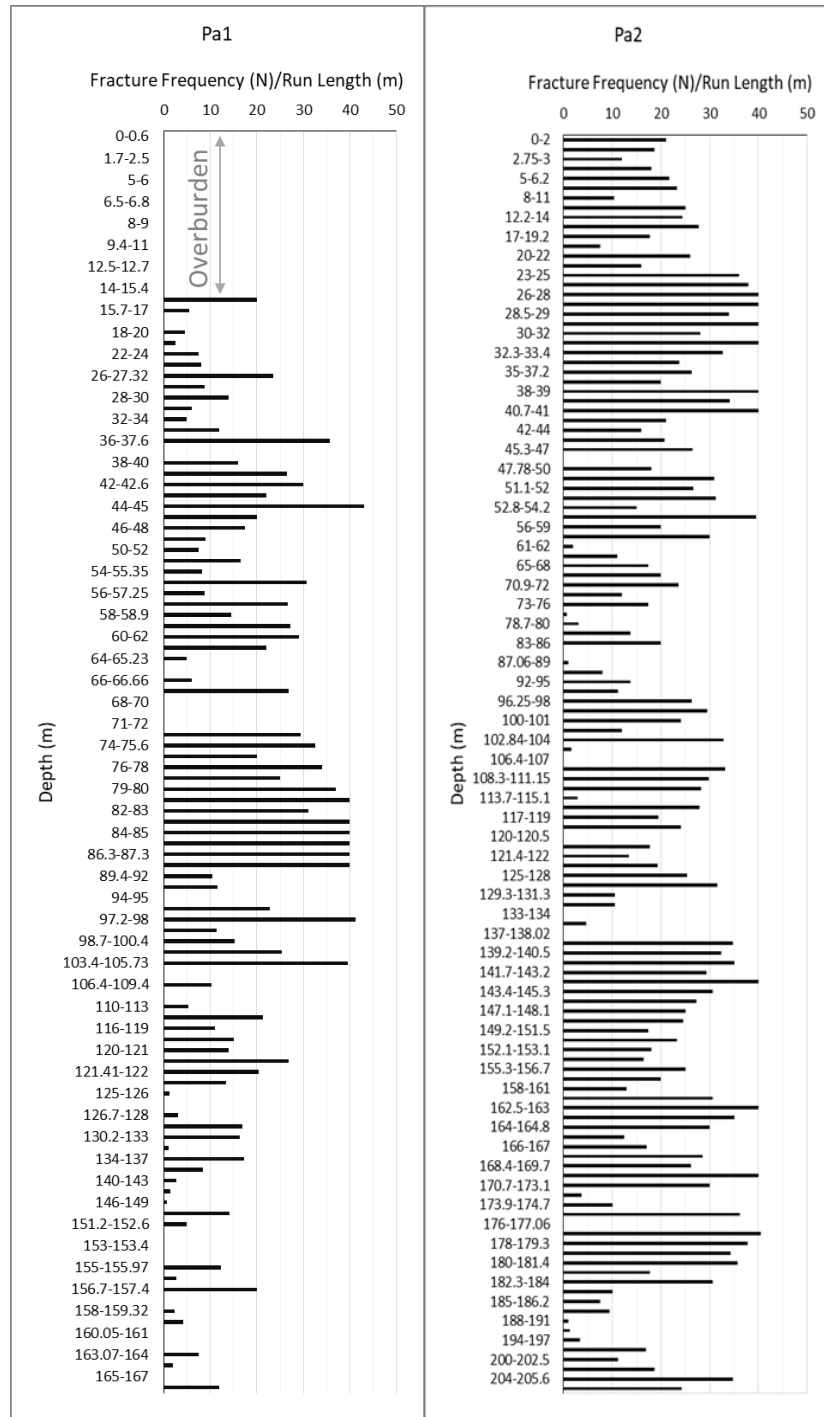
Figure A-1. Fracture Frequency (N)/Run Length (m) of Pa1 and Pa2
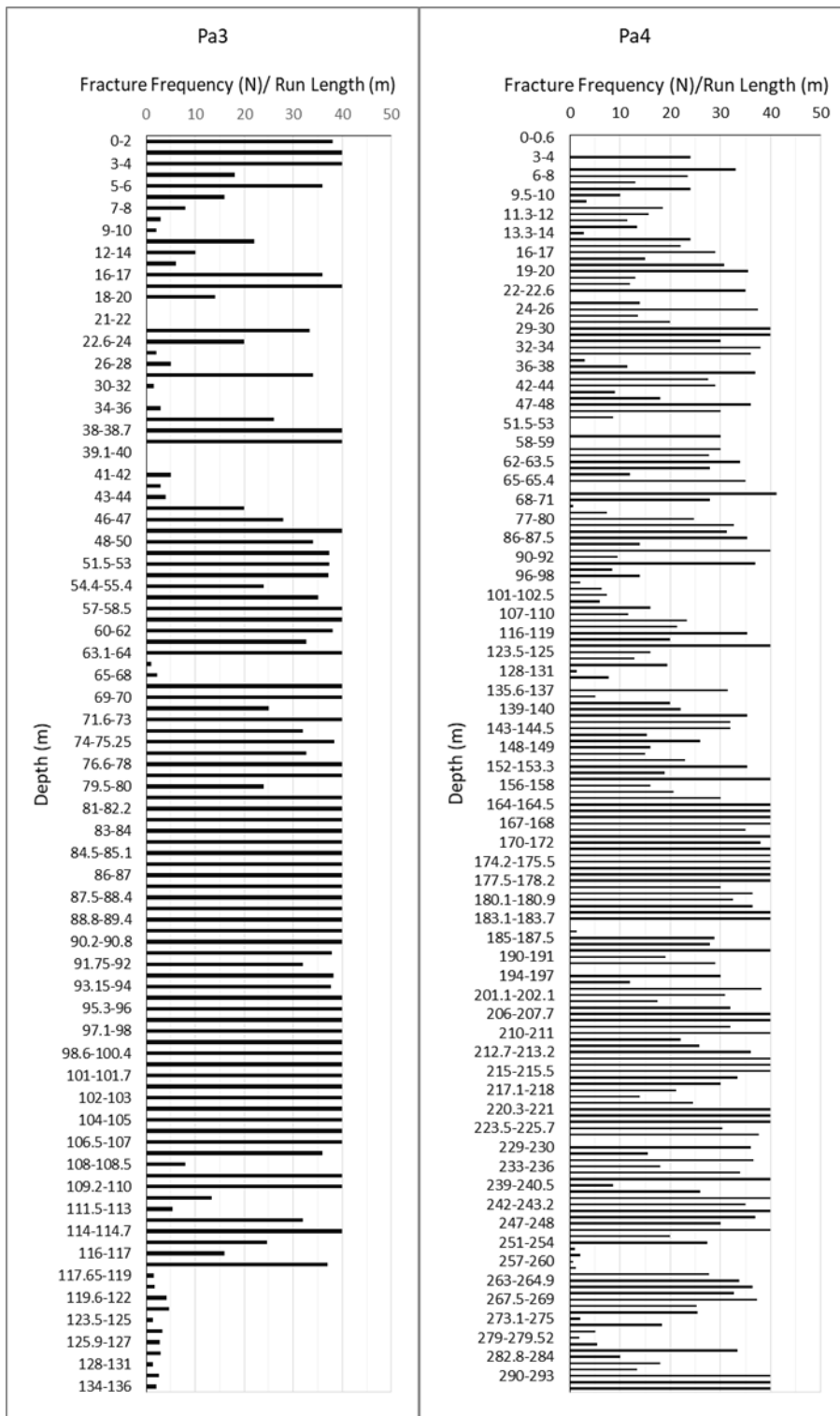
Figure A-2. Fracture Frequency (N)/Run Length (m) of Pa3 and Pa4
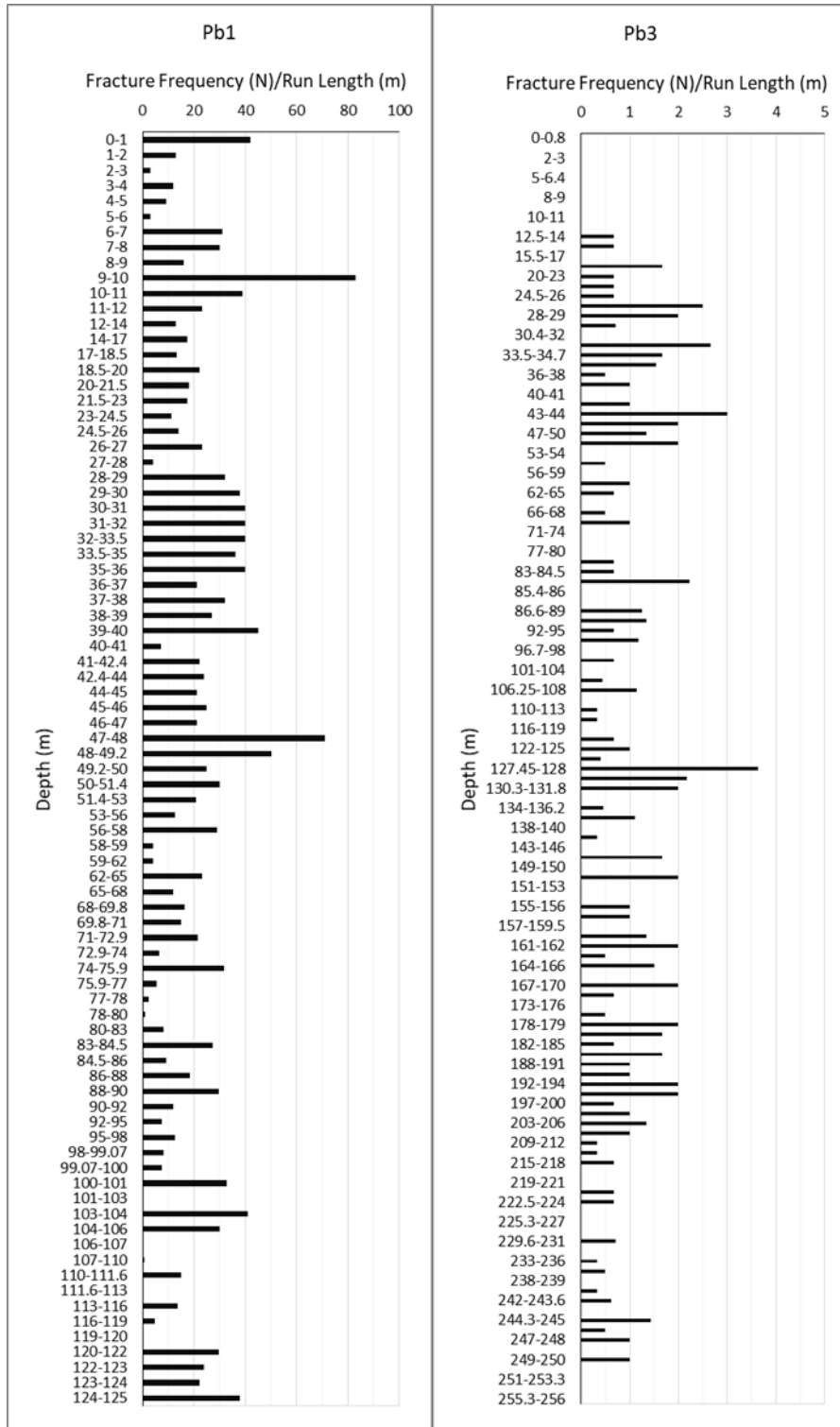
Figure A-3. Fracture Frequency (N)/Run Length (m) of Pb1 and Pb3
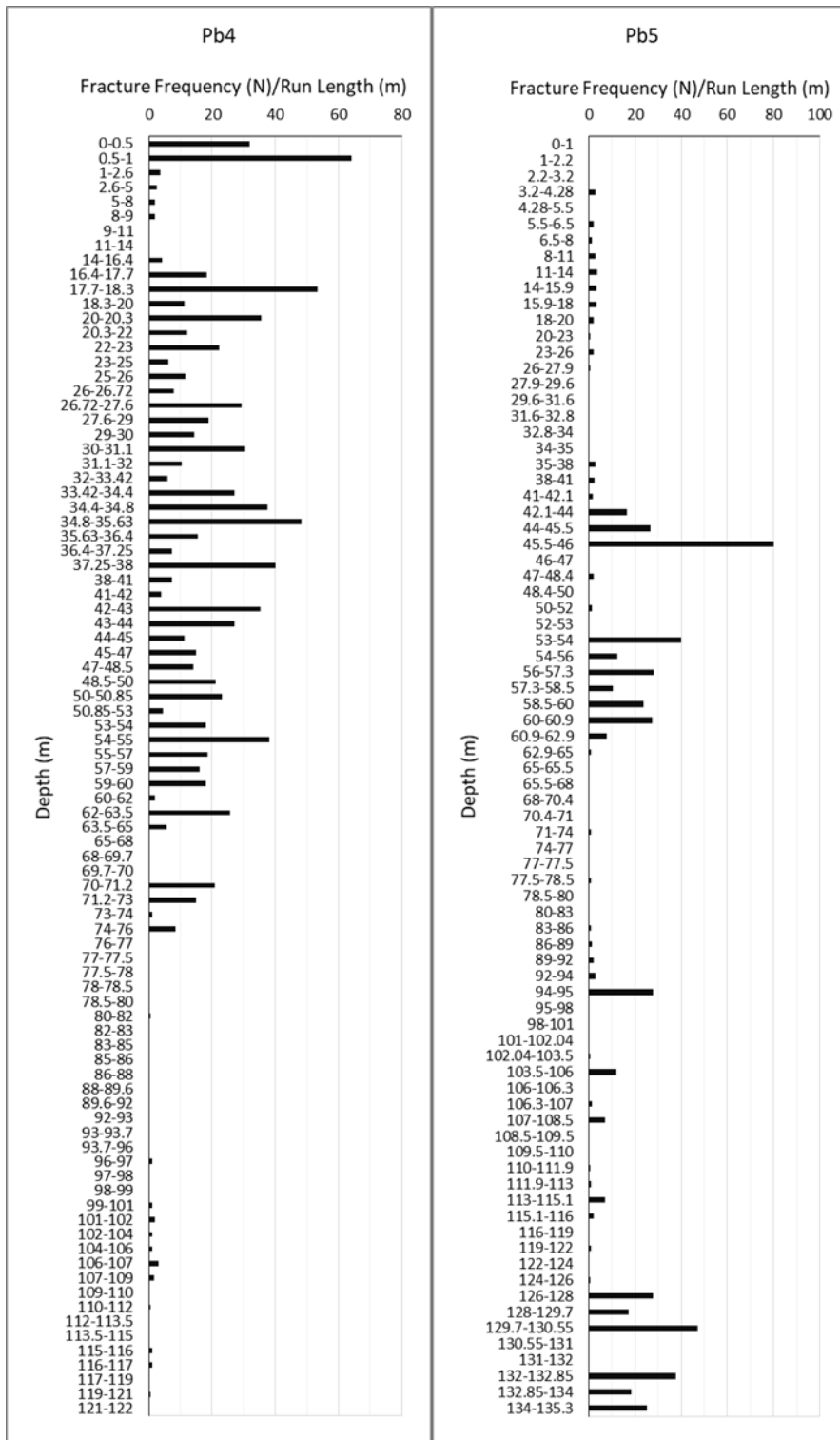
Figure A-4. Fracture Frequency (N)/Run Length (m) of Pb4 and Pb5
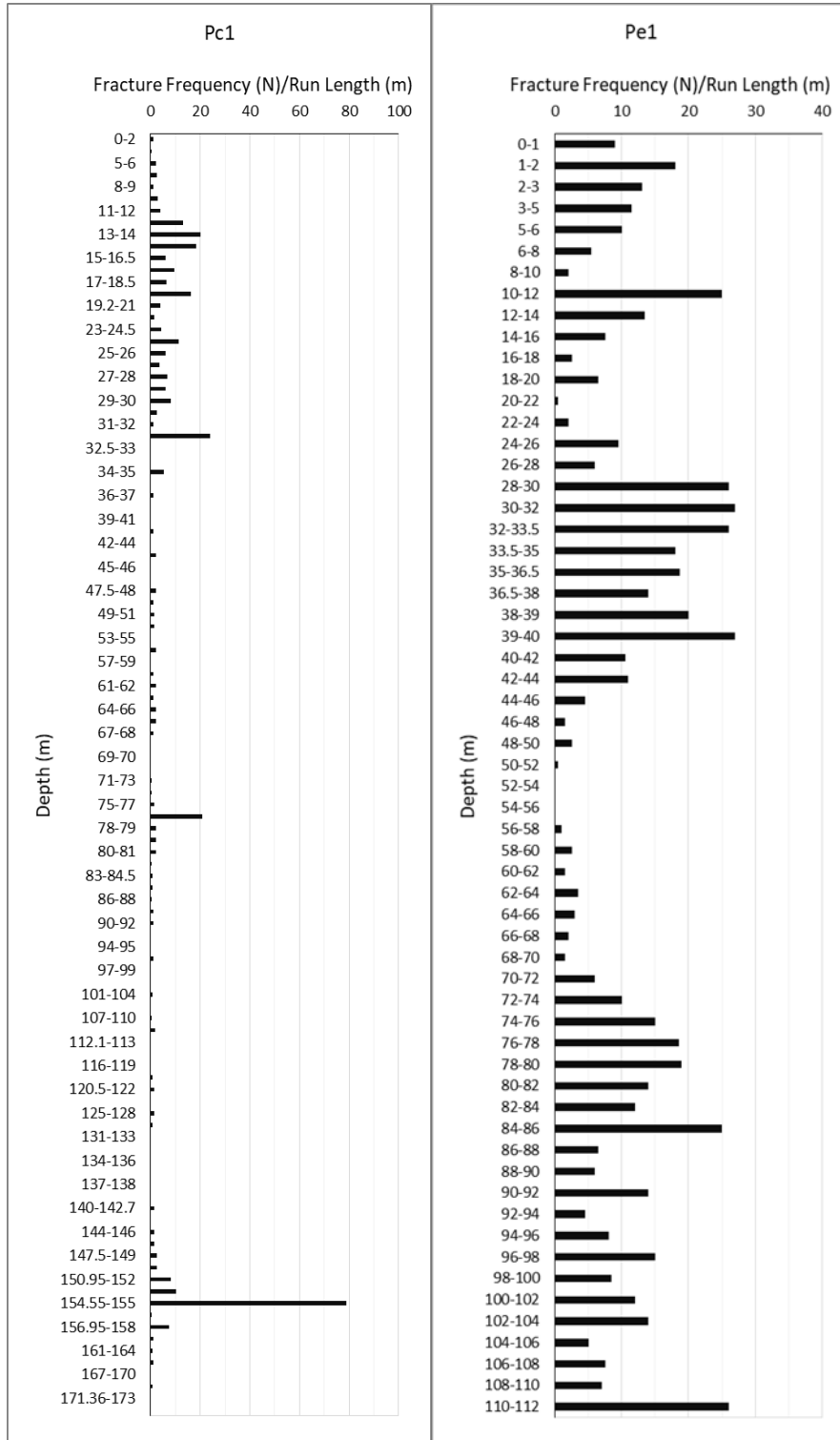
Figure A-5. Fracture Frequency (N)/Run Length (m) of Pc1 and Pe1
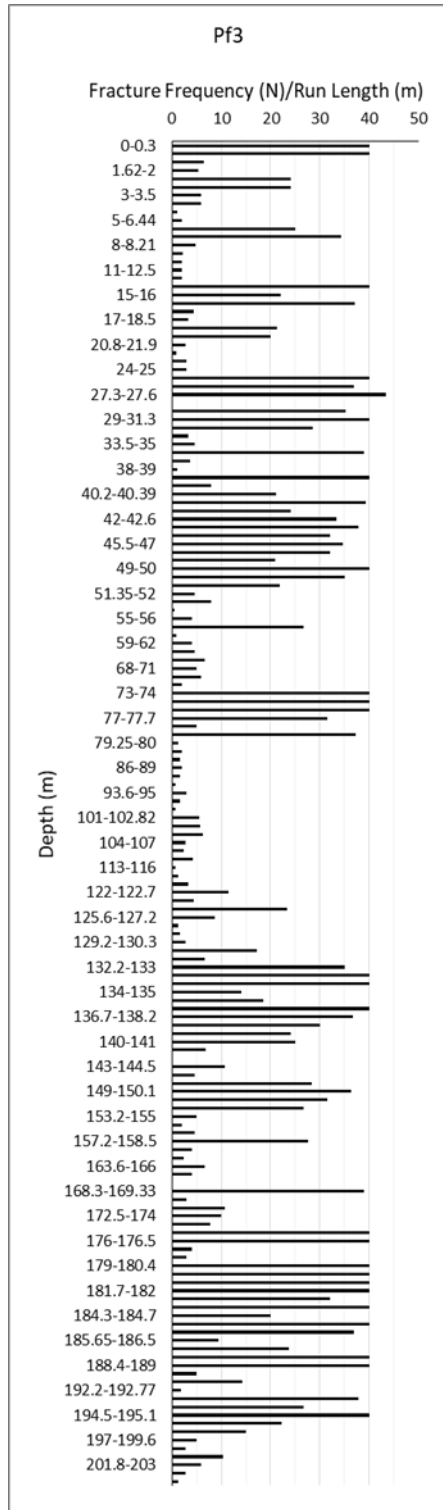
Figure A-6. Fracture Frequency (N)/Run Length (m) of Pf3
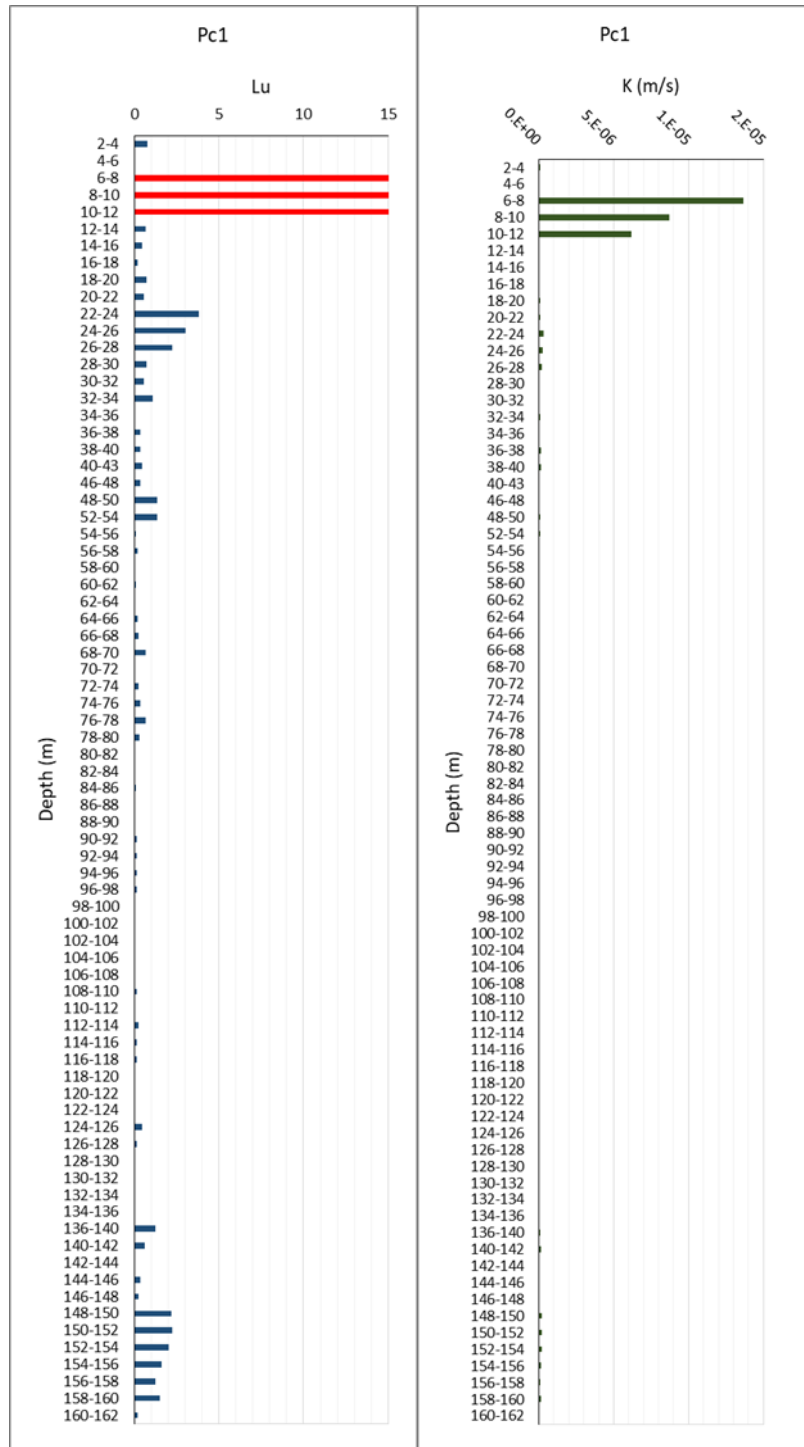
Permeability (Lu) and Hydraulic Conductivity (m/s) Profiles for Drill Holes
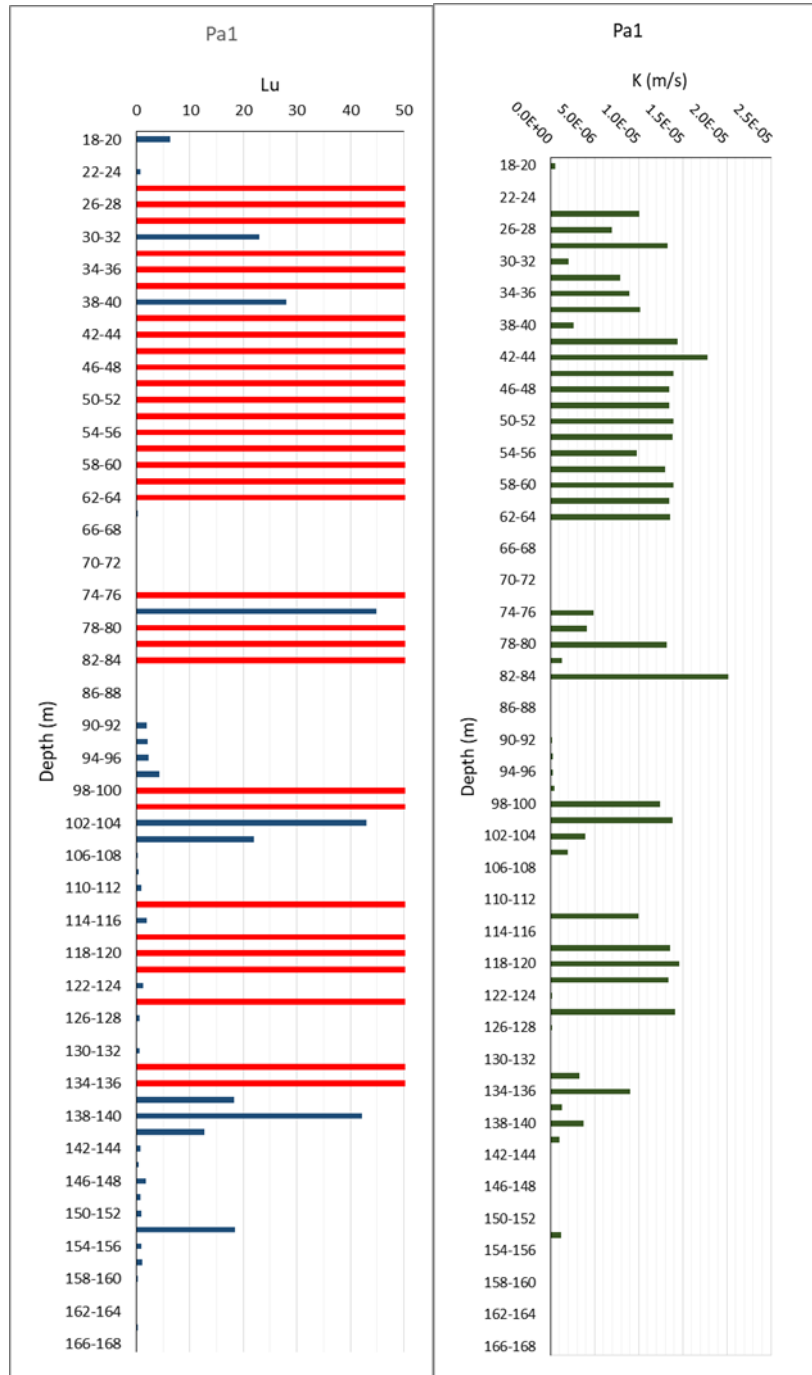
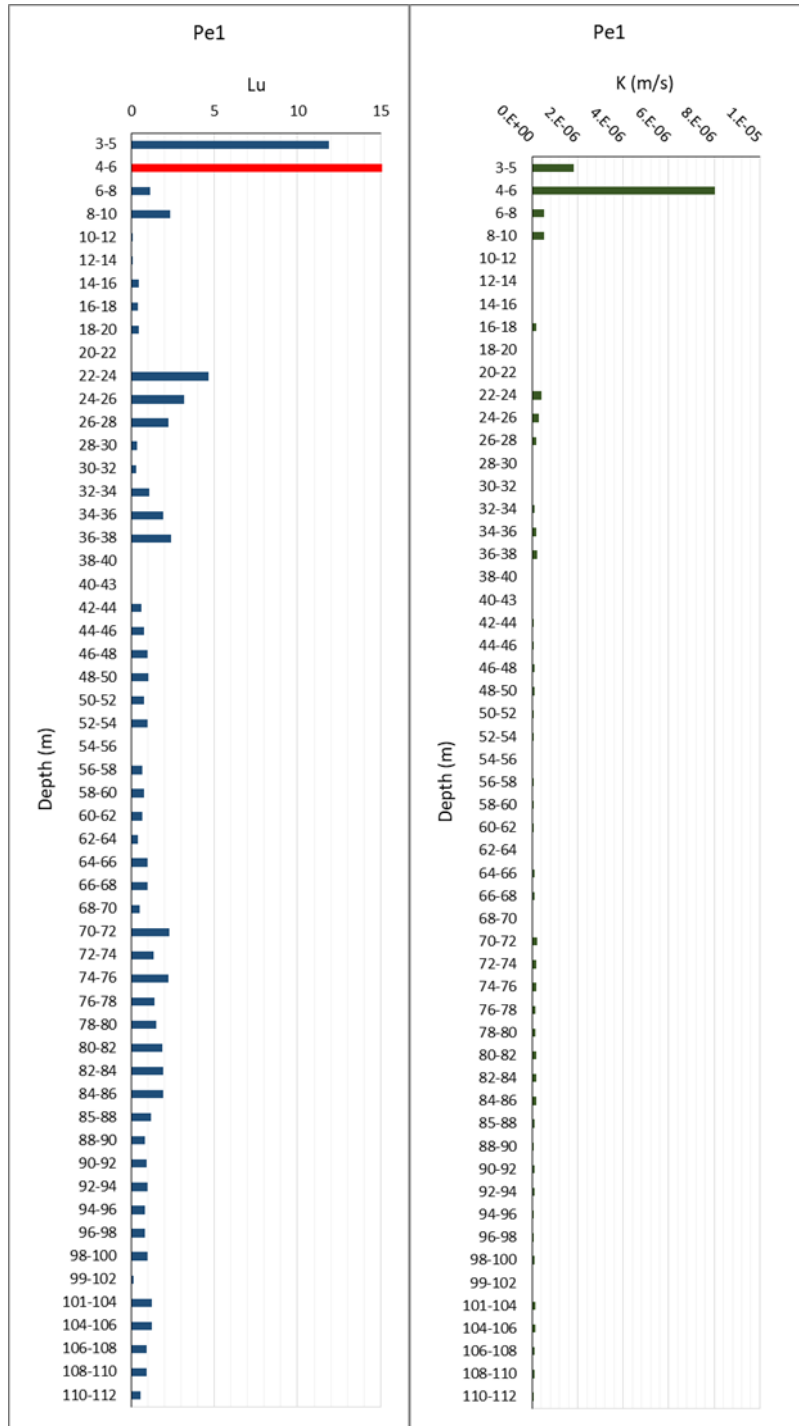

Figure B-1. Permeability (Lu) on the left and Hydraulic Conductivity (m/s) on the right for Pa1
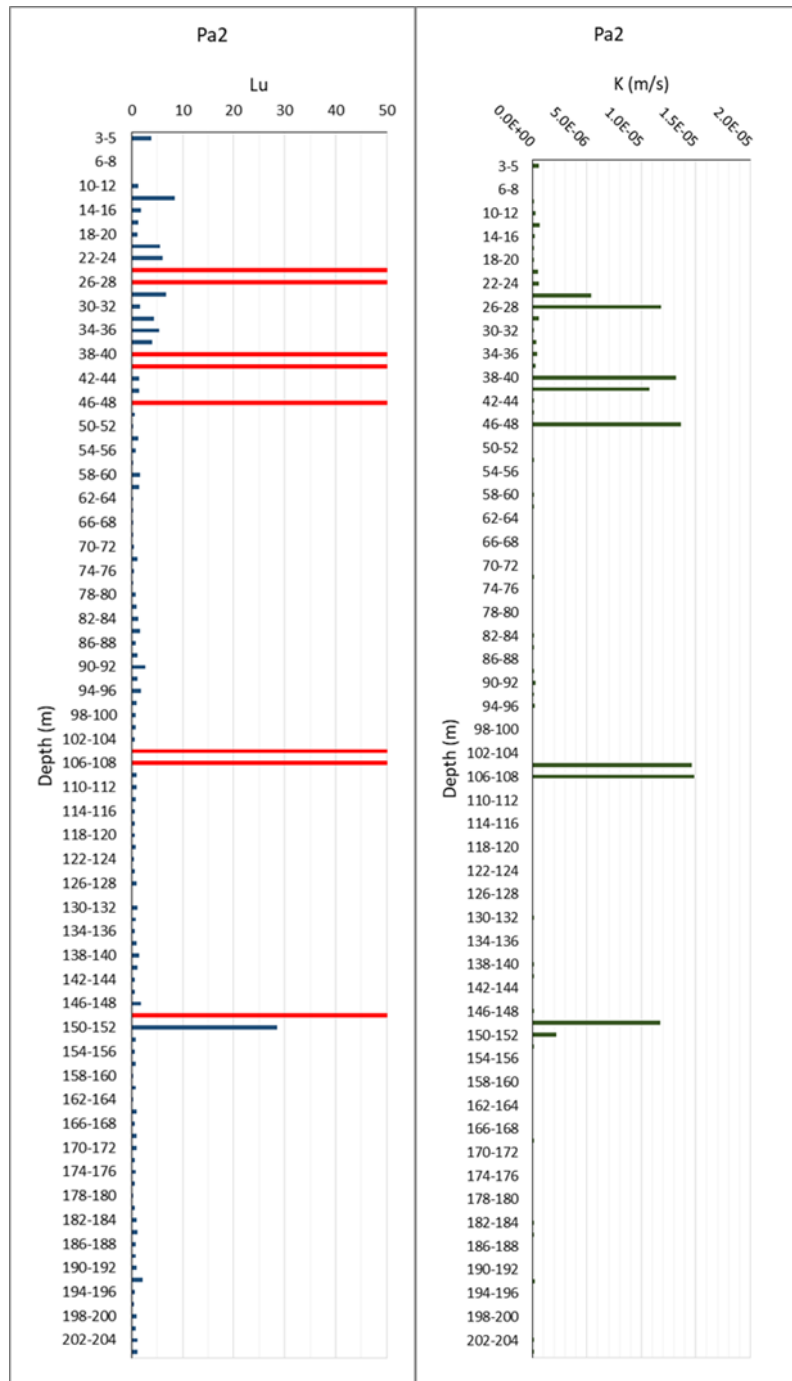
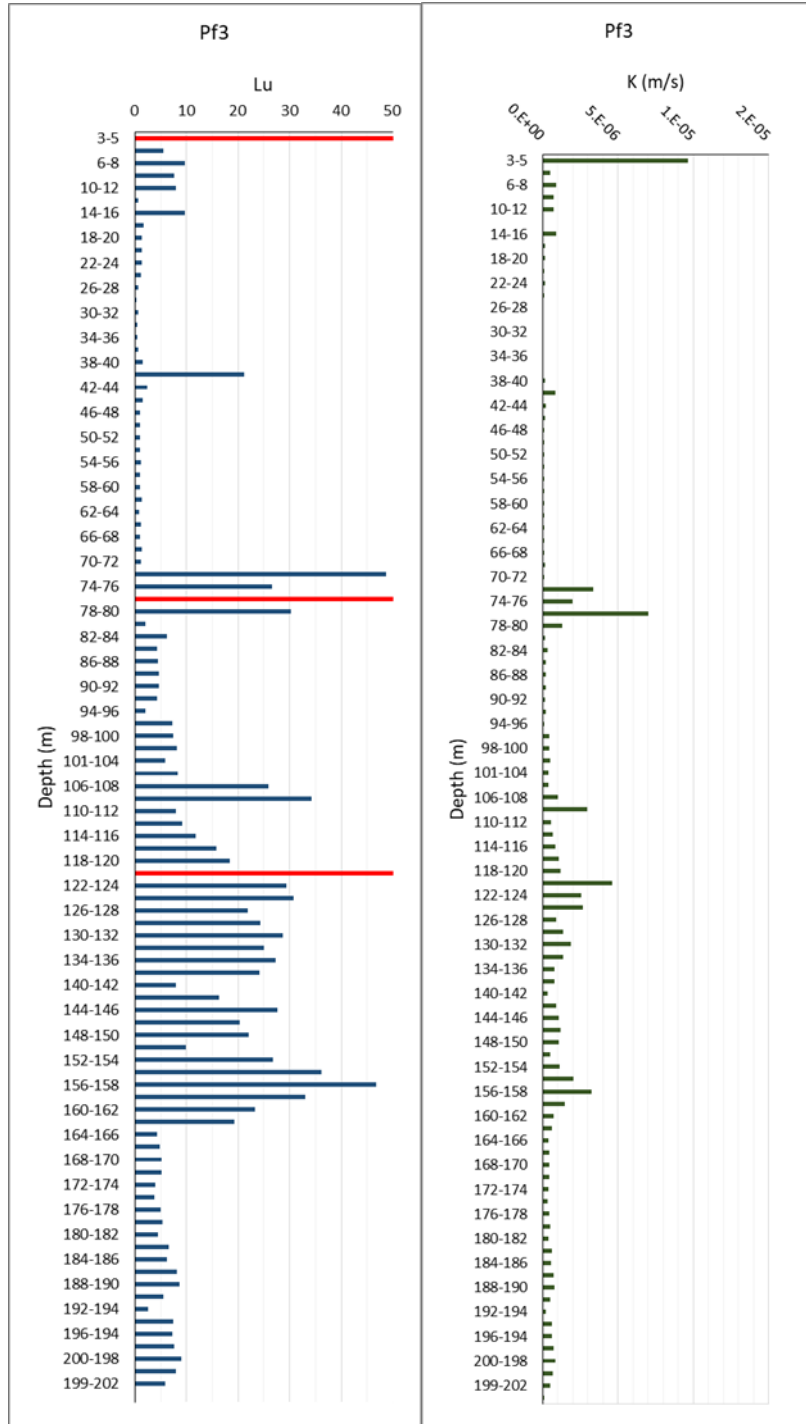Figure B-2. Permeability (Lu) on the left and Hydraulic Conductivity (m/s) on the right for Pa2
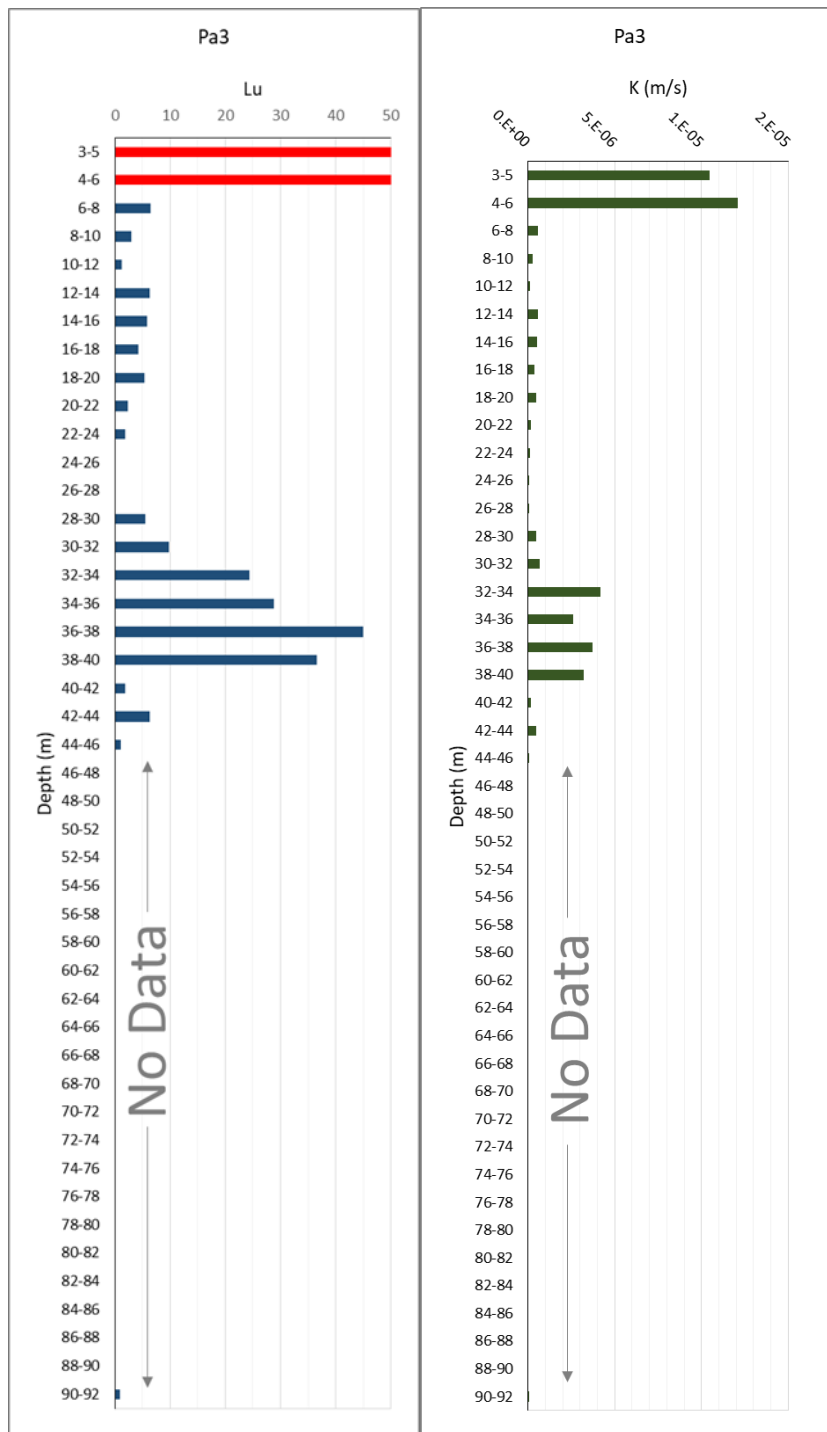
Figure B-3. Permeability (Lu) on the left and Hydraulic Conductivity (m/s) on the right for Pa3
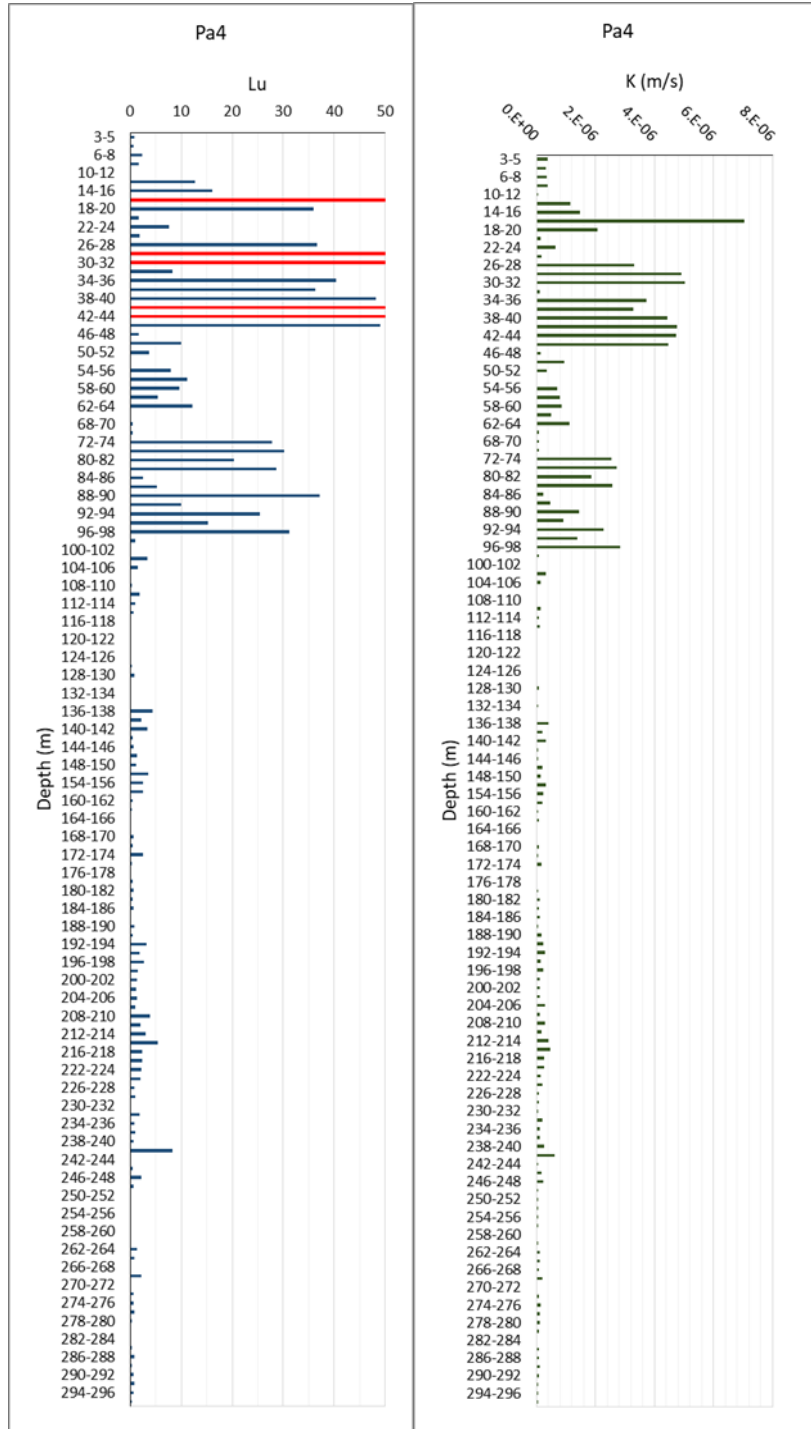
Figure B-4. Permeability (Lu) on the left and Hydraulic Conductivity (m/s) on the right for Pa4
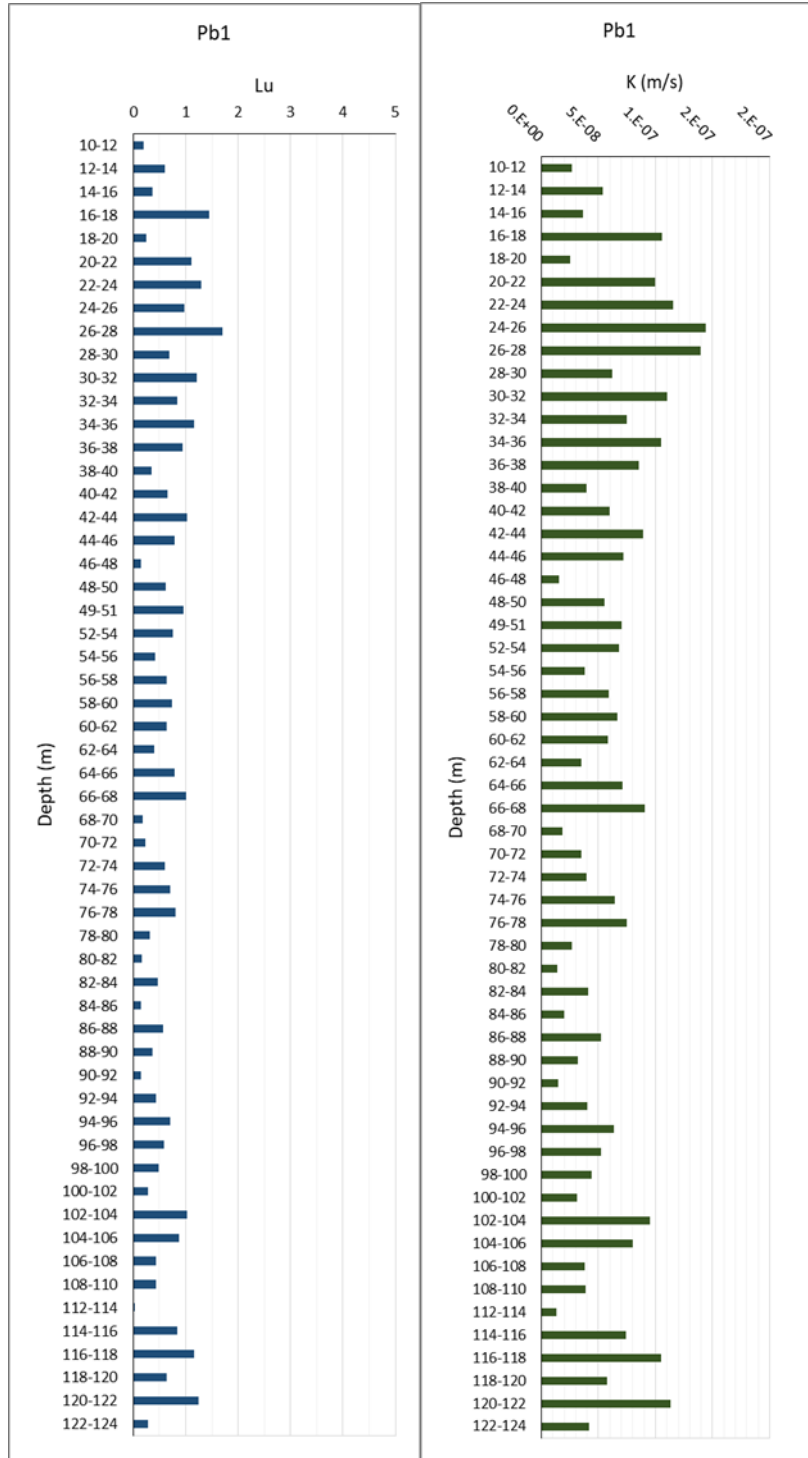
Figure B-5. Permeability (Lu) on the left and Hydraulic Conductivity (m/s) on the right for Pb1
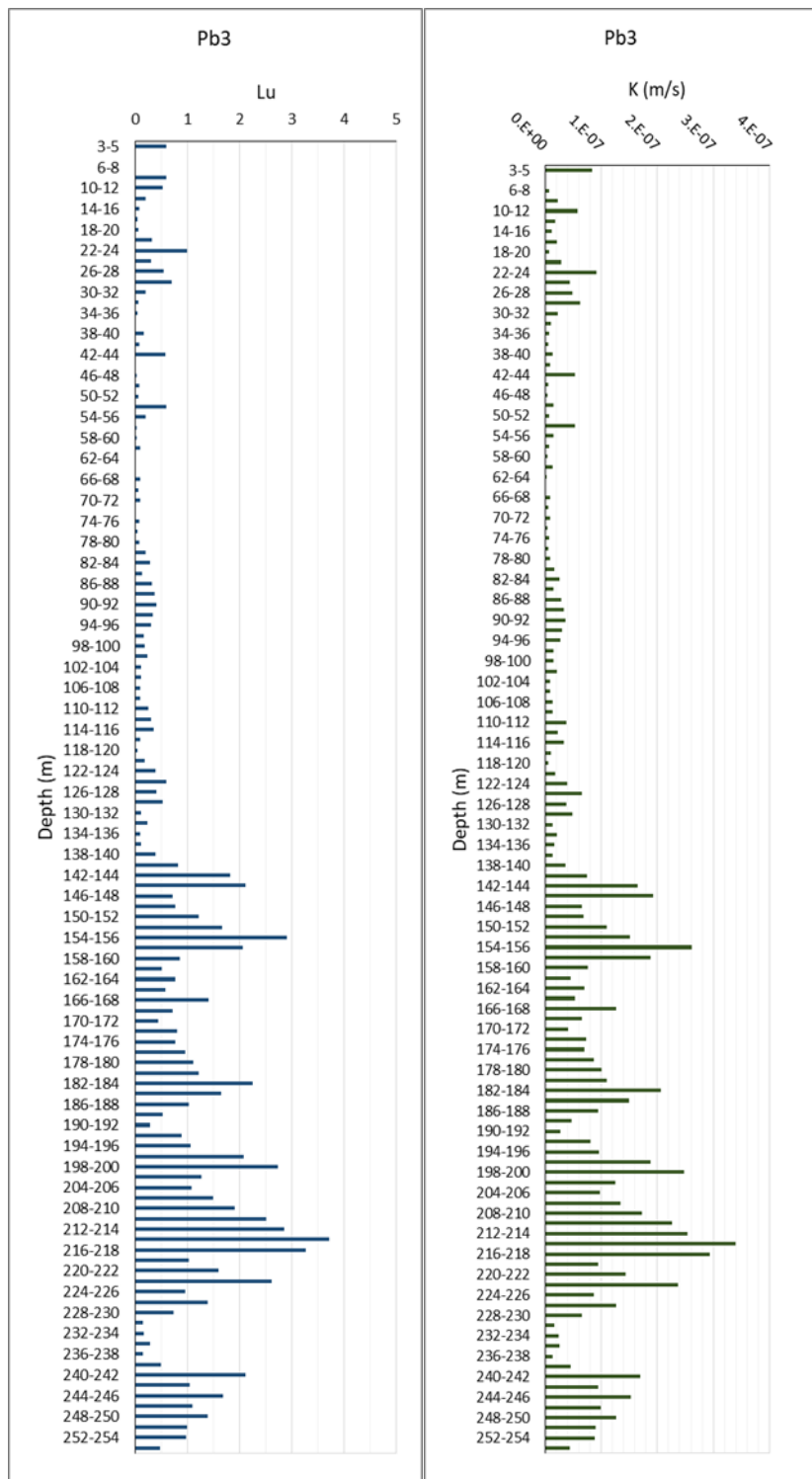
Figure B-6. Permeability (Lu) on the left and Hydraulic Conductivity (m/s) on the right for Pb3
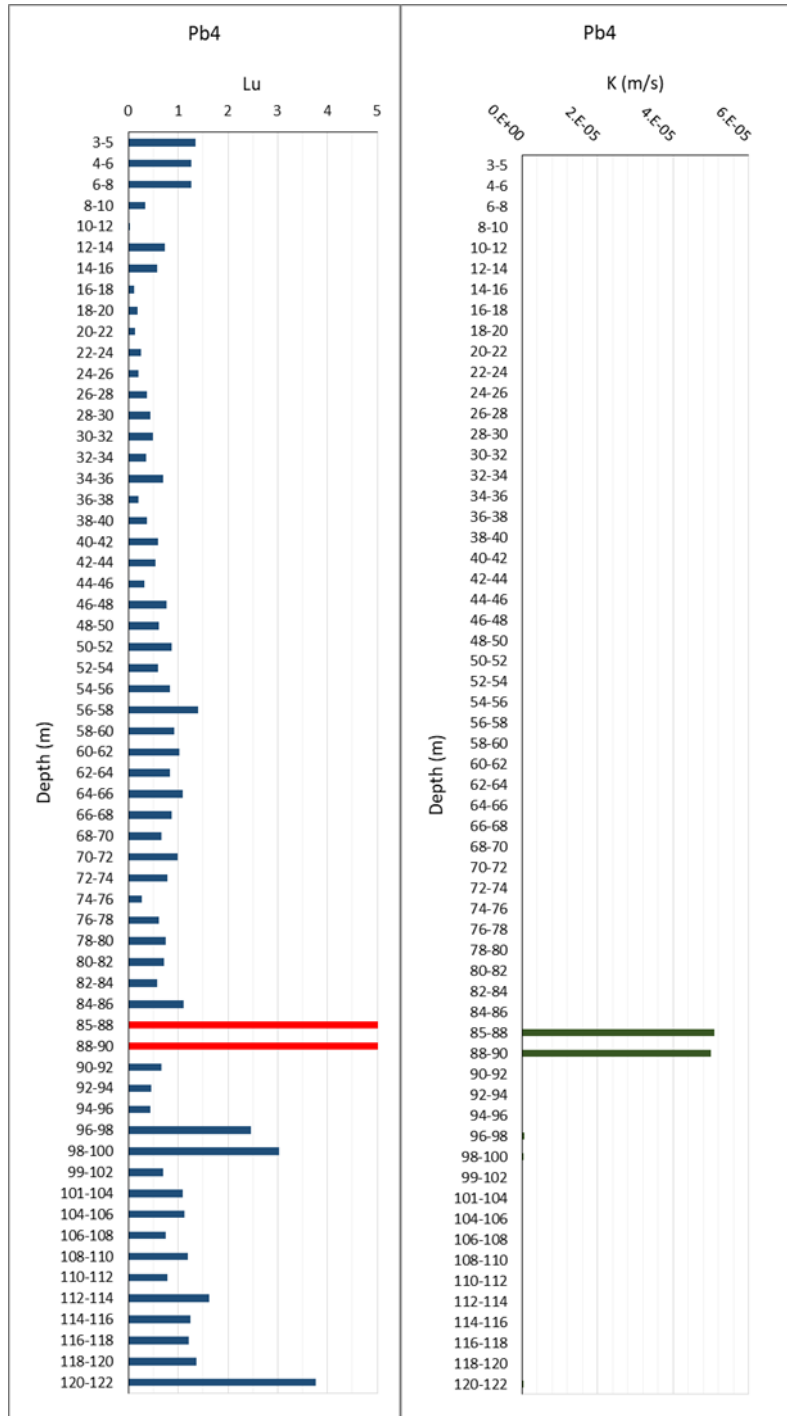
Figure B-7. Permeability (Lu) on the left and Hydraulic Conductivity (m/s) on the right for Pb4
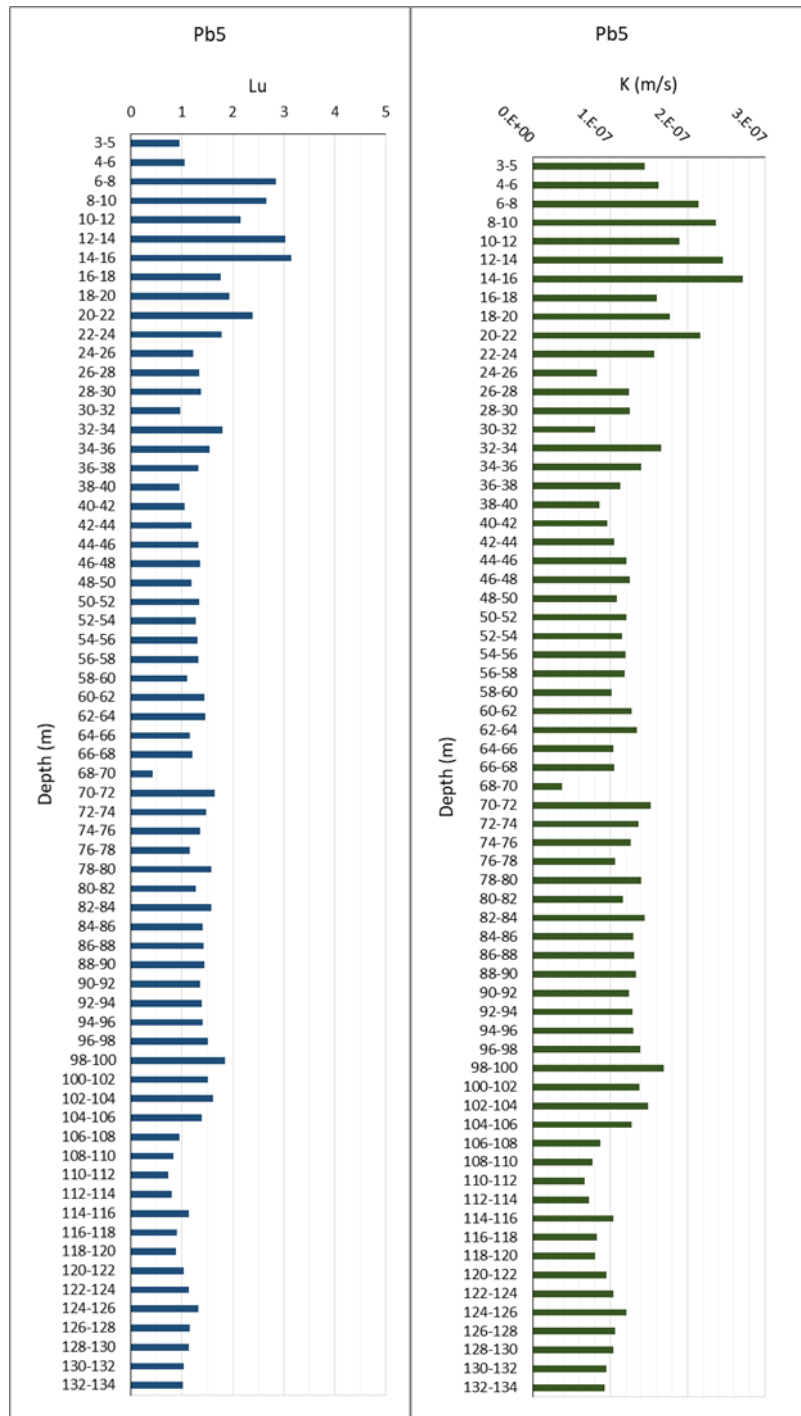
Figure B-8. Permeability (Lu) on the left and Hydraulic Conductivity (m/s) on the right for Pb5

Figure B-9. Permeability (Lu) on the left and Hydraulic Conductivity (m/s) on the right for Pc1

Figure B-10. Permeability (Lu) on the left and Hydraulic Conductivity (m/s) on the right for Pe1

Figure B-11. Permeability (Lu) on the left and Hydraulic Conductivity (m/s) on the right for Pf3

Cross Sections with Hydraulic Conductivity distribution
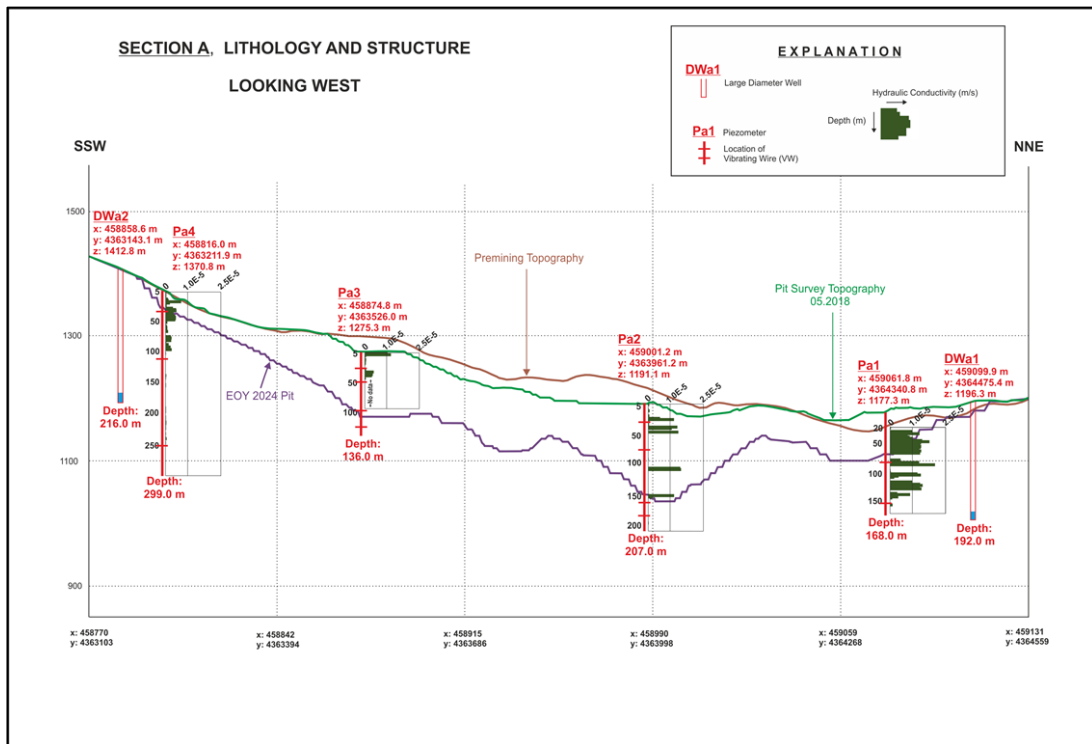
Figure C-1. Hydraulic Conductivity Distribution in Section A
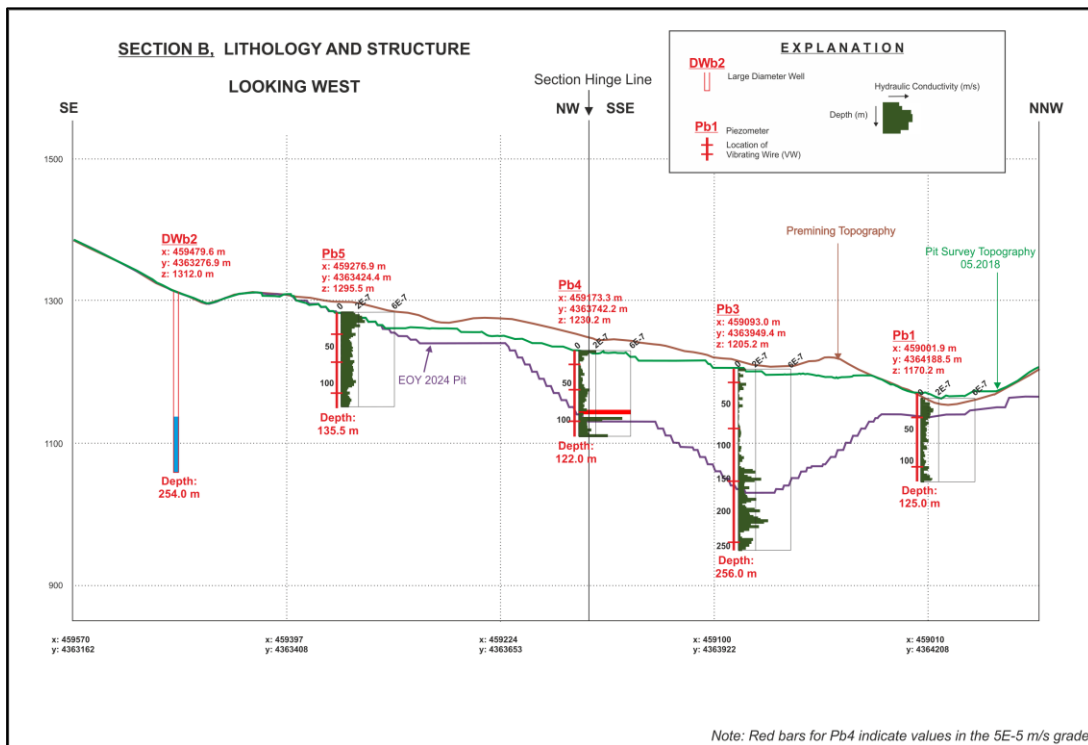
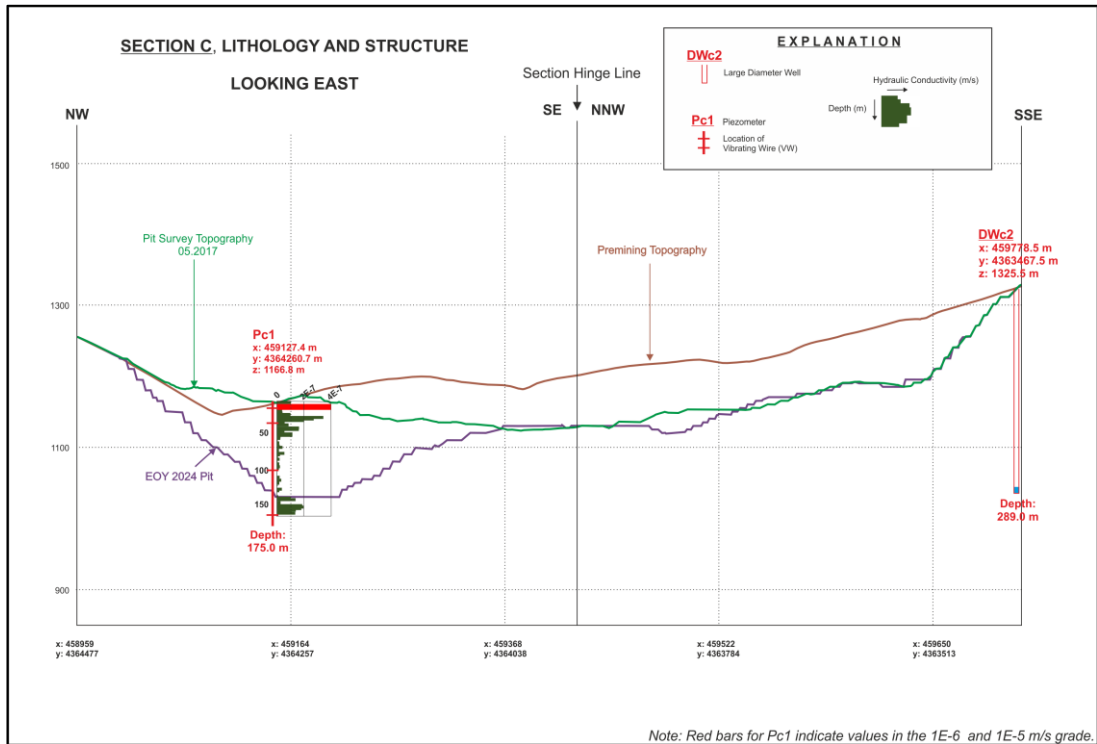Figure C-2. Hydraulic Conductivity Distribution in Section B

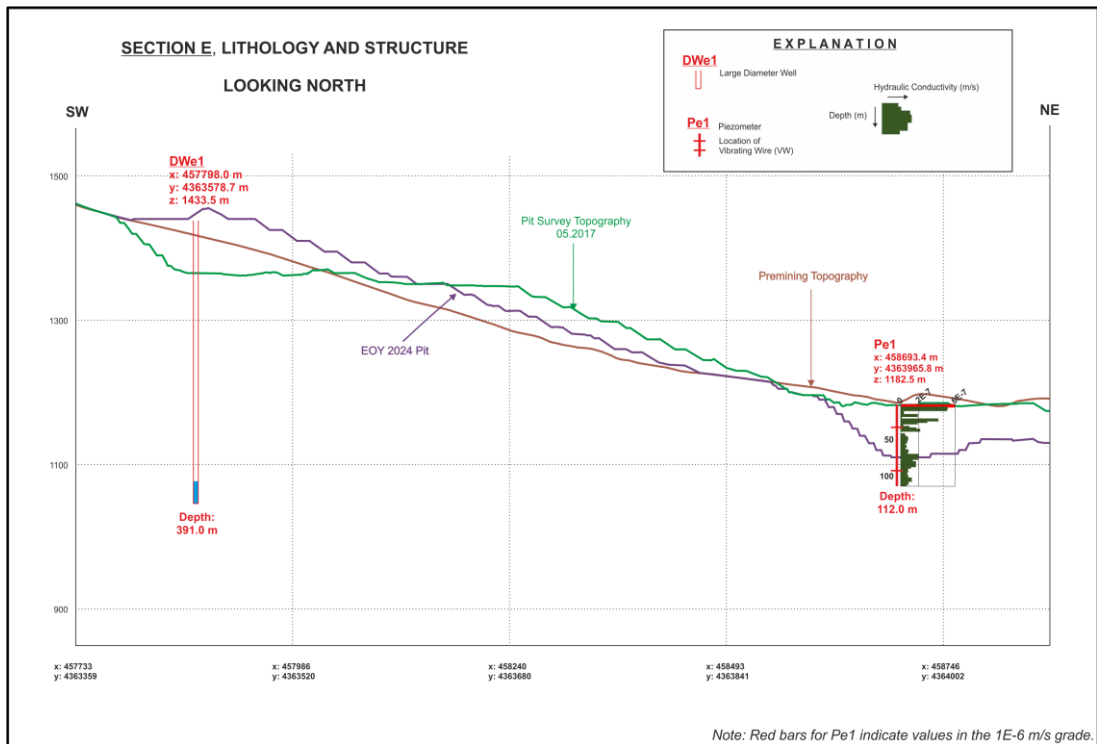Figure C-3. Hydraulic Conductivity Distribution in Section C
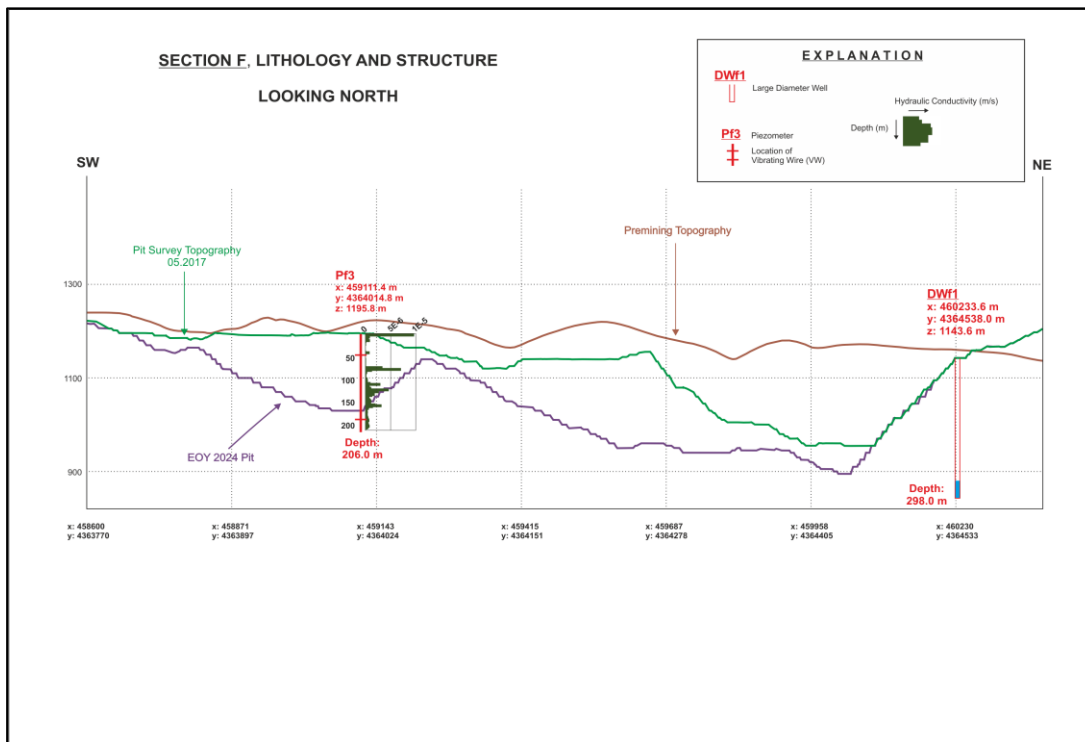

Figure C-4. Hydraulic Conductivity Distribution in Section E

Figure C-5. Hydraulic Conductivity Distribution in Section F